Dissertation zur Erlangung des Doktorgrades
der Fakultät für Chemie und Pharmazie
der Ludwig-Maximilians-Universität München

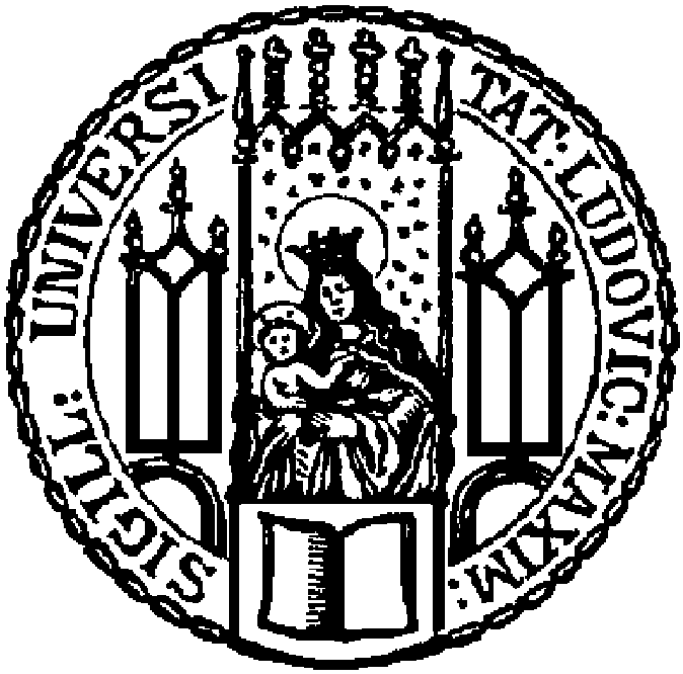

pH-Responsive PEGylation Enhances Colloidal Stability and Promotes Ligand-Mediated Targeting of LAF-Xenopeptide Nanoparticles

Paul Folda

aus

Fürth, Deutschland

2025

Erklärung

Diese Dissertation wurde im Sinne von § 7 der Promotionsordnung vom 28. November 2011 von Herrn Prof. Dr. Ernst Wagner betreut.

Eidesstattliche Versicherung

Diese Dissertation wurde eigenständig und ohne unerlaubte Hilfe erarbeitet.

München, 19.12.2025

……..

Paul Folda

Dissertation eingereicht am:	19.12.2025
1. Gutachter:	Prof. Dr. Ernst Wagner
2. Gutachter:	Prof. Dr. Wolfgang Frieß
Mündliche Prüfung am:	10.02.2026

Für meine Familie

TABLE OF CONTENTS

1 Introduction 1

1.1 Messenger Ribonucleic Acid (mRNA) 1

1.2 Therapeutic Potential 2

1.3 mRNA Engineering 3

1.4 Viral Delivery 4

1.5 Non-Viral Delivery 5

1.5.1 Requirements for Intravenous Administration 5

1.6 Physical Principles of Colloidal Stability 7

1.7 Protein Corona 9

1.8 Steric Stabilization 10

1.9 Classes of Non-Viral Delivery Systems 13

1.9.1 Lipid Nano Particles and Polyplexes 13

1.9.2 LAF-Xenopeptides 15

1.10 Targeting 16

1.11 Aim of the Thesis: 18

2 Materials 19

3 Methods 21

3.1 Synthesis of LAF-XP Carriers 21

3.2 Copper Free Click Reaction for DSPE-PEG-GE11 Conjugate Formation 21

3.3 Unmodified and PEGylated LAF-XP Polyplex Formation 21

3.4 Zetasizer Measurements 22

3.5 Cell Culture 22

3.6 Transfections 22

3.7 Luciferase Gene Expression Assay 23

3.8 Cellular Uptake Study - Flow Cytometry 23
3.9 Steric Stabilization of LAF-XP mRNA Polyplexes Against Salt-Induced Aggregation Through PEGylation 24
3.10 pH-Triggered Deshielding and Destabilization of LAF-XP mRNA Polyplexes 24
3.11 Steric Stabilization of LAF-XP mRNA Polyplexes Against Protein Induced Aggregation Through PEGylation 24
3.12 Serum Assay – Preparation of Serum Incubated LAF-XP mRNA Polyplexes..... 24
3.13 DLS Measurements of Serum Incubated LAF-XP mRNA Polyplexes 25
3.14 Nanoparticle Tracking Analysis of Serum Incubated LAF-Xp mRNA Polyplexes..... 25
3.15 Transfection Efficiency Assessment of Serum Incubated LAF-XP mRNA Polyplexes..... 25
3.16 Isolation and Purification of Protein Corona Coated LAF-XP mRNA Polyplexes 25
3.17 Protein Corona Determination via Mass Spectrometry (MS) Analysis of Serum Coated mRNA LAF-XP Polyplexes..... 26
3.18 SDS-PAGE and Silver Staining of Protein Corona Coated mRNA LAF-XP Polyplexes 27
3.19 Statistical Analysis:..... 27
3.20 Synthesis of GE11 and scrGE11:..... 28
3.21 Lyophilization..... 28
3.22 MALDI-TOF Mass Spectrometry (MS) 29
3.23 Analytical Reversed-Phase HPLC 29
3.24 Preparative HPLC 29
3.25 Ethidium Bromide (EtBr) Exclusion Assay..... 29
3.26 Agarose Gel Shift Assay..... 30
3.27 Cell Viability Assay by MTT..... 30
3.28 Ribo Green Assay 31
3.29 pH Dependent Changes in ZEta Potential of Unmodified and Shielded LAF-XP mRNA Polyplexes..... 31
3.30 In Vivo Performance of mRNA LAF-XP-Polyplexes in Tumor-Bearing Mice: 32
3.31 Ex Vivo Luciferase Expression Assay of Organs and Tumors:..... 32

4 Results and Discussion: 34

4.1 Formulation, Physicochemical and In Vitro Assessment of PEGylated LAF-XP mRNA Polyplexes 36

4.2 Targeting of LAF-XP mRNA Polyplexes with GE11 42

4.3 PEGylation and GE11 Targeting of LAF-XP pDNA Polyplexes 47

4.4 Colloidal Stability 50

4.4.1 Steric Stabilization of LAF-XP mRNA Polyplexes Against Salt-Induced Aggregation Through PEGylation 50

4.4.2 Reduction of the N/P ratio Through PEGylation 53

4.4.3 Overcoming mRNA LAF-XP mRNA Polyplex Instability Through PEGylation 54

4.5 Protein Corona 56

4.6 Steric Stabilization of LAF-XP mRNA Polyplexes Against Protein and Serum Induced Aggregation Through PEGylation 60

4.7 In Vivo Dose Study: 1621 and 1752 68

5 Summary 72

6 Appendix 74

7 References 76

8 Publications 92

8.1 Research 92

8.2 Poster Presentation 92

8.3 Patent Application 92

9 Acknowledgements 93

1 INTRODUCTION

This chapter provides a brief introduction on the fundamental principles of mRNA therapeutics, with a focus on the physicochemical and biological challenges associated with their systemic delivery. It is not considered to be a complete review of the entire scientific field.

1.1 MESSENGER RIBONUCLEIC ACID (MRNA)

Gene expression is a complex and tightly regulated process. Both coding and non-coding genetic information are stored in deoxyribonucleic acid (DNA). The human genome comprises approximately 20,000 protein-coding genes, which are transcribed into messenger ribonucleic acid (mRNA) and subsequently translated into proteins [1, 2]. mRNA serves as a transient and tightly regulated intermediary that carries a copy of the nucleotide sequence encoded by a gene.

Structurally, mRNA is a single-stranded heteropolymer composed of numerous nucleotides, which are linked by 3'-5' phosphodiester bonds. Each nucleotide consists of a nitrogenous base, adenine, cytosine, guanine, or uracil, covalently attached to a ribose sugar [3]. Transcription is the process by which the genetic information encoded in a DNA sequence is copied into a complementary precursor messenger RNA (pre-mRNA). In eukaryotic cells, transcription is carried out by RNA polymerase II and regulated by cis-regulatory elements and transcription factors that control promoter recognition, initiation, elongation, and termination. The resulting pre-mRNA undergoes several processing steps to generate a functional transcript, the mature mRNA. This processing includes the addition of a 5' cap, splicing of introns, and polyadenylation at the 3' end. The 5' cap, consisting of a 7-methylguanosine-triphosphate moiety protects mRNA from degradation and is essential for ribosomal recognition during translation initiation. Splicing removes non-coding introns and joins exons to generate a continuous protein-coding sequence [4]. The poly(A) tail contributes to mRNA stability, nuclear export, and translation efficiency. Once fully processed, mature mRNA, comprising a 5' untranslated region (UTR), an open reading frame

(ORF), and a 3’ UTR, is transported from the nucleus into the cytoplasm, where translation of the ORF into a protein occurs [5-7].

1.2 THERAPEUTIC POTENTIAL

mRNA has the potential to revolutionize modern medicine. Because mRNA can be readily designed and modified to encode virtually any protein, it offers, the ability to therapeutically address a wide range of diseases. Potential applications of mRNA-based therapeutics range from vaccines and in vivo antibody production to protein replacement therapies, genome editing, and cell-based therapy [8]. During the COVID-19 pandemic, this approach played a pivotal role. The mRNA vaccines Spikevax (mRNA-1273) and Comirnaty (BNT162b2) were rapidly developed and demonstrated high efficacy, preventing SARS-CoV-2 infections in approximately 95% of vaccinated individuals [9]. Most recently, the U.S. Food and Drug Administration (FDA) approved Moderna’s next-generation, lower-dose mRNA vaccine mNexspike for COVID-19 [10]. Beyond the application for COVID-19, mRNA technology is increasingly being applied to other viral infections. In this context, both the FDA and the European Medicines Agency (EMA) approved mRESVIA (Moderna Therapeutics), an mRNA-based vaccine for the prevention of respiratory syncytial virus-associated (RSV) lower respiratory tract diseases [11].

Several mRNA vaccines are currently undergoing clinic trails for personalized cancer immunotherapy. For example, BioNTech's autogene cevumeran (BNT122/RO7198457), an individualized neoantigen mRNA vaccine that is being tested for the treatment of solid tumors. It is currently in phase II clinical trials [12].

Moreover, an in vivo CRISPR-Cas9 mRNA LNP therapy, nexiguran ziclumeran, is presently in late-stage (phase III) clinical development [13]. These clinical trials and technological advances collectively highlight the innovation and expanding potential of mRNA therapeutics [14].

Unlike DNA, which needs to be translocated into the nucleus, mRNA only needs to be delivered into the cytosol. This leads to more rapid and efficient protein expression and eliminates the risk of accidental genomic integration [15]. Thanks to in vitro transcription (IVT) technology, mRNA can be easily designed, modified, and produced at a large and cost-

effective scale [16]. This is a major advantage over classical biologics, such as antibodies or recombinant proteins. Here, synthesis relies on traditional cell-based protein production systems, which are difficult to scale and need extensive purification to obtain the required purity. This substantially increases production costs [17, 18].

mRNA was first described in 1961 [19]. In 1990, it was demonstrated that direct administration of mRNA into mice resulted in successful protein expression [20]. However, its therapeutic use has only become recently possible. This is due to several limitations which make mRNA difficult to apply as a drug. mRNA is inherently unstable, negatively charged, and large in size and therefore cannot cross biological lipid bilayers on its own efficiently [21]. Moreover, unmodified mRNA is highly immunogenic and is recognized by the innate immune system through a range of pattern recognition receptors (TLR3, TLR7, TLR9, RIG-1 and MDA5) [22-26].

To enable the development of mRNA as a clinical drug two major aspects have to be addressed. First, the mRNA itself requires extensive optimization to increase stability and modulate immunogenicity. Second, an effective delivery system is needed to protect the mRNA from degradation by endogenous nucleases and ensure its delivery to the intended target site.

1.3 mRNA Engineering

The presence of the 2'-hydroxyl group in the ribose renders mRNA chemically unstable as it can perform intramolecular nucleophilic addition and elimination reactions with the phosphodiester backbone, leading to degradation. A mechanism exploited by endogenous nucleases [27]. Modifying the different structural elements of mRNA can be used to tailor immunogenicity, translational efficiency and stability.

Incorporating specific base modifications into mRNA has been shown to enhance stability and efficiency, while reducing immunogenicity. Important modifications include 5-methylcytidine (m5C) and pseudouridine (Ψ), an isomer of uridine that reduces activation of innate immune receptors such as TLR7/8 and RIG-I. An additional modification, N1-methylpseudouridine exhibits even lower immunogenicity and leads to higher protein

production. This particular modification was used in both the Comirnaty and Spikevax COVID-19 mRNA vaccines [24, 28, 29].

In eukaryotic mRNA, 5’ capping results in enhanced stability and translation and enables the discrimination from foreign RNA [30]. The major cap structures include Cap0, Cap1, and Cap2. The innate immune receptor RIG-I recognizes uncapped and, to a lesser extent, Cap0 mRNA as foreign [31]. Cap0 consists of a 7-methlyguanosine (m7G) linked to the first nucleotide of the mRNA via a triphosphate bridge (m7GpppN). 2’-O-methylation of the ribose of the first nucleotide is termed Cap1, while an additional 2’-O-methylation of the second nucleotide results in Cap2. In the COVID-19 vaccines, a Cap1 modification was employed to minimize immunogenicity and to ensure optimal function [32].

The poly(A) tail is also crucial for mRNA stability. In mammalian cells the poly(A) tail is about 100-250 nucleotides (nt) long [33, 34]. For therapeutic mRNA, however, 100 nt is optimal, as it reduces degradation while still enabling efficient manufacturing [8, 35].

1.4 VIRAL DELIVERY

Viral vectors, such as adeno-associated viruses (AAVs), lentiviruses, and adenoviruses, were among the first delivery systems used in gene therapy. Their high transduction efficiency, in vivo stability and, intrinsic or engineerable targeting capabilities have demonstrated their effectiveness. Their application is highly versatile, ranging from life-saving gene therapies to use as platforms for vaccines, including against COVID-19. However, viral vectors are primarily suited for delivering DNA rather than mRNA and have limited packaging capacity [36, 37].

1.5 NON-VIRAL DELIVERY

Non-viral delivery systems represent promising alternatives to viral vectors. A major advantage is that encapsulation of nucleic acids is achieved through electrostatic interactions, enabling the delivery of large nucleic acid cargos. This makes non-viral delivery particularly attractive for mRNA therapeutics.

1.5.1 Requirements for Intravenous Administration

mRNA therapeutics can be administered via multiple routes, including local injection into muscle, ocular or pulmonary delivery [38-40]. Intravenous (i.v.) administration has the advantage that any internal organ is addressable. However, successful delivery requires overcoming multiple barriers. In this context, the delivery system plays an integral role.

First of all, it must be designed to efficiently encapsulate the mRNA and ensure that resulting nanoparticles do not aggregate but remain colloidally stable during the formulation. Secondly, the delivery system must address several extracellular challenges. Again, the colloidal stability of mRNA nanoparticles is critical. Upon intravenous injection, nanoparticles encounter ionic stress from salts, interactions with negatively charged serum proteins and blood cells, and have to endure shear forces and physiological temperature [41, 42]. Aggregation would not only reduce delivery efficiency but also pose significant safety risks, such as thrombotic events [43]. Moreover, the delivery system must ensure efficient targeting of the intended tissue and cell type. The treatment becomes ineffective otherwise and may even cause adverse effects.

Lastly, the delivery system must facilitate intracellular delivery. It needs to promote cellular uptake, enable endosomal escape and subsequently release the mRNA into the cytosol (Figure 1).

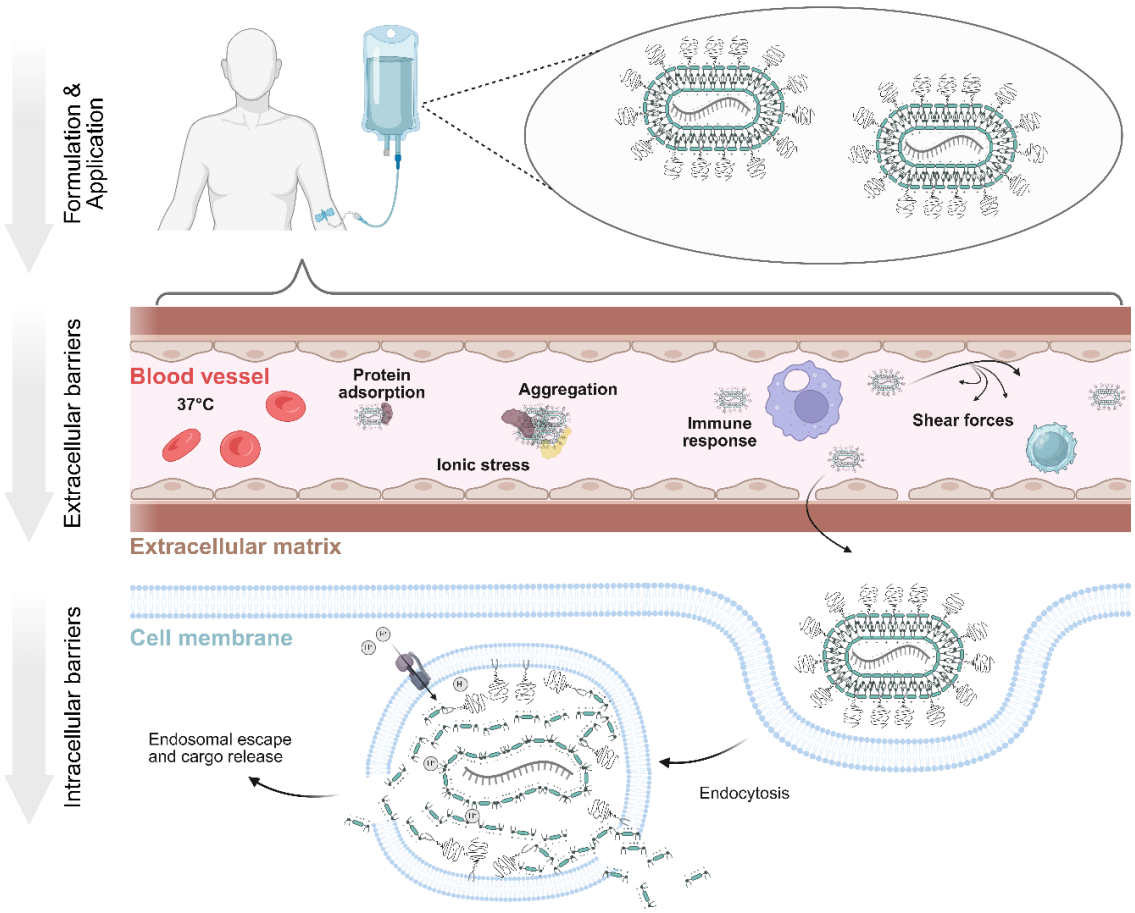

Figure 1. *Schematic overview of extra- and intracellular barriers encountered by mRNA nanoparticles following i.v. administration. mRNA nanoparticles must remain colloidally stable during and after formulation and withstand ionic stress, serum protein adsorption, shear forces, immune recognition, and physiological temperature in the bloodstream. For efficient delivery, intracellular barriers such as cellular uptake, endosomal escape and mRNA release into the cytosol must be overcome. Created with BioRender.com*

1.6 PHYSICAL PRINCIPLES OF COLLOIDAL STABILITY

In a colloidal system, particles are dispersed within a medium. Colloidal stability describes how long these particles stay dispersed without coagulation (aggregation). It depends on the balance between attractive and repulsive forces. According to the Derjaguin–Landau–Verwey–Overbeek (DLVO) theory, the attractive forces are determined by van der Waals forces, whereas the repulsive forces arise from the electric double-layer interactions [44]. The electric double layer forms due to the attraction of counter ions. A portion of these counter ions accumulates directly at the charged surface, forming a compact layer known as the Stern layer. The rest of the ions form a loosely bound cloud, termed the diffuse layer [45].

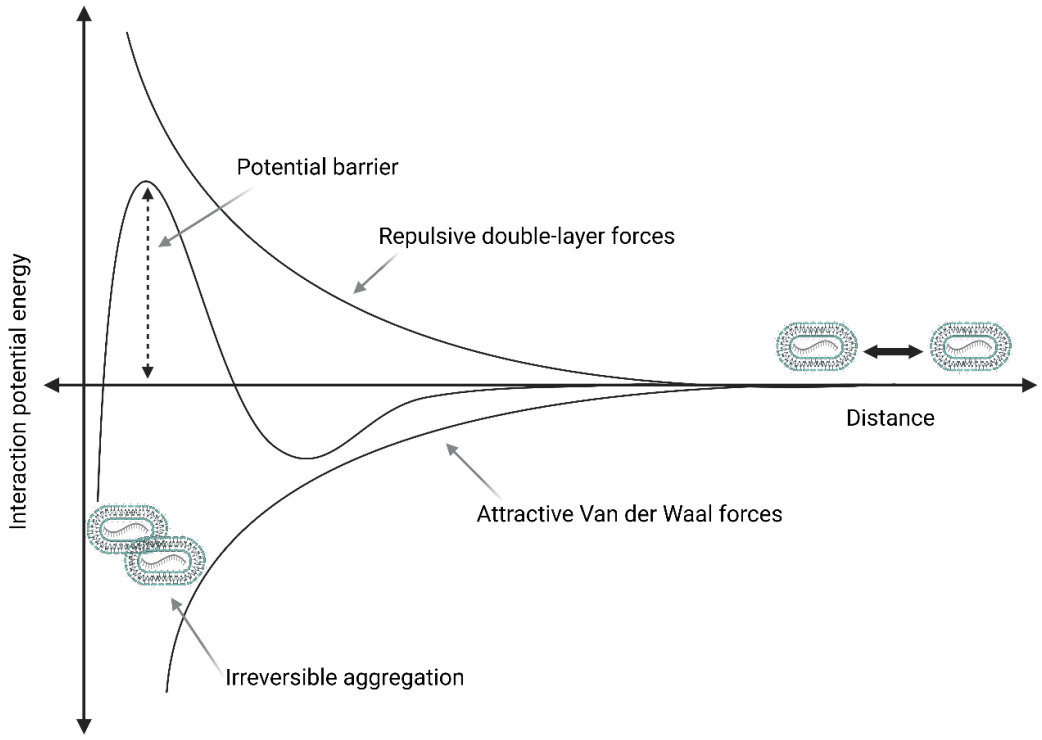

Figure 2. *Schematic illustration of DLVO theory, depicting the opposing attractive van der Waals forces and repulsive electrostatic double-layer forces. At short interparticle distances, van der Waals forces dominate, resulting in a primary energy minimum and irreversible aggregation, whereas increased electrostatic repulsion raises the potential barrier and stabilizes the dispersion. Created with BioRender.com*

The x-axis represents the distance between two particles, while the y-axis shows the interaction potential energy, together creating the energy-distance curve. This curve reflects the sum of the attractive van der Waals forces and repulsive double-layer forces. When two particles approach each other closely enough van der Waals attraction can overcome the double-layer repulsion. At this point, the interaction energy drops into the primary minimum and the particles irreversibly aggregate. A higher surface charge on particles increases the double-layer repulsive forces and thereby enhances colloidal stability (Figure 2) [44].

The ionic strength of the surrounding medium has a strong effect on colloidal stability. As the concentration of ions increases, the diffuse layer gets compressed and its repulsive force decreases. As a result, the likelihood of aggregation increases [44].

This model can be applied to the behavior of mRNA nanoparticles during formulation or in a biological system, particularly following i.v. administration. Under physiological conditions, the salt concentration is approximately 145 mM. In addition, adsorption of negatively charged serum proteins can further mask or neutralize the surface charge and reduce electrostatic repulsion. Protein adsorption may also enhance van der Waals attraction. Furthermore, physiological temperature and shear forces, present in the bloodstream, increase the kinetic energy of the mRNA nanoparticles. This further enhances the chance of collisions with each other or blood cells, consequently promoting aggregation [46].

However, forces beyond those described by classical DLVO theory also play a critical role in determining colloidal stability. These are referred to as non-DLVO forces. One important example is the repulsive steric force generated by polymer coatings. When attached to the particles, highly flexible polymer chains move freely in many directions, giving them a high conformational entropy. As polymer-coated particles approach each other, the polymer chains begin to overlap, creating a crowded region between the particles. This overlap restricts the conformational freedom of the chains and results in a loss of entropy. An energetically unfavorable state according to the second law of thermodynamics, which generates an entropic steric repulsion. In addition, overlapping polymer layers form regions of increased polymer concentrations. This causes water to flow into these zones by osmosis. The resulting osmotic pressure further pushes the particles apart, creating an additional

repulsive force. Together, these entropic and osmotic repulsion are referred to as steric stabilization [44, 47].

1.7 PROTEIN CORONA

Following i.v. administration, nanoparticles are rapidly exposed to blood components and adsorb plasma proteins and other biomolecules, leading to the formation of a dynamic protein corona. The protein corona is primarily composed of apolipoproteins, immunoglobulins, complement factors, coagulation proteins, and acute phase proteins [48, 49].

The composition of the protein corona can influence the efficiency, biodistribution, and circulation time of nanoparticles. Protein adsorption is the result of multiple types of interactions. These include covalent bonding, electrostatic interactions, hydrogen bonding, and weaker forces such as van der Waals. Among these, electrostatic interactions are considered to be the main driving force for protein interaction. For instance, positively charged nanoparticles exhibit strong adsorption of plasma proteins with low isoelectric points ($pI < 5.5$), such as serum albumin and fibrinogen [50-52].

The protein corona can be separated into two layers, commonly referred to as the hard and soft corona. The hard corona comprises proteins that are bound to the surface with high affinity. Protein exchange within this layer is slow, with proteins remaining attached to the surface for minutes and even hours. In contrast, the soft corona is formed by proteins which are weakly bound. Association typically persists on the surface for only seconds before being replaced [53].

Moreover, the composition of the protein corona is highly dynamic. Initially, smaller proteins bind to the nanoparticles. Eventually larger and bulkier proteins, such as fibrinogen replace them - a process known as the Vroman effect. Once adsorbed, these large proteins tend to exhibit greater surface coverage and increased binding stability. This is attributed to their larger size, allowing for stronger and multivalent binding [54, 55].

Protein corona formation may also induce adverse effects. Adsorption of opsonins, including complement factors, immunoglobulins, and fibrinogen, may promote immune recognition

and clearance through the reticuloendothelial system (RES) and trigger the activation of inflammatory signaling pathways [56, 57].

1.8 STERIC STABILIZATION

Steric stabilization is widely utilized in pharmaceutical formulations. As discussed above, it relies on the functionalization of highly flexible and hydrophilic polymers. Polyethylene glycol (PEG) has proven to be particularly well suited for this purpose. Each PEG unit forms hydrogen bonds with approximately two to three water molecules, generating a dense hydration shell that increases the hydrodynamic diameter [58]. PEG is generally well tolerated and, in addition to providing steric stabilization, enhances drug solubility. Upon i.v. administration, PEGylation reduces protein adsorption and prolongs systemic circulation half-life, an effect termed stealth effect [59].

Both the molecular weight and surface density of PEG strongly influence the stealth effect. PEG chains with a molecular weight of at least 2 kDa have been shown to provide effective steric stabilization [60, 61]. Depending on grafting density, PEG chains adopt different conformations on the nanoparticle surface. At low surface densities, PEG chains form a mushroom conformation, whereas at higher surface densities they extend into a brush conformation (Figure 2). Proteins can only reach the nanoparticle surface if they push PEG chains aside. However, displacing PEG chains restricts their conformational freedom and removes associated hydration water, leading to a substantial loss of entropy. This is energetically unfavorable. As a result, approaching proteins are repelled. However, this repulsion depends on protein size. Small proteins may slip through wider gaps between the PEG chains with only minimal loss in entropy. This happens particularly in mushroom conformation. In contrast, at brush densities, the spacing between the PEG chains becomes narrower, reducing this possibility (Figure 3) [62, 63]. Moreover, PEGylation reduces surface charge, thereby diminishing electrostatic attraction forces. This effect is particularly important for cationic nucleic acid delivery systems [64].

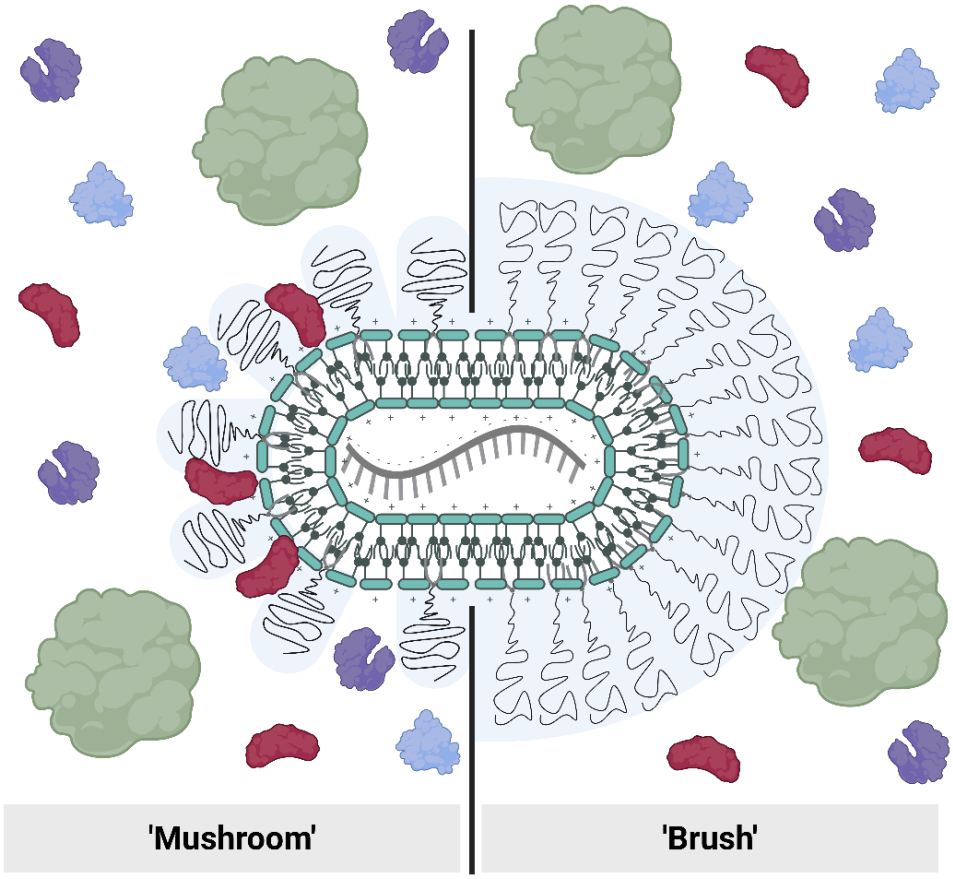

Figure 3. *Schematic display of PEG polymer conformations on mRNA nanoparticles. At low grafting density, PEG chains adopt a "mushroom" conformation, leaving small gaps through which small proteins can access and adsorb onto the nanoparticle surface. At higher grafting density, PEG chains extend into a "brush" conformation with minimal gaps, thereby acquiring stealth characteristics. Created with BioRender.com*

Initially, PEG was first applied in therapeutics through covalent attachment to proteins to increase circulation half-life and therapeutic efficiency [59]. This concept was subsequently applied to liposomal drug delivery by introducing PEG via lipid anchoring (non-covalent). For example, PEGylated liposomal doxorubicin demonstrated markedly prolonged circulation times and enhanced therapeutic effect [65-67] .This principle was later adapted to non-viral nucleic acid delivery. PEG was introduced either through lipid anchoring or by covalent conjugation. Similar to liposomes, PEGylation of nucleic acid nanoparticles prevents aggregation, reduces protein adsorption, and prolongs circulation time [68-70].

Despite these advantages, PEGylation has notable limitations for nucleic acid delivery. By masking surface charge, PEG can also reduce interactions with negatively charged cellular or endosomal membranes. As a result, cellular uptake and endosomal escape are reduced, thereby lowering transfection efficiency. This phenomenon is known as the PEG dilemma.

Several strategies have been developed to overcome this dilemma [71-73]. For lipid-anchored PEG, shorter anchors have been employed to promote desorption. For covalently attached PEG, enzymatically cleavable, reducible, or pH-sensitive linkers have been employed [74-79]. An alternative strategy includes active targeting of specific cell-surface receptors.

More recently, it has become evident that PEG can be recognized by the immune system, in particularly by pre-existing anti-PEG IgM antibodies [80]. Because PEG is widely used in cosmetic products, a considerable fraction of the population may be repeatedly exposed and develop anti PEG immunity. For mRNA therapeutics, especially those requiring repeated dosing, such as protein replacement therapy, this immune recognition presents a significant challenge that must be addressed.

Consequently, the development of PEG alternatives remains an active area of research. Suitable alternatives must fulfill the same physicochemical criteria: high hydrophilicity and high chain flexibility. Promising alternatives include polysarcosine (pSar), poly(N-(2-hydroxylpropyl) methacrylamide (pHPMA), and poly(2-oxazoline) [81-87].

1.9 CLASSES OF NON-VIRAL DELIVERY SYSTEMS

1.9.1 Lipid Nano Particles and Polyplexes

Historically, nucleic acid delivery was first achieved by using cationic lipid-based lipoplexes or polymer-based polyplexes [64, 88-99]. Lipoplexes typically contain a cationic lipid such as 1,2-di-O-octadecenyl-3-trimethylammonium-propane (DOTMA) or 1,2-dioleoyl-3-trimethylammonium-propane (DOTAP), which possess quaternary ammonium head groups. They bind and encapsulate mRNA through strong electrostatic interactions. Although lipoplexes exhibited high transfection efficiencies, their highly cationic nature causes significant colloidal instability and toxicity following i.v. administration [100, 101]. As a consequence, PEGylation in the form of PEGylated lipids was introduced, cationic lipids were replaced by ionizable lipids. Moreover, helper lipids such as phosphor- and sterol lipids were incorporated. Together, these advances led to the development of lipid nanoparticles (LNPs) [102, 103].

LNPs are now state-of-the-art for the delivery of mRNA and are used in the mRNA COVID-19 vaccines [104, 105]. The ionizable lipids used in the clinically approved mRNA vaccines Comirnaty (ALC-0315) and Spikevax (SM102) contain tertiary amine head groups with a low pKa. At physiological pH, they remain neutral, reducing toxicity. In the acidic endosomal environment, they become protonated, promoting the formation of fusogenic phases. Consequently, resulting in endosomal escape and cytosolic mRNA release [106].

Phospholipids such as 1,2-dioctadecanoyl-sn-glycero-3-phosphocholine (DSPC), which contain fully saturated fatty acyl chains, promote the formation and stabilization of lamellar phases. In contrast, 1,2-di-(9Z-octadecenoyl)-sn-glycero-3-phosphoethanolamine (DOPE), with its unsaturated oleyl chains, induces fusogenic phase formation, improving endosomal escape. Cholesterol, a sterol lipid, acts as a stabilizing component by filling gaps within the lipid bilayer. It can further enhance membrane fusion [107-112].

During LNP assembly, the lipids are diluted in organic solvents, typically ethanol, whereas the nucleic acid is diluted in an acidic aqueous buffer. During turbulent mixing, the ionizable lipid becomes protonated, enabling electrostatic binding and encapsulation of the mRNA. After particle formation, the formulation must be diluted and subjected to buffer exchange to

remove the organic solvent and adjust the pH to physiological conditions (pH 7.4). During this process, the ionizable lipid head groups deprotonate and return to their deprotonated state. This results in largely neutral particles, meaning that electrostatic repulsive forces are minimal and insufficient to maintain colloidal stability. For this reason, PEGylation is essential during LNP formulation, as it prevents the particles from aggregating throughout the manufacturing process and during subsequent storage [113-116].

Lipid-conjugated PEG is also essential for maintaining the colloidal stability after i.v. administration. In current formulations, 2 kDa PEG lipids such as 1,2-dimyristoyl-rac-glycero-3-methoxypolyethylene glycol (DMG-PEG) and 1,2-distearoyl-sn-glycero-3-phosphoethanolamine-N-[amino(polyethylene glycol)-2000] (DSPE-PEG) are frequently used. These conjugates consist of a PEG polymer attached to a hydrophobic lipid anchor. DMG-PEG contains a relatively short C14 myristic diacyl anchor. It embeds only weakly within the LNP surface and gradually dissociates from the LNP after administration ("sheddable PEG"). In contrast, DSPE-PEG featuring longer C18 stearoyl chains, are strongly anchored, which results in extended circulation times in vivo [117-121].

In contrast, polyplexes offer a much simpler formulation procedure. The nucleic acid and the cationic polymer are directly combined in an aqueous buffer, eliminating the need for downstream steps such as dilution or dialysis. No additional PEGylation is needed during formulation, as electrostatic repulsion between the cationic carrier-nucleic acid complexes contributes to colloidal stability. Early polyplex systems were based on simple cationic polymers such as polylysine or polyarginine. However, these polymers exhibited limited transfection efficiency [122, 123]. The introduction of polyehtyleneimine (PEI) represented a major advancement, as its pH-responsive protonation at endosomal pH significantly enhanced endosomal escape and thus transfection efficiency [124]. However, similar to cationic lipids, cationic polymer delivery systems suffered from poor in vivo colloidal stability and toxicity [43, 64]. Moreover, the strong positive charge triggers complement activation, which potentially triggers inflammation [125-127]. Again, surface modification with PEG has been used to mitigate these effects [70, 128-136].

1.9.2 LAF-Xenopeptides

Prof. Ernst Wagner, a pioneer in the field of non-viral delivery, introduced a virus-inspired development strategy termed “chemical evolution” (CEvo) [137]. Viruses achieve highly efficient delivery through evolutionary processes in which continuous mutation and selection pressure give rise to ever more effective variants. Drawing on this principle, Wagner’s group employed solid-phase peptide synthesis (SPPS) to generate libraries of sequence-defined xenopeptides (XP). Within this framework, an artificial amino acid, succinoyl tetraethylene pentamine (Stp), was developed and incorporated together with natural amino acids to create a new class of delivery systems [92, 138].

To tune carrier properties such as stability and efficiency, a variety of different amino acid motifs were introduced. Cysteine residues enable intermolecular disulfide bridge formation, while tyrosine tripeptides induce π-π stacking, with both modifications leading to increased stability [139-141]. Histidine integration increases endosomal buffering thus enhancing endosomal escape and transfection efficiency [142]. These combinatorial libraries were then screened for delivery performance, and the most promising candidates served as the basis for subsequent iterations of synthesis, mirroring an evolutionary cycle that continuously refines carrier potency. Ultimately, repeated CEvo iterations yielded a highly efficient class of delivery agents known as lipo-amino fatty acid (LAF) xenopeptides (LAF-XPs) [91, 143].

In this carrier class, the polar Stp domain is linked to hydrophobic LAF moieties through lysine-branching, allowing the generation of diverse sequences, compositions, and topologies. The resulting carriers represent a sweet spot between classical lipoplexes and polyplexes [143, 144]. Although they share similarities with conventional cationic lipids, these carriers feature a considerably larger ionizable polycationic domain instead of a small cationic head group. With approximately eight to more than ten protonatable nitrogen atoms, these constructs are much smaller than typical cationic polymers yet still provide sufficient charge density and aqueous solubility to enable polyplex formation [143].

Another major distinction lies in the lipophilic LAF domain, which is pH-responsive. Upon acidification and protonation in the endosome, this domain switches from a hydrophobic, nonpolar state to a hydrophilic, polar state. In contrast, the hydrophobic domain of lipids of

lipoplexes typically consists of a fatty acid which cannot undergo such pH-dependent polarity switches.

Increasing the proportion of LAF units shifts the physicochemical behavior of these carriers toward that of ionizable lipids, permitting their use in LNP formulations. Whether formulated as polyplexes or LNPs, LAF-XP carriers have demonstrated outstanding transfection performance for mRNA, siRNA and pDNA [144-146].

1.10 TARGETING

Besides ensuring colloidal stability, the precise delivery of mRNA to the appropriate organ and cell type is critical for the success of mRNA therapeutics. Various strategies have been developed to direct nanoparticles to their intended target sites. In this context, PEG is not only used to ensure colloidal stability but also plays a central role in modulating their biodistribution. Generally, a distinction is made between passive and active targeting strategies. Passive targeting refers to the accumulation of nanoparticles in the desired target tissue not through specific cell interactions, but instead due to the result of their physicochemical properties.

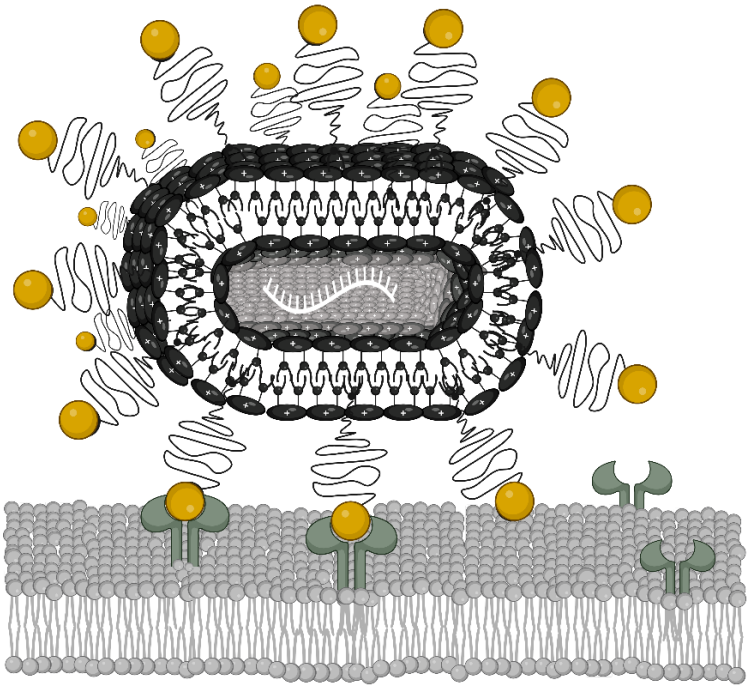

Figure 4. *Schematic illustration of active targeting, in which ligand-PEG-functionalized mRNA nanoparticles bind to specific cell-surface receptors. Created with BioRender.com*

These include size, shape, surface charge, and protein adsorption [38]. Different PEGylation strategies have been utilized to exploit these effects. A classic example is passive tumor targeting via the enhanced permeability and retention effect (EPR). Tumor endothelium differs markedly from normal healthy endothelium, as it is characterized by large interendothelial junctions. In addition, tumor tissue often exhibits inefficient or absent lymphatic drainage. Together, these features enable the accumulation of nanoparticles within the tumor tissue [147, 148]. PEGylation prolongs systemic circulation time, thereby increasing the probability of eventual accumulation in the tumor [145, 149]. For LNPs, this has been achieved by using long anchored DSPE-PEG. Another form of PEG-mediated passive targeting is exemplified by the siRNA therapeutic Onpattro [150]. Detachment of the short-anchored DMG-PEG permits apolipoprotein E (ApoE) adsorption, which mediates uptake into hepatocytes via the low-density lipoprotein (LDL) receptor [151]. This process is considered an intermediate between active and passive targeting.

Active targeting, in contrast, relies on specific interactions between the nanoparticles and the target cells (Figure 4). Here, PEG also plays an essential role. Terminal functionalization of PEG chains with targeting ligands such as antibodies, peptides, carbohydrates, or small molecules enables active and specific delivery. For lipid anchoring, the PEG-lipids of choice are the ones with long anchors, such as DSPE-PEG, as they are firmly anchored [152-158].

Ligand functionalization is not the only role of PEG. Its surface density must be sufficiently high to confer stealth characteristics, either to reduce unspecific uptake or to minimize protein adsorption that could otherwise mask surface-displayed ligands [159].

A combination of passive and active targeting is especially suitable for tumor targeting, as tumors often overexpress certain types of receptors. Passive accumulation is achieved via the EPR effect [145, 160]. Subsequently, target cells are addressed through specific ligand-receptor interactions. Prominent receptors include the epidermal growth factor receptor (EGFR), transferrin receptors, folate receptors, and integrin $\alpha v\beta 3$ [161-167].

1.11 AIM OF THE THESIS:

mRNA therapeutics face several fundamental challenges that limit their successful systemic application. These include insufficient colloidal stability, protein adsorption and a lack of specificity. As outlined, PEGlyation presents a powerful and versatile tool to address these limitations by providing steric stabilization, reducing serum protein adsorption, and enabling selective delivery.

LAF-XP carriers have previously been demonstrated to be highly potent in delivering mRNA [143]. However, they display limited colloidal stability, lack cell-specific targeting, and for some carriers, exhibit considerable cytotoxicity.

This thesis aimed to overcome these limitations by transferring PEGylation principles from liposomal and LNP systems to the LAF-XP platform, while preserving its simple formulation technique. In this context, PEG lipids DMG-PEG and DSPE-PEG-N_3 were to be incorporated and the impact of PEGylation on key physicochemical properties, such as particle size, surface charge and encapsulation efficiency to be systematically investigated. Particular emphasis had to be placed on evaluating and improving colloidal stability during formulation and under physiological conditions. In addition, differences in the protein corona composition of different LAF-XP carriers and the influence of PEGylation had to be analyzed. Beyond improving colloidal stability, selective tumor targeting was aimed at by combining high-density PEG shielding with receptor specific ligands.

2 MATERIALS

This chapter has been adapted from:

Folda, Paul, Eric Weidinger, Johanna Seidl, Mina Yazdi, Jana Pöhmerer, Melina Grau, David P. Minde, Mayar Ali, Ceren Kimna, and Ernst Wagner. "PEGylation Enhances Colloidal Stability and Promotes Ligand-Mediated Targeting of LAF–Xenopeptide mRNA Complexes." Polymers 17, no. 22 (2025): 2979. https://www.mdpi.com/2073-4360/17/22/2979.

Chemically modified CleanCap® FLuc mRNA (5moU), was acquired from Trilink Biotechnologies (San Diego, CA, USA). EZ Cap™ Cy5 Firefly luciferase mRNA (5-moUTP) was bought from Apexbio Technology LLC (Houston, USA). Plasmid pCMVLuc (encoding Photinus pyralis firefly luciferase regulated of a cytomegalovirus promoter and enhancer) was obtained from Plasmid Factory GmbH (Bielefeld, Germany). 1,2-dimyristoyl-rac-glycero-3-methoxypolyethylene glycol-2000 (DMG-PEG) and 1,2-distearoyl-sn-glycero-3-phosphoethanolamine-N-[carbonyl-azido(polyethylene glycol)-2000] (DSPE-PEG-N_3) were bought from Avanti Polar Lipids (Alabaster, AL, USA). Agarose BioReagent low EEO, boric acid, bromophenol blue, ethidium bromide (EtBr) (1% solution in H2O), glycerol, RNase-free water, tris(hydroxymethyl) aminomethane hydrochloride (Tris-HCl) and triton X-100 were procured from Sigma Aldrich (Munich, Germany), 4-(2-hydroxyethyl) 1-piperazineethanesulfonic acid (HEPES) from Biomol (Hamburg, Germany), GelRed (1000x) from VWR (Darmstadt, Germany) and D-(+)-glucose monohydrate, silver nitrate ($AgNO_3$), disodium carbonate (Na_2CO_3), sodium thiosulfate ($Na_2S_2O_3$) and ethylene diamine tetraacetic acid (EDTA) from Merck (Darmstadt, Germany). The Quant-iT™ RiboGreen RNA Assay-Kit was purchased from Thermo Fisher Scientific (Schwerte, Germany) and heparin (5000 I.U. mL-1) from B. Braun SE (Melsungen, Germany). All cell culture consumables were purchased from Faust Lab Science (Klettgau, Germany). N2a cells (murine neuroblastoma cell line Neuro2a) and HepG2 cells (human hepatocellular carcinoma) were from the American Type Culture Collection (ATCC, Manassas, VA, USA), human adherent hepatic carcinoma cell lines Huh7 wild-type from the Japanese Collection of Research Bioresources Cell Bank (Osaka, Japan). Human cervical

cancer cell line KB were purchased from the German Collection of Microorganisms and Cell Cultures (DSMZ; Braunschweig, Germany). Dulbecco's Modified Eagle's medium (DMEM) low glucose, DMEM Ham's F12 medium, fetal bovine serum (FBS), penicillin (100 U mL-1) and streptomycin (100 µg mL-1), trypsin/EDTA as well as paraformaldehyde (PFA), were bought from Sigma Aldrich (Munich, Germany) and PAN-Biotech (Aidenbach, Germany). Cell culture 5 x cell culture lysis buffer, and D-luciferin sodium salt were acquired from Promega (Mannheim, Germany. β-mercaptoethanol, 3-(4,5-dimethylthiazol-2-yl)-2,5-diphenyiltetrazolium bromide (MTT), 4′,6-diamidino-2-phenylindole (DAPI), dithiothreitol (DTT), adenosine 5′-triphosphate (ATP) disodium salt trihydrate, coenzyme A trilithium salt, glycylglycine, magnesium chloride ($MgCl_2$) and 2,5-DHB and 2-hydroxy-5-methoxybenzoic acid (super-DHB), from Sigma-Aldrich (Munich, Germany). Polypropylene syringe microreactors were obtained from Multisyntech (Witten, Germany). Trifluoroacetic acid (99%, extra pure) (TFA), sodium hydroxide (1M NaOH), dichloromethane, HPLC reagent grade (DCM), acetonitrile, HPLC reagent grade (ACN) and N,N-dimethylformamide, 99.8 %, extra dry over molecular sieve, croSeal (dry DMF), acetic acid (CH_3COOH) was purchased from Thermo Fisher Scientific GmbH (58239 Schwerte, Germany). Sodium dodecyl sulfat (SDS) was purchased from SERVA Electrophoressis GmbH (69115, Heidelberg, Germany). Formaldehyde (CH_2O) was bought from Grüssig GmbH (26849, Flisum, Germany). Fmoc-protected amino acids, 2-chlorotritylchloride polystyrene resin, dimethylformamide, N-methyl-2-pyrrolidone (NMP), DBCO-NHS, O-(benzotriazol-1-yl)-N, N, N′, N′-tetramethyluronium hexafluorophosphate (HBTU) and piperidine were acquired from Iris Biotech (Marktredwitz, Germany). Diisopropylethylamine (DIPEA), 1-hydroxybenzotriazole hydrate (HOBt), methanol (CH_3OH), bromophenol blue and triisopropylsilane (TIS) were purchased from Sigma-Aldrich (Munich, Germany). (Benzotriazol-1-yloxy)-tripyrrolidinophosphonium hexafluorophosphate (PyBOP) was procured from Millipore (Oakville, Canada). Trifluoroacetic acid was obtained from Acros Organics (Geel, Belgium). Linear polyethylenimine (LPEI) 22 kDa was synthesized according to previously published procedure [168].

3 METHODS

This chapter has been adapted from:

Folda, Paul, Eric Weidinger, Johanna Seidl, Mina Yazdi, Jana Pöhmerer, Melina Grau, David P. Minde, Mayar Ali, Ceren Kimna, and Ernst Wagner. "PEGylation Enhances Colloidal Stability and Promotes Ligand-Mediated Targeting of LAF–Xenopeptide mRNA Complexes." Polymers 17, no. 22 (2025): 2979. https://www.mdpi.com/2073-4360/17/22/2979.

3.1 SYNTHESIS OF LAF-XP CARRIERS

The ionizable LAF-Stp carriers were synthesized using solid-phase peptide synthesis (SPPS) according to the protocol reported by Thalmayr et al [143].

3.2 COPPER FREE CLICK REACTION FOR DSPE-PEG-GE11 CONJUGATE FORMATION

Equimolar amounts of DSPE-PEG-N_3 and DBCO-GE11/DBCO-GE11scr peptide were mixed and incubated in HBG overnight on a shaker at 25°C and 250 rpm.

3.3 UNMODIFIED AND PEGYLATED LAF-XP POLYPLEX FORMATION

The nucleic acid was first diluted in HBG (20 mm of HEPES, 5% (w/v) glucose, pH 7.4). Separately, the LAF-XP carrier at the specified N/P ratios, along with the selected PEG-lipid at defined molar ratios, was diluted in Milli-Q water. For calculating the N/P ratio, all secondary amines within the Stp (succinoyl tetraethylene pentamine) units, the amine groups, and the tertiary amines of the LAFs were taken into account. Equal volumes of nucleic acid solution and LAF carrier/PEG lipid solution were mixed by rapid pipetting and incubated for 40 min at RT in a closed Eppendorf reaction tube. The final concentration of nucleic acid in the LAF-XP polyplex solution was 12.5 µg/mL for mRNA, 10 µg/mL for pDNA, if not otherwise stated. Each carrier was formulated at its respective optimal nitrogen-to-phosphate ratios (N/P). For mRNA: bundles 1621 and 1752 at N/P 24, 1611 at N/P 18, and 1719 at N/P 12. For pDNA: 1719 and 1730 at N/P ratio 12, 1611 at N/P ratio of 18

3.4 ZETASIZER MEASUREMENTS

Measurements were carried out using a Zetasizer Nano ZS (Malvern Instruments, Malvern, Worcestershire, United Kingdom) using a folded capillary cell (DTS1070) by dynamic and electrophoretic laser light scattering (DLS, ELS). To assess particle size and polydispersity index (PDI), 40 µL of LAF - polyplex solutions were prepared as described above (sections 2.2.3), diluted with 40 µL HBG and analyzed under the following settings: 30 sec of equilibration time, temperature 25 °C, refractive index 1.330, viscosity 0.8872 mPa*s. Each sample was measured three times with six sub-runs per measurement. To determine the zeta potential, the polyplex solution was diluted with 720 µL of HBG and thoroughly mixed by pipetting prior to measurement. Measurement settings were identical to size determination, with the exception of an increase in equilibration time of 60 sec. Each sample was measured with 15 sub-runs (10 sec each) and zeta potential were calculated by Smoluchowski equation. All results (size, PDI and zeta potential) were reported as mean ± SD out of these measurements.

3.5 CELL CULTURE

The human adherent hepatic carcinoma cell lines Huh7 and HepG2 were cultured in Dulbecco's Modified Eagle Medium (DMEM) supplemented with F12 Ham. KB and N2a (murine adherent neuroblastoma cell line Neuro2a) was cultivated in DMEM low glucose (1 g/L glucose). All Cell culture media were supplemented with 100 U/mL penicillin, 10% fetal bovine serum (FBS), 4 mM of stable glutamine, and 100 µg/mL streptomycin.

3.6 TRANSFECTIONS

LAF - polyplexes were prepared as described above (section 2.2.3) for transfections. Cells were seeded 24 h prior to the transfection. For Huh7, 8 000 cells/well, for KB, 5 000 cells/well, for N2a and HepG2 cells, 10 000 cells/well, were seeded on a 96-well plate. The medium was replaced with fresh medium, before transfection. For mRNA, the volumes of 2.0 and 1.25 µL of LAF - polyplex solution (12.5 µg/mL mRNA-luc) were added to the corresponding wells in triplicate. In case of pDNA, 5.0 µL of LAF - polyplex solution (10 µg/mL) was added to each well. HBG/H2O (50/50) was used as negative control.

3.7 Luciferase Gene Expression Assay

Transfections of LAF-polyplexes were carried out as described (section 2.2.6) After 24 h incubation time, the medium was removed. 100 µL of 0.5x lysis buffer was added to each well and the cells were stored and frozen overnight at -80 °C. Prior to luciferase expression anlaysis, plates were brought to RT for 1 h under constant gentle shaking. For mRNA, the cell lysates were diluted 1:100 in PBS. 35 µL of cell lysate was dispensed into an opaque 96-well plate for measurement. Luciferase activity was recorded for 10 seconds in a Centro LB 960 plate reader luminometer (Berthold Technologies, Bad Wildbad, Germany) after addition of 100 µL LAR buffer (20 mM glycylglycine; 1 mM $MgCl_2$; 0.1 mM ethylenediaminetetraacetic acid; 3.3 mM dithiothreitol; 0.55 mM adenosine 5′-triphosphate; 0.27 mM coenzyme A, pH 8-8.5) supplemented with 5% (v/v) of a mixture of 10 mM luciferin and 29 mM glycylglycine. Transfection efficiency as relative light units (RLU) per well. For mRNA, a background (i.e., RLU values of HBG-treated cells) subtraction was performed.

3.8 Cellular Uptake Study - Flow Cytometry

At 24 h before the experiment, KB cells were seeded in 24-well plate at a density of 50 000 cells/well. Transfection was then carried out by applying a volume of 6 µL of LAF-polyplexes prepared at a mRNA concentration of 12 µg/mL (20% Cy5-labeled) as described (section 2.2.3). After 2 h of incubation, the medium was removed and cells were washed with 400 µL phosphate-buffered saline (PBS). Subsequently 400 µL of heparin was added (1000 IE/mL) and the plate was placed on ice for 10 min to remove polyplexes non-specifically bound to the cell surface. After incubation, heparin was removed and the cells were again washed with PBS. Then, cells were detached using 100 µL trypsin/EDTA and diluted in 200 µl FACS buffer (PBS supplemented with 10% FBS), supplemented with 0.1% (v/v) DAPI (1 mg/mL) to stain the nuclei of dead cells. Cellular uptake was quantified using a CytoFLEX S flow cytometer (Beckman Coulter, Brea, CA, USA) with Cy5 excitation at 635 nm and emission detection at 665 nm. Cells were gated based on their forward- and sideward-scatter profiles. At least 14 000 - 20 000 events were recorded and data was analyzed by FlowJo 7.6.5 flow cytometric analysis software (FlowJo, Ashland, OR, USA). The results are presented as mean fluorescence intensity (MFI; n=1) of all live cells.

3.9 Steric Stabilization of LAF-XP mRNA Polyplexes Against Salt-Induced Aggregation Through PEGylation

40 µL of LAF-XP polyplex solutions were formed as described above (section 2.2.3) and diluted with 70 µL PBS. Subsequently, size was measured as described above (section 2.2.4).

3.10 pH-Triggered Deshielding and Destabilization of LAF-XP mRNA Polyplexes

20 µL of LAF-XP polyplex solutions were formed as described above (section 2.2.3) at a concentration of 25 µg/mL. Subsequently, 180 µL of 0.01 mM HCl (pH 4) was added and the samples were incubated for 30 min at 37°C under constant shaking (300 rpm). For control groups, 180 µL HBG (pH 7.4) was added and the samples were incubated under identical conditions. Subsequently, samples were diluted with 700 µL PBS and the size was measured as described above (section 2.2.4).

3.11 Steric Stabilization of LAF-XP mRNA Polyplexes Against Protein Induced Aggregation Through PEGylation

Equal volumes of nucleic acid solution and LAF-XP carrier/PEG lipid solution were mixed by rapid pipetting and incubated for 40 min at RT in a closed Eppendorf reaction tube to give 25 µL of LAF-XP polyplex solution with a concentration of 25 µg/mL mRNA. Subsequently, 15 µL of human transferrin solution was added, resulting in a final mRNA concentration of 12.5 µg/mL, with the indicated molar ratios of human transferrin to carrier. After an incubation of 10 min size, PDI and zeta potential was measured as described above (section 2.2.4)

3.12 Serum Assay – Preparation of Serum Incubated LAF-XP mRNA Polyplexes

LAF-XP polyplexes were formed as described above (section 2.2.3), using a concentration of 10µg mRNA/150 µL. The polyplexes were incubated in 90% fetal bovine serum (FBS) for 2h at 37°C under continuous shaking at 300 rpm.

3.13 DLS Measurements of Serum Incubated LAF-XP mRNA Polyplexes

For DLS measurements, 40 µL of the FBS-incubated samples was mixes with 40 µL of HBG, yielding a final volume of 80 µL. The solution was transferred to a folded capillary cell. Size was analyzed with the settings describe above (section 2.2.3).

3.14 Nanoparticle Tracking Analysis of Serum Incubated LAF-Xp mRNA Polyplexes

Particle concentration was determined at 25°C using a NanoSight NS300 (Malvern Instruments, Malvern, UK) equipped with a blue 488 nm laser and sCMOS camera. The FBS-incubated samples (serum dilution 1:10) were diluted 1:200 with HEPES buffer (7.4), resulting in a total dilution of 1:2000. The diluted samples were injected via the integrated syringe pump at a speed of 20AU following the manufacturer's instructions. Five runs per sample were conducted. Videos were recorded at a frame rate of 25 fps, with a total of 1498 frames analyzed per measurement. The detection threshold was set to 10. Maximum jump mode, blur and minimum track length were operated in automatic mode.

3.15 Transfection Efficiency Assessment of Serum Incubated LAF-XP mRNA Polyplexes

2.25 µL of the serum-incubated LAF-polyplexes were added to the corresponding wells in triplicate. As a control, a portion of the original LAF-polyplexes was diluted in HBG instead of serum prior to transfection and also added at a volume of 2.25 µL per well in triplicate.

3.16 Isolation and Purification of Protein Corona Coated LAF-XP mRNA Polyplexes

LAF-XP mRNA polyplexes were formed as described above (section 2.2.3), using a concentration of 1µg mRNA/50 µL. The polyplexes were then mixed with mouse serum at a 1:1 volume ratio and incubated for 15 minutes at 37 °C at 300 rpm. A 0.7 M sucrose solution was prepared by dissolving solid sucrose in Milli-Q H_2O. The serum incubated polyplexes (100 µL) were carefully pipetted onto a 300 µL cushion of 0.7 M sucrose and centrifuged at

15.300 g for 1 hour at 4 °C. Following centrifugation, the supernatant was discarded. The resulting pellet was washed with 400 µL sterile PBS. The pellet was centrifuged again at 15.300 g for 5 minutes at 4 °C and the supernatant was removed. This washing step was repeated two additional times, for a total of three washes. All pipetting steps were performed using sterile filter tips. Subsequent, samples were stored at -20 °C until further analysis (MS analysis and SDS-PAGE).

3.17 Protein Corona Determination via Mass Spectrometry (MS) Analysis of Serum Coated mRNA LAF-XP Polyplexes

Prior to mass spectrometry analysis, samples were prepared as follows: Evotip PURE tips were rinsed with Buffer B (comprising 80% ACN, water and 0.1% formic acid) and spun down at 800g for 60 s. The tips were then equilibrated in 20 µl of Buffer A (0.1% formic acid) and impulse spun at 800g for storage until the acidified samples were ready to load. Samples were acidified in 0.4% TFA, and the Evotip PURE was emptied by centrifuging at 800g for 1 min. The acidified samples were loaded onto the PURE Evotips and spun at 800g for 1 min. The samples were washed twice with 20 µl of Buffer A and spun down at 800g for 1 min. Elutions were collected in PCR strips by eluting with 20 µl of 45% Buffer B (containing 45% ACN, water and 0.1% TFA) at 450g. After drying in a SpeedVac and resuspended in 0.1% TFA supplemented with 0.015% DDM, samples were analyzed using liquid chromatography with tandem mass spectrometry (LC−MS/MS; EASY nanoLC 1200, Thermo Fisher Scientific) coupled with a trapped ion mobility spectrometry quadrupole time-of-flight single-cell proteomics mass spectrometer (timsTOF SCP; Bruker Daltonik) via a CaptiveSpray nano-electrospray ion source. 50 ng of sample per injection was loaded on a 5.5-cm High Throughput µPAC Neo HPLC Column (Thermo Fisher Scientific) and analyzed using an 80-min active gradient method at a flow rate of 250 nl min−1. Data were analyzed using scanpy (v. 1.10.2) and anndata (v. 0.10.8) in Python 3.11. Thirty independent samples were analyzed from each group (N=2). All proteins expressed in less than half of the samples in each group were filtered out, resulting in 684 proteins used for downstream analyses. The data was log-transformed and normalized per sample. The missing values were input using KNNImputer (n_neighbors=5) from sklearn package (v. 1.5.1). With scanpy's dendrogram function scipy's hierarchical linkage clustering was calculated on a Pearson correlation

matrix over groups which was calculated for 50 averaged principal components. Differential expression analysis was conducted using Scanpy's method `rank_genes_groups` with method set to `t-test`. A threshold of $p < 0.05$ and $|\log \text{fold change}| > 1.0$ were applied to identify differentially expressed proteins (DEPs). These DEPs were subsequently visualized using volcano plots.

3.18 SDS-PAGE AND SILVER STAINING OF PROTEIN CORONA COATED mRNA LAF-XP POLYPLEXES

Samples were thawed on ice and 20 µl of Milli Q H_2O and 10 µL reducing loading buffer (30% glycerol (v/v); 0.7 mM Tris pH 6.8; 10% SDS (w/v); 0.12 mg/ml bromophenol blue; 0.93 mg/mL DTT, 0.01% β-mercaptoethanol (v/v)) was added. Subsequently, the samples were shaken (300 rpm) at 95°C for 5 min and applied on to a 3.5 - 10% gradient SDS gel according to the Laemmli method and separated at 30 mA for 120 min in a Mini-PROTEAN II electrophoresis cell (Bio-Rad, Hercules, CA, USA).

After electrophoresis, the gel was placed in a clean tray and washed three times for 5 min each with 50 – 100 mL pure H_2O. The Imperial Protein Stain was gently mixed before use by inverting the bottle several times. Gels were stained for 2 h at room temperature, followed by destaining in ultrapure H_2O for three days with several water changes until background staining was minimized. Quantification was performed using ImageJ. Percentage change (% change) was calculated by using the formula $\% \, change = 100 \text{ x} \left(1 - \frac{Intensity\ 1752}{Intensity\ 1611}\right)$ and $\% \, change = 100 \text{ x } \left(1 - \frac{Intensity\ PEGylated}{Intensity\ unmodified}\right)$. Three protein bands were quantified at approximately 70, 15 and 8 kDa.

3.19 STATISTICAL ANALYSIS:

Results are presented as mean values (arithmetic mean) of triplicates. Error bars display the standard deviation (SD). Statistical analysis of the results (mean ± SD) was evaluated by unpaired t-test with Welch's correction; ns, not significant; *$p \leq 0.05$, **$p \leq 0.01$, **$p \leq 0.001$, ****$p \leq 0.0001$

3.20 SYNTHESIS OF GE11 AND SCRGE11:

The peptides GE11 (YHWYGYTPQNVI) and scrambled GE11 (scrGE11; YWGPNIHYYTQV) were synthesized using standard Fmoc-based solid-phase peptide synthesis (SPPS) on either isoleucine- or valine-preloaded 2-chlorotityl resin. Synthesis was conducted out on an automated Syro Wave peptide synthesizer (Biotage, Uppsala, Sweden) using Fmoc-protected amino acids and HBTU (2-(1H-benzotriazol-1-yl)-1,1,3,3-tetramethyluronium-hexafluorophosphat), HOBt (1-hydroxybenzotriazol), and DIPEA (diisopropylethylamine) as standard coupling reagents. Following synthesis, peptides were cleaved from the resin with a mixture of trifluoroacetic acid (TFA), water, and triisopropylsilane (TIS) in a ratio of 95:2.5:2.5 (v/v/v) for 1 hour at room temperature. The cleavage solution was precipitated by dropwise addition into pre-cooled n-hexane/methyl tert-butyl ether (MTBE) (3:1, v/v), followed by centrifugation at 4000 rpm at 4 °C for 15 minutes. The supernatant was discarded, and the resulting pellets was dried under nitrogen stream. For DBCO-functionalization, the crude peptides (15 mg, 0.0096 mmol) were dissolved in 20 mM HEPES buffer and adjusted to pH 8.0-8.5 using 1 M NaOH. DBCO-NHS ester (1.2 eq., 0.0117 mmol, 5.03 mg) was dissolved in anhydrous, degassed DMF and kept on ice for 10 minutes prior to reaction. The DBCO-NHS solutions was combined with the peptide solutions, and the reaction mixture was vortexed briefly. The conjugation reaction was carried out at room temperature for 16 hours. Purification of the peptides was achieved via preparative high-performance liquid chromatography (HPLC) using a LaPrep system (VWR International GmbH, Darmstadt, Germany) and a SymmetryPrep C18 column (7 μm, 19 x 150 mm). The purified ligands were subsequently lyophilized. The molecular structures were confirmed by matrix-assisted laser desorption/ionization time-of-flight mass spectrometry (MALDI-TOF MS) and analytical reversed-phase HPLC (RP-HPLC)

3.21 LYOPHILIZATION

The synthesized product was lyophilized using a freeze-dryer ALPHA 3-4 LSCbasic (Martin Christ Gefriertrocknungsanlagen GmbH, Osterode am Harz, Germany) with the condenser temperature at -105 °C and a pressure of 0.050 mbar.

3.22 MALDI-TOF MASS SPECTROMETRY (MS)

MALDI-TOF mass spectrometry was performed using an Autoflex II mass spectrometer (Bruker Daltonics, Germany). A solution of 10 mg mL-1 super-DHB (9/1 (w/w) mixture of 2,5-dihydroxybenzoic acid and 2-hydroxy-5-methoxybenzoic acid) in 69.93/30/0.07 (v/v/v) H_2O/ACN/TFA was used as matrix. 1 µL of matrix solution was added onto a MTP AnchorChip (Bruker Daltonics, Germany). Then, 1 µL of sample dissolved in H_2O/EtOH at a concentration of 1 mg mL-1, was added onto the matrix, co-crystallized and examined. Spectra were recorded in positive ionization mode.

3.23 ANALYTICAL REVERSED-PHASE HPLC

Reversed-phase high-performance liquid chromatography (RP-HPLC) was performed using a VWR-Hitachi Chromaster 5160 pump system, a VWR-Hitachi Chromaster 5260 autosampler, and a diode array detector (DAD) (VWR-Hitachi Chromaster 5430; VWR, Darmstadt, Germany) with detection at 214, 260, 280 and 308 nm. Separation was performed on a Hydrosphere C18 column (5 µm, 150 x 4.6 mm I.D.; YMC Europe GmbH, Dinslaken, Germany). The mobile phase consisted of ACN/H_2O containing 0.1% TFA, with a linear gradient from 95:5 (v/v) to 0:100 (v/v) over 25 minutes.

3.24 PREPARATIVE HPLC

Preparative high-performance liquid chromatography (prep-HPLC) was carried out using a Büchi Pure C-830 Prep system (BÜCHI Labortechnik GmbH, Essen, Germany) equipped with a SymmetryPrep™ C18 column (7 µm, 19 x 150 mm; Waters, Milford, Massachusetts, USA). Purification was performed with solvent A (100% ACN with 0.1% TFA) and solvent B (100% H2O with 0.1% TFA), applying a gradient from 95% B to 0% B over 30 minutes at a flow rate of 20 mL/min. Eluents were monitored using a UV/vis detector at 254, 265, 290 and 308 nm.

3.25 ETHIDIUM BROMIDE (ETBR) EXCLUSION ASSAY

Quantification of EtBr fluorescence was performed using a microplate reader (Spectrafluor Plus, Tecan, Switzerland) with an excitation wavelength of λex = 535 nm and an emission wavelength of λem = 590 nm. LAF-polyplexes were prepared as described above (sections

2.2.8) with a total volume of 50 µL at a final pDNA concentration of 10 µg/mL. After an incubation time of 40 min, LAF-polyplexes were diluted with 250 µL of aqueous EtBr solution (c = 0.5 µg/mL). After further incubation for 10 min at RT, 260 µL of each sample was pipetted into a TPP-ft 96-well-plate and fluorescence intensity was measured. For quantification, a standard calibration curve with free pDNA (linear concentration range from 0 to 10 µg/mL) diluted in HBG was used. The amount of free, i.e., non-compacted pDNA was determined based on the calibration of free pDNA and displayed as percentage of EtBr fluorescence in relation to 100% of free pDNA.

3.26 Agarose Gel Shift Assay

1% (w/v) agarose gel was prepared by microwave-assisted heating of agarose in TBE buffer (18.0 g of tris(hydroxymethyl)aminomethane, 5.5 g of boric acid, 2 mM EDTA at pH 8 in 1 L of H_2O). 1x GelRed was added to the solution (i.e., 1:1000-dilution of 1000x GelRed stock solution), after the solution cooled down to about 50 °C. The solution was then poured into an electrophoresis chamber and allowed to cool down further to allow gelation. LAF-polyplexes were formulated as described above (sections 2.2.8) with a total volume of 15 µL at a mRNA concentration of 12.5 µg/mL. Following a 40 min incubation, 3 µL of loading dye (6x; prepared from 6 mL of glycerol, 1.2 mL of 0.5 M EDTA, 2.8 mL of H_2O, 0.02 g of bromophenol blue) was added to the LAF-polyplex solution. Subsequently, 15 µL of each sample was loaded to the gel and electrophoresis was conducted at 120 mV for 70 min in 1x TBE buffer. As a control, free mRNA diluted in HBG/H_2O 50/50 to a concentration of 12.5 mg/mL was used.

3.27 Cell Viability Assay by MTT

Transfections of LAF - polyplexes were performed as described (section 2.2.8). At 24 h post transfection, 10 µL of MTT solution (3-(4,5-dimethylthiazol-2-yl)-2,5-diphenyltetrazolium bromide; 5 mg/mL) was added to each well. Plates were then incubated for further 2 h at 37°C. Subsequently, the supernatant was carefully removed. The plates were stored overnight at -80°C. The resulting purple formazan was then solubilized in 100 µL of DMSO and incubated for 30 min at 37°C with gentle, continuous shaking. Spectophotometric analysis was performed with a Tecan microplate reader

(Spectrafluor Plus, Tecan, Männedorf, Switzerland). Absorbance was measured at wavelength λ = 590 nm with a background correction at λ = 630 nm. Relative metabolic activity was related to control well treated with HBG/H_2O (50/50) and calculated by dividing [A]sample/[A]control.

3.28 RIBO GREEN ASSAY

Encapsulation efficiency [ee(%)] of mRNA LAF - polyplexes was evaluating using the Quant-iT™ RiboGreen RNA Assay-Kit (Thermo Fisher Scientific). LAF - polyplex solutions were formed as described above (sections 2.2.8) and subsequently diluted with 1 x TE (10 mM Tris-HCl, 1 mM EDTA, pH 7.5 in RNase-free water) to a concentration of 2 µg/mL. 50 µL aliquotes were either mixed with 50 µL of 1x TE as untreated controls or added to 50 µL of 1x TE containing 2% (v/v) TritonX-100 and 250 I.U. mL-1 heparin to fully dissociated complexes. All samples were incubated at 37 °C for 10 min, while constantly shaking at 150 rpm. Following 5 min cooling period at RT, 100 µL of RiboGreen reagent diluted 200-fold in 1x TE were added to every sample. Then after 5 min, the fluorescence intensity was measured in duplicates using a Tecan microplate reader (Spectrafluor Plus, Tecan, Männderdorf, Switzerland) at excitation/emission wavelength of 485/535 nm. Background signals were measured with pure HBG in 1x TE, or in 1x TE supplemented with TritonX- 100 and heparin, which were treated identically to the respective LAF - polyplex samples. Encapsulation efficiency [ee(%)] was calculated using the following formula after background subtraction of each sample:

$$ee\ (\%) = 100\% - \frac{\text{mean emission untreated control}}{\text{mean emission treated sample}}\ x\ 100\%$$

3.29 PH DEPENDENT CHANGES IN ZETA POTENTIAL OF UNMODIFIED AND SHIELDED LAF-XP MRNA POLYPLEXES

LAF-XP mRNA polyplexes were formulated as described in section 2.2.3, using a concentration of 25 µg/mL at a total volume of 80 µL. The polyplex solution was evenly split into two portions. One portion was diluted with 760 µL of HEPES buffer at pH 7.4 and the other with 760 µL of Hepes buffer at pH 5.4, resulting in a final volume of 800 µL

for each sample. After 10 minutes of incubation, size and zeta potential were measured by DLS.

3.30 In Vivo Performance of mRNA LAF-XP-Polyplexes in Tumor-Bearing Mice:

In vivo experiments were performed according to the guidelines of the German Animal Welfare Act and were approved by the animal experiments ethical committee of the Government of Upper Bavaria (accreditation number Gz. ROB-55.2-2532.Vet_02-19-20). N2a cells (10^6 cells/150 μL PBS) were subcutaneously inoculated into the left flank of 6-week-old female A/Jmice (Envigo RMS GmbH, Düsseldorf, Germany) and NMRI mice (Janvier, Le Genest-Saint-Isle, France). Mice were randomly divided into groups of five and were housed in isolated ventilated cages under specific pathogen-free conditions with a 12 h day/night cycle, and food and water provided ad libitum. Body weight and general well-being were monitored regularly. Tumor size was measured with a caliper and determined by the formula: [0.5 xx (longest diameter) x (shortest diameter)^2]. When tumors reached a size of 250-500 mm^3, the experiments were performed by intravenous tail vein injection of polyplexes formed at indicated N/P ratio, containing 2.5 or 5 μg of mRNA-luc in 150 μL HBG/H_2O (50:50 v/v). An HBG with double the amount of glucose was used to reach isosmotic conditions. Mice were euthanized 24 h after injection. The organs (tumor, lungs, liver, kidneys, spleen, brain, heart, muscle, i.e., hamstring muscles and calves) were carefully dissected and washed with PBS, followed by analysis via *ex vivo* luciferase gene expression assay. The luciferase expression was determined as described below and presented as relative light units per gram organ after background subtraction (lysis buffer).

3.31 Ex Vivo Luciferase Expression Assay of Organs and Tumors:

Tumor tissues and organs were homogenized in Luciferase Cell Culture Lysis Reagent 1x, supplemented with 1% (v/v) protease and phosphatase inhibitor cocktail with mechanical a tissue and cell homogenizer (FastPrep-24, MP Biomedicals, USA). Subsequently, the samples were stored frozen overnight at −80 °C to ensure full lysis and complete cell disruption. Before measurement, the samples were thawed and centrifuged for 10 min at maximum speed (≈13 000 rpm) and 4 °C. Luciferase activity in 25 μL of the supernatant

was determined in a Centro LB 960 plate reader luminometer (Berthold Technologies, Bad Wildbad, Germany) for 10 s after addition of 100 µL/well of a LAR assay buffer solution (composition see above) supplemented with 5% (v/v) of a mixture of 10 mm luciferin and 29 mm glycyl- glycine.

4 RESULTS AND DISCUSSION:

This chapter has been adapted from:

Folda, Paul, Eric Weidinger, Johanna Seidl, Mina Yazdi, Jana Pöhmerer, Melina Grau, David P. Minde, Mayar Ali, Ceren Kimna, and Ernst Wagner. "PEGylation Enhances Colloidal Stability and Promotes Ligand-Mediated Targeting of LAF–Xenopeptide mRNA Complexes." Polymers 17, no. 22 (2025): 2979. https://www.mdpi.com/2073-4360/17/22/2979.

DLS measurements and luciferase gene expression (HepG2 and HUH7 cells) of GE1-functionalized LAF-XP mRNA polyplexes were performed by Eric Weidinger, Pharmaceutical Biotechnology, Department of Pharmacy, Ludwig-Maximilians-Universität (LMU), 81377 Munich, Germany. Center for NanoScience (CeNS), LMU Munich, 80799 Munich, Germany

GE11 and GE11scr ligands were synthesized and characterized by Johanna Seidl, Pharmaceutical Biotechnology, Department of Pharmacy, Ludwig-Maximilians-Universität (LMU), 81377 Munich, Germany.

Animal experiments (i.v. application and organ harvesting) were performed by veterinarians Dr. Mina Yazid and Dr. Jana Pöhmerer. Pharmaceutical Biotechnology, Department of Pharmacy, Ludwig-Maximilians-Universität (LMU) Munich, 81377, Germany.

Measurement, analysis, and statistical evaluation of the protein corona composition of LAF-XP mRNA polyplexes was performed by Dr. Ceren Kimna, Dr. David-Paul Minde and Dr. Mayar Ali. Institute for Intelligent Biotechnologies (iBIO), Helmholtz Center Munich, 85764 Neuherberg, Germany.

LAF-XP carriers were synthesized by Melina Grau, Pharmaceutical Biotechnology, Department of Pharmacy, Ludwig-Maximilians-Universität (LMU), 81377 Munich, Germany

For mRNA delivery, the current best performing carriers, two U1 U-shape (1611 and 1719) and two B2 bundle LAF-XPs (1621 and 1752) were applied. (Scheme 1b, Scheme 1c).

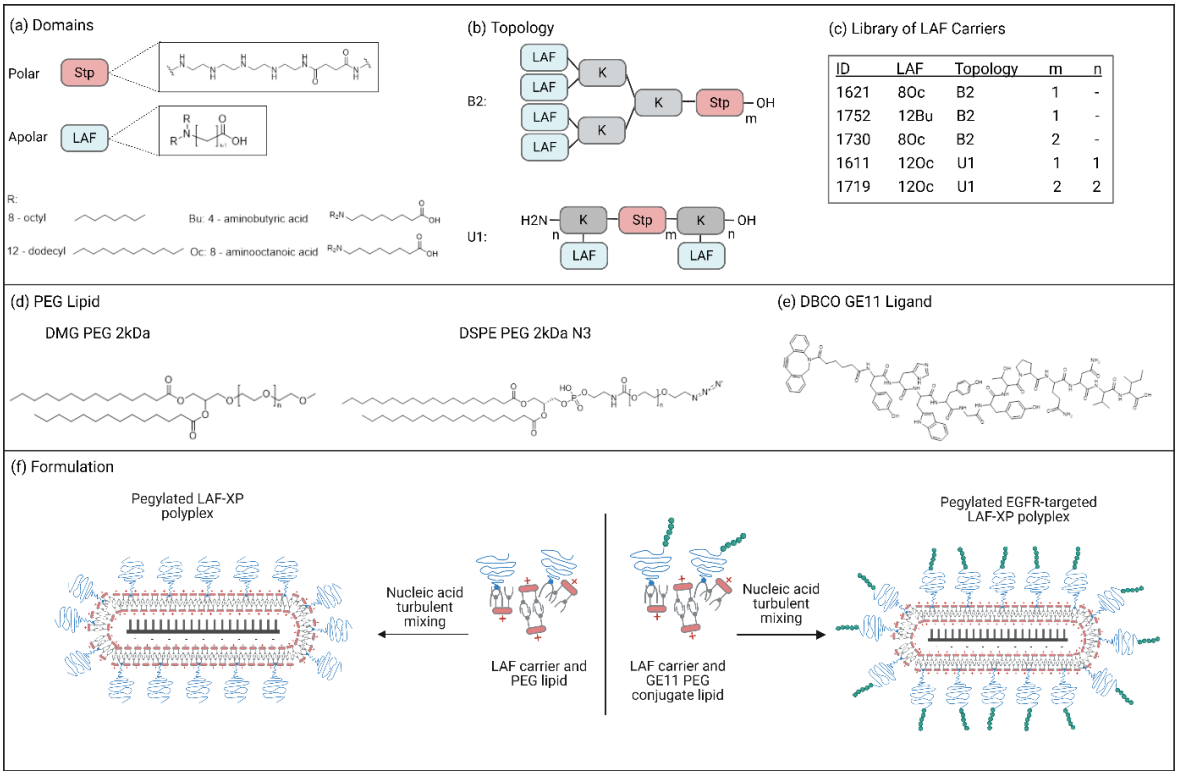

Scheme 1. *LAF-XP carriers.* ***(a)*** *Polar succinoyl tetraethylene pentamine (Stp) domain and apolar lipoamino fatty acid (LAF) domains as structural elements of the carriers. The position of the tertiary amine within the LAF domain can be adjusted by varying the carbon chain length of the ω-amino fatty acids (Bu, Oc) and the length of the N,N-dialkyl substituents (N,N-dioctyl or N,N-didodecyl groups).* ***(b)*** *The LAF and Stp domain can be assembled into distinct topologies (B2 and U1) through lysine (K) branching.* ***(c)*** *Library of investigated LAF-XP carriers.* ***(d)*** *Structures of the two different PEG lipids: polydisperse 1,2-dimyristoyl-rac-glycero-3-methoxypolyethylene glycol-2k (DMG-PEG) and polydisperse 1,2-distearoyl-sn-glycero-3-phosphoethanolamine-N [azido (polyethylene glycol)-2k] (DSPE-PEG-N_3) (Average MW 2kDa, n~45).* ***(e)*** *Structure of the DBCO functionalized GE11 peptide. DBCO-modified GE11 is coupled to DSPE-PEG-N_3 via strain-promoted azide-alkyne cycloaddition (SPAAC) to form a DSPE-PEG-GE11 conjugate.* ***(f)*** *Formulation of standard PEGylated (left) or EGFR-targeted LAF-XP polyplexes, (right) by adding (rapid pipetting) nucleic acid to LAF carrier/ lipid-PEG-GE11 conjugate solution at equal volumes. LAF-XP carriers were synthesized by Melina Grau, Pharmaceutical Biotechnology, Department of Pharmacy, Ludwig-Maximilians-Universitätm (LMU), 81377 Munich, Germany.*

4.1 Formulation, Physicochemical and In Vitro Assessment of PEGylated LAF-XP mRNA Polyplexes

LAF-XP polyplexes are assembled in a 50:50 (V/V) solvent of HBG (HEPES-buffered glucose) and water [169]. To utilize the solvent advantages of LAF-XP polyplexes, DMG-PEG and DSPE-PEG-N_3 stock solutions were also prepared in water. This enables their use in the classic LAF-XP polyplex preparation protocol. A new, slightly modified preparation method was established. Nucleic acid is diluted in HBG. The PEG lipid was co-diluted with the LAF-XP carrier in water at indicated molar ratios of total lipid. Equal volumes of nucleic acid solution and the LAF-XP / PEG lipid solution are mixed by rapid pipetting and incubated for 40 min at RT in a closed Eppendorf reaction tube (Scheme 1f).

To assess the impact of the PEGylation, an in depth physicochemical characterization, which includes dynamic light scattering (DLS), Ribogreen assay and an agarose gel shift, was conducted. Subsequently, the PEGylated LAF-XP polyplexes were tested regarding their transfection efficiency and metabolic activity in N2A and KB cell lines. Each carrier was formulated at its respective optimal nitrogen-to-phosphate ratios (N/P) [143, 169].

For B2 LAF-XP mRNA polyplexes, PEGylation had a particularly favorable effect on the Z-average. Both PEG lipids lead to the formation of smaller particles, whereas for U-shapes, only DMG-PEG had a size reducing effect. In terms of PDI no notable changes could be seen (Figure 1a). Regarding the zeta potential, PEGylation led to a reduction for all carriers and no considerable differences were observed between DMG-PEG and DSPE-PEG-N_3 in this regard (Figure 1b).

(a)

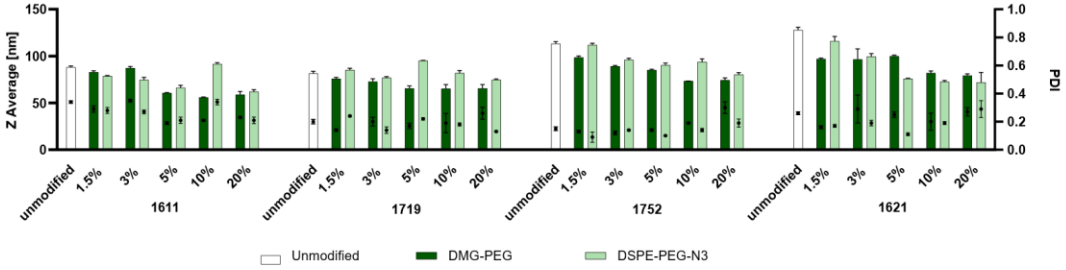
Z Average [nm]
PDI
unmodified
1.5%
3%
5%
10%
20%
1611
1719
1752
1621
Unmodified
DMG-PEG
DSPE-PEG-N3

(b)

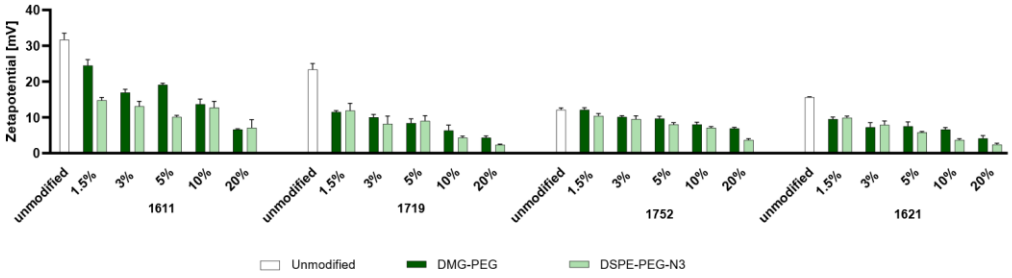
Zetapotential [mV]
unmodified
1.5%
3%
5%
10%
20%
1611
1719
1752
1621
Unmodified
DMG-PEG
DSPE-PEG-N3

(c)

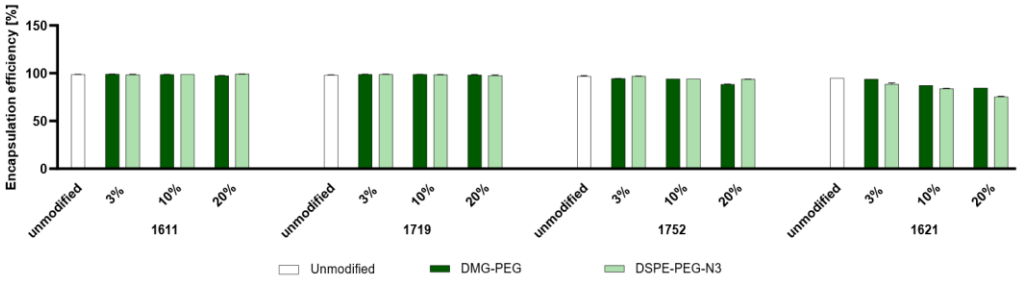
Encapsulation efficiency [%]
unmodified
3%
10%
20%
1611
1719
1752
1621
Unmodified
DMG-PEG
DSPE-PEG-N3

(d)

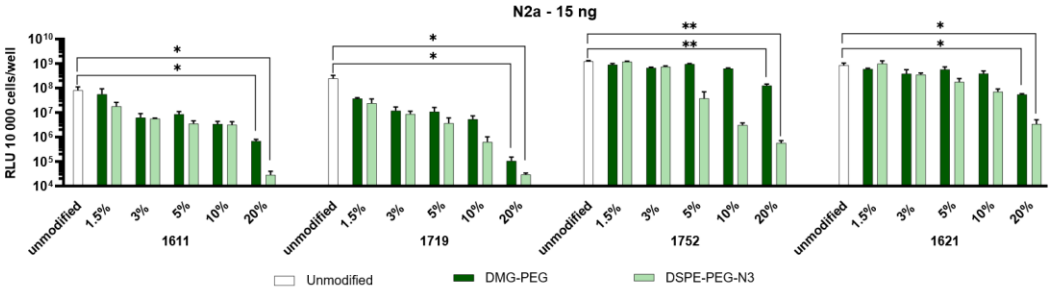
N2a - 15 ng
RLU 10 000 cells/well
unmodified
1.5%
3%
5%
10%
20%
1611
1719
1752
1621
Unmodified
DMG-PEG
DSPE-PEG-N3

Figure 1. *Variation in molar % of PEGylation of LAF-XP mRNA polyplexes with DMG-PEG and DSPE-PEG-N_3.* ***(a)*** *Hydrodynamic sizes and polydispersity index (PDI) values unmodified and pegylated (at different molar ratios) LAF-polyplexes, measured by dynamic light scattering (DLS) and* ***(b)*** *Zeta potential analysis determined using electrophoretic light scattering (ELS).* ***(c)*** *mRNA encapsulation efficiency at different molar ratios of DMG-PEG and DSPE, determined by the RiboGreen assay.* ***(d)*** *Gene transfer activity of unmodified PEGylated LAF-polyplexes in N2a cells 24 h after transfection. Comparison of unmodified and PEGylated LAF-XP polyplexes at a dose of 15 ng mRNA-LUC/well. Transfection efficacy was determined by luciferase gene expression assay (n = 3, mean + SD). The statistical significance was determined by unpaired t-test with Welch's correction; ns, not significant; *p ≤ 0.05, **p ≤ 0.01, ***p ≤ 0.001, ****p ≤0.0001.*

Previous studies have shown that PEGylation can interfere with nucleic acid compaction [170, 171]. Therefore, a RiboGreen assay and a gel shift was conducted. The results indicated that PEGylation did not compromise encapsulation efficiency for the U-shapes 1611 and 1719. However, when incorporated into B2 bundles 1752 and 1621, a reduction in encapsulation especially at higher molar ratios could be seen (Figure 1c). These results were confirmed in an agarose gel shift assay. For bundles, PEGylation induced smearing particularly at higher molar ratios. For U-shapes, again no notable impact on compaction efficiency could be observed (Figure 2).

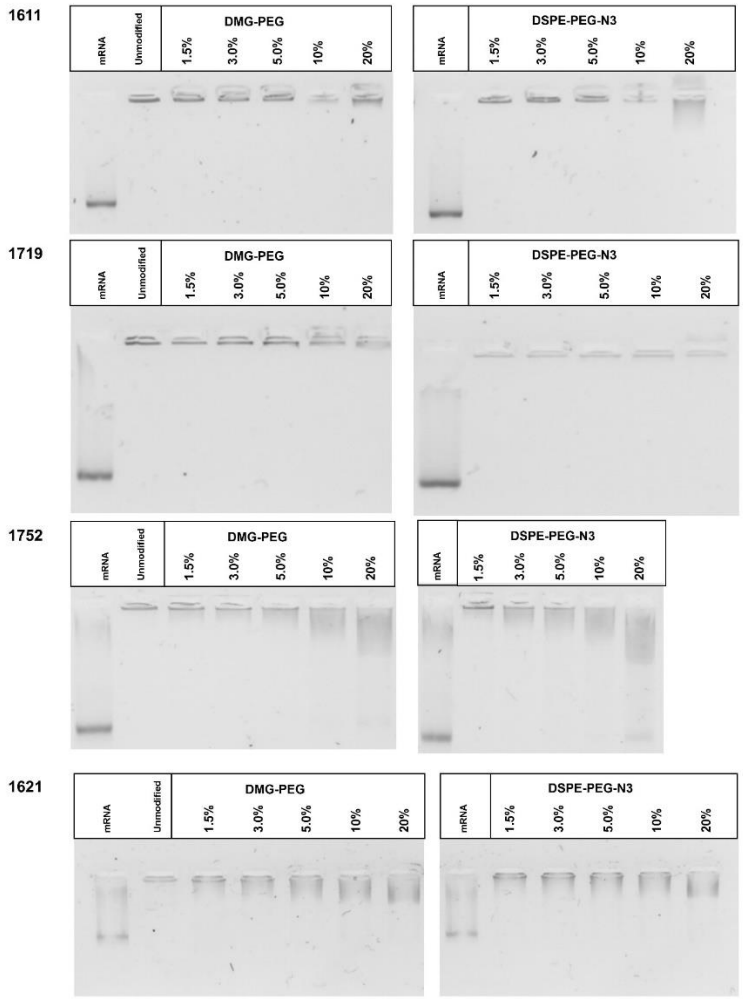

Figure 2. *Agarose gel shift. Variation in PEGylation (molar %) of LAF-XP mRNA polyplexes with DMG-PEG and DSPE-PEG-N_3. Comparison of unmodified with PEGylated polyplexes.*

An increase in PEGylation universally resulted in a decline in transfection efficiency, (Figure 2d, Figure 3a). These findings are consistent with the results obtained from DLS measurements, where the zeta potential was decreased by PEG. Previous work has shown, that due to a reduced zeta potential, interactions with cellular and endosomal membranes are inhibited. Both cellular uptake and endosomal escape is hindered, which ultimately leads to a reduced transfection efficiency [71, 73, 172-174]. This may also explain why the transfection efficiency of U-shapes was more strongly affected by PEGylation compared to

bundles. The decrease in zeta potential was substantially more prominent in U-shapes. In addition, other factors may contribute to the observed differences in behavior. For bundles, PEGylation reduced mRNA compaction, which can often lead to reduced transfection efficiency. However, excessive mRNA compaction can also hinder its release. In case of the bundles PEGylation may simultaneously lower cellular uptake and endosomal escape, while facilitating mRNA release in the cytoplasm. These opposing effects could partially counterbalance each other.

For all carriers, DSPE-PEG-N_3 led to a stronger reduction in transfection efficiency than DMG-PEG (Figure 1d, Figure 3a).

DSPE-PEG-N_3, featuring a longer lipid anchor (two C18 hydrocarbon chains), likely forms stronger lipophilic interactions with the LAF domain of the carriers. This results in more stable anchoring and long lasting PEG shielding. In contrast, weaker anchoring of DMG-PEG, due to its shorter lipid anchor (two times C14 hydrocarbon chains), allows dissociation from LAF-XP mRNA polyplexes promoting cell interactions. This likely accounts for the higher transfection efficiency.

This makes DSPE-PEG-N_3 suitable for incorporating targeting ligands. Its azido group enables functionalization with targeting moieties via copper-free azido / DBCO click chemistry.

Furthermore, an MTT assay revealed no substantial effect of PEGylation on metabolic activity (Figure 3b, Figure 3c).

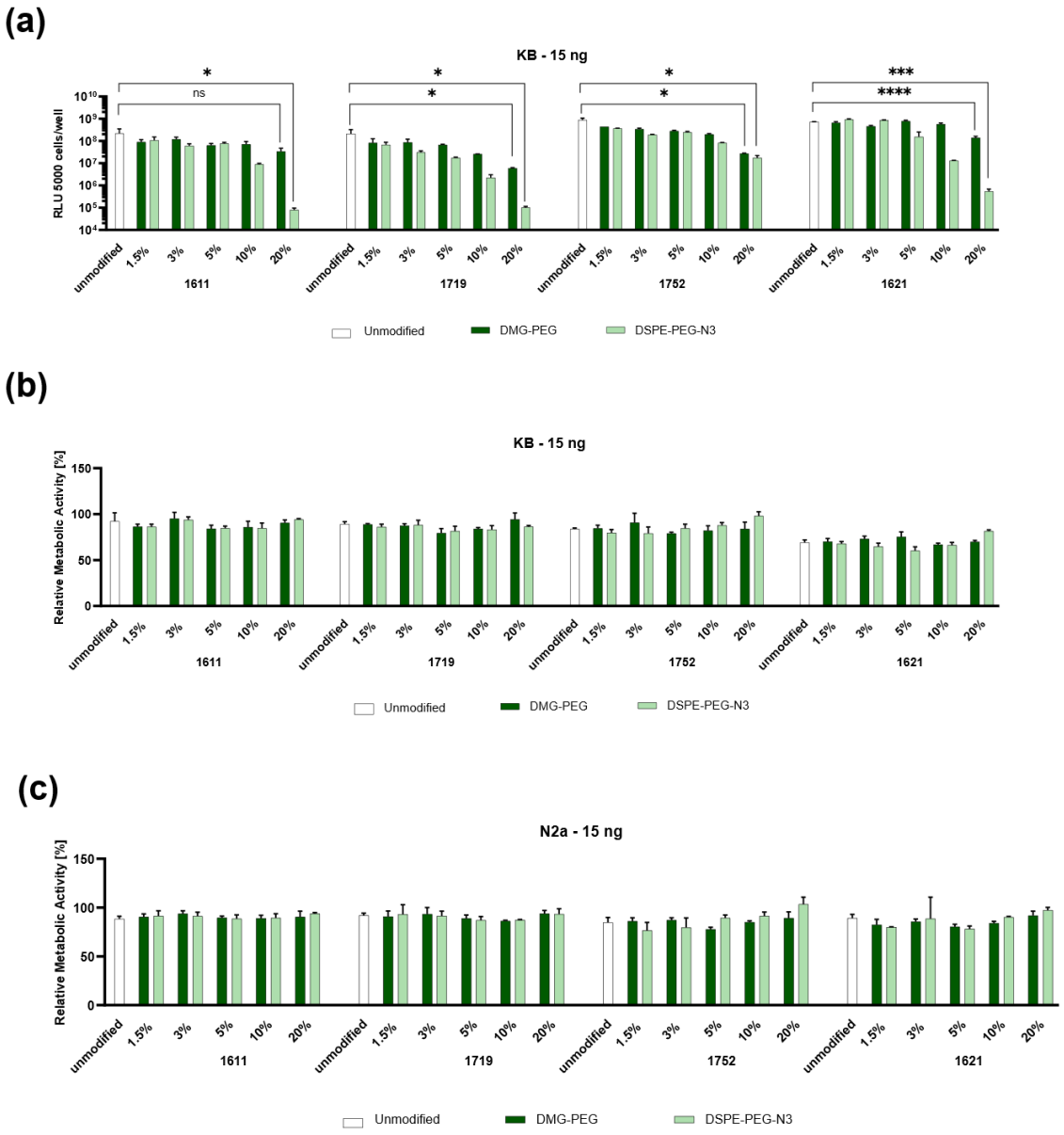

Figure 3. *Variation in molar % PEGylation of LAF-XP mRNA polyplexes with DMG-PEG and DSPE-PEG-N3.* ***(a)*** *Gene transfer activity of unmodified PEGylated polyplexes in KB cells 24 h after transfection. Comparison of unmodified with PEGylated polyplexes at a dose of 15 ng mRNA-LUC/well. Transfection efficacy was determined by luciferase gene expression assay (n = 3, mean + SD).* ***(b) (c)*** *Metabolic activity in relation to HBG-treated control cells determined by MTT assay on KB and N2a cells at a dose of 15 ng mRNA-LUC/well (n = 3, mean + SD). The statistical significance was determined by unpaired t-test with Welch's correction; ns, not significant; *p ≤ 0.05, ***p ≤ 0.001, ****p≤0.0001.*

Finally, the anchoring mechanism of the PEG lipids under physiological and endosomal acidic conditions was evaluated. (Figure 4). Size and zeta potential of unmodified and fully shielded (20% DSPE-PEG-N_3) LAF-XP mRNA polyplexes were compared, after an incubation at either pH 7.4 or at pH 5.4. As observed before, at physiological conditions the shielded particles exhibited a strongly reduced zeta potential. Upon acidification, however, the zeta potential experienced a sharp increase (9.4-fold for 1611, 3.8-fold for 1621), suggesting a loss in shielding. These findings support the hypothesis that the PEG lipids would be released from polyplexes under endosomal protonation of the lipidic LAF domains. (Scheme 2) For the unmodified formulations, the rise in zeta potential (1.4 for 1611, 1.9 for 1621) was not as drastic as for the shielded ones.

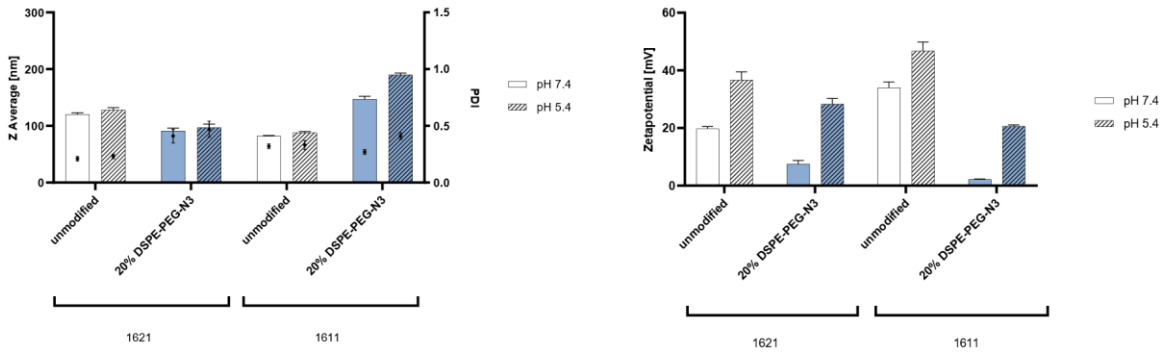

Figure 4. *Unmodified (white) and PEGylated (blue) LAF-XP mRNA polyplexes were formulated and subsequently either diluted with HEPES buffer at pH 7.4 (non-dashed) or at pH 5.4 (dashed). After dilution, size and zeta potential were measured by DLS.*

4.2 TARGETING OF LAF-XP MRNA POLYPLEXES WITH GE11

Tumor specific nucleic acid delivery still remains challenging [160]. The particles must be shielded, meaning they should exhibit a neutral zeta potential to prevent nonspecific cellular interactions. To ensure delivery to the intended site a targeting moiety has to be incorporated. A promising approach involves the use of ligands, which have demonstrated high potential in various studies [131, 175-182]. For instance, GE11 is a phage derived peptide ligand and consists of 12 amino acids with the sequence H_2N-YHWYGYTPQNVI-COOH, specifically targeting the epidermal growth factor receptor (EGFR). It has shown encouraging results

both *in vitro* and *in vivo* [167, 183-186]. In the following study (Scheme 2) the GE11 peptide was functionalized with an N-terminal DBCO moiety (Table1). This enables azido / DBCO copper free click reactions to DSPE-PEG-N_3 yielding a DSPE-PEG-2k-GE11 conjugate (DSPE-PEG-GE11). Identity and purity of the DBCO-GE11 peptide conjugate was confirmed by MALDI-TOF-MS and HPLC (Figure 5).

	Sequence	***Calculated molecular weight [DA]***	***Mass by MALDI-TOF***
GE11-DBCO	*H_2N-YHWYGYTPQNVI-COOH*	*1854.84*	*1851.03*
GE11scr-DBCO	*H_2N-YWGPNIHYYTQV-COOH*	*1854.84*	*1851.27*

Table 1. *Overview of GE11-DBCO ligands and the corresponding mass analyses by MALDI-TOF-MS*

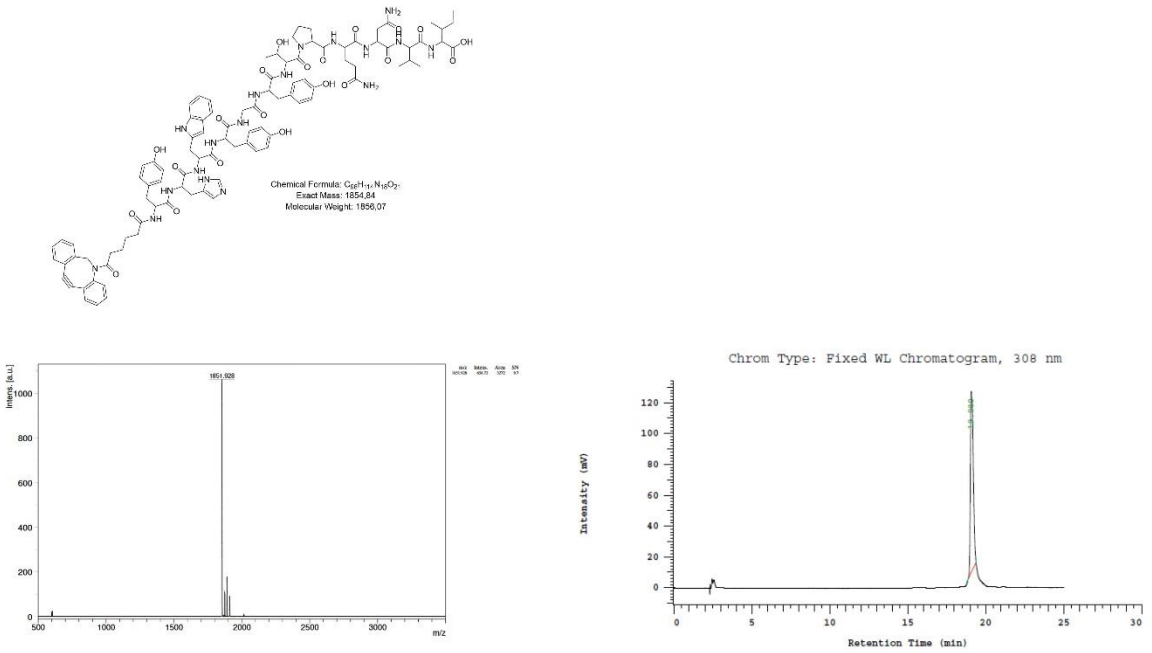

Figure 5. *Structure, MALDI-TOF-MS spectra and HPLC analysis of DBCO-GE11. [M+H]+ calculated 1854.84 [M+H]+ found 1851.27 GE11 ligand was synthesized and analyzed by Johanna Seidl, Pharmaceutical Biotechnology, Department of Pharmacy, Ludwig-Maximilians-Universitätm (LMU), 81377 Munich, Germany.*

For mRNA, DSPE-PEG-N_3 at molar ratios of 10% and 20%, significantly decreased zeta potential and transfection efficiency for all carriers. These molar ratios are ideal for targeting. Consequently, 1611 was selected for targeting studies due to its superior mRNA compaction at high molar ratios of PEG. In accordance with the newly established formulation protocol, the DSPE-PEG 2kDa-GE11 conjugate was used in the same manner as DSPE-PEG-N_3 (Scheme 1f).

DLS measurements revealed that GE11-functionalized mRNA particles exhibited small, uniform sizes with a neutral zeta potential (Figure 7a).

Three EGFR-expressing cell lines HEPG2, HUH7, and KB cells were selected to assess the transfection efficiency of GE11-functionalized 1611 LAF-XP polyplexes. Unmodified, shielded (10% and 20% DSPE-PEG-N_3), and targeted (10% and 20% DSPE-PEG-GE11)

formulations were evaluated. Shielded 1611 exhibited lower transfection efficiency, which was restored by GE11 functionalization (Figure 7b).

In order to investigate the specificity of the ligand-receptor interaction, a constitutional isomer of GE11 (GE11-scr) was synthesized (Figure 6). This was first reported by Yu et al., where the original amino acid sequence (H_2N-YHWYGYTPQNVI-COOH) was scrambled, resulting in a new sequence: H_2N-YWGPNIHYYTQV-COOH [187]. In the same way as for the GE11 peptide, the GE11-scr peptide was functionalized with a DBCO group and conjugated with DSPE-PEG-N_3.

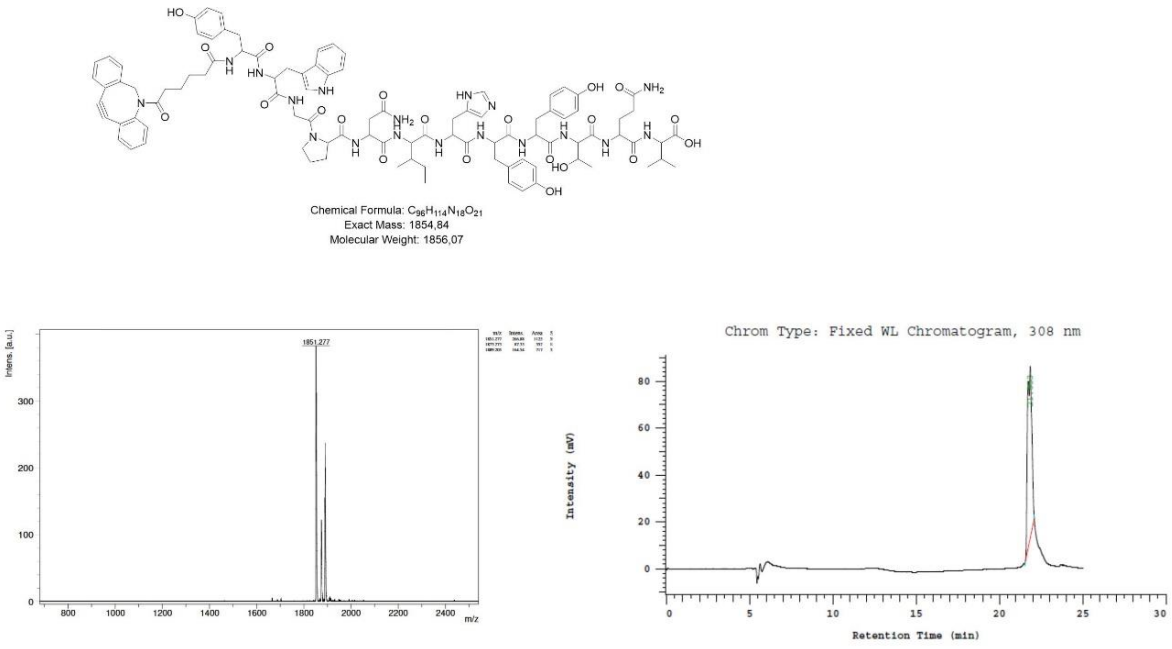

Figure 6. *Structure, MALDI-TOF-MS spectra and HPLC analysis of DBCO-scrGE11. [M+H]+ calculated 1854.84 [M+H]+ found 1851.27. GE11scr ligand was synthesized and analyzed by Johanna Seidl, Pharmaceutical Biotechnology, Department of Pharmacy, Ludwig-Maximilians-Universitätm (LMU), 81377 Munich, Germany.*

GE11-scr-functionalized 1611 LAF-XP polyplexes formed smaller particles with a higher zeta potential compared to those functionalized with GE11 (Figure 7a, Figure 7c). However, unlike GE11, the scrambled GE11 did not enhance transfection efficiency. No considerable differences were observed between shielded and GE11-scr-functionalized particles (Figure 7d). Subsequent uptake measurements supported these findings. Shielding reduced cellular

uptake, while GE11-functionalized LAF-XP polyplexes recovered uptake nearly to the extent of unmodified LAF-XP polyplexes. In contrast, GE11-scr-functionalized LAF-XP polyplexes exhibited uptake levels similar to shielded particles (Figure 7e).

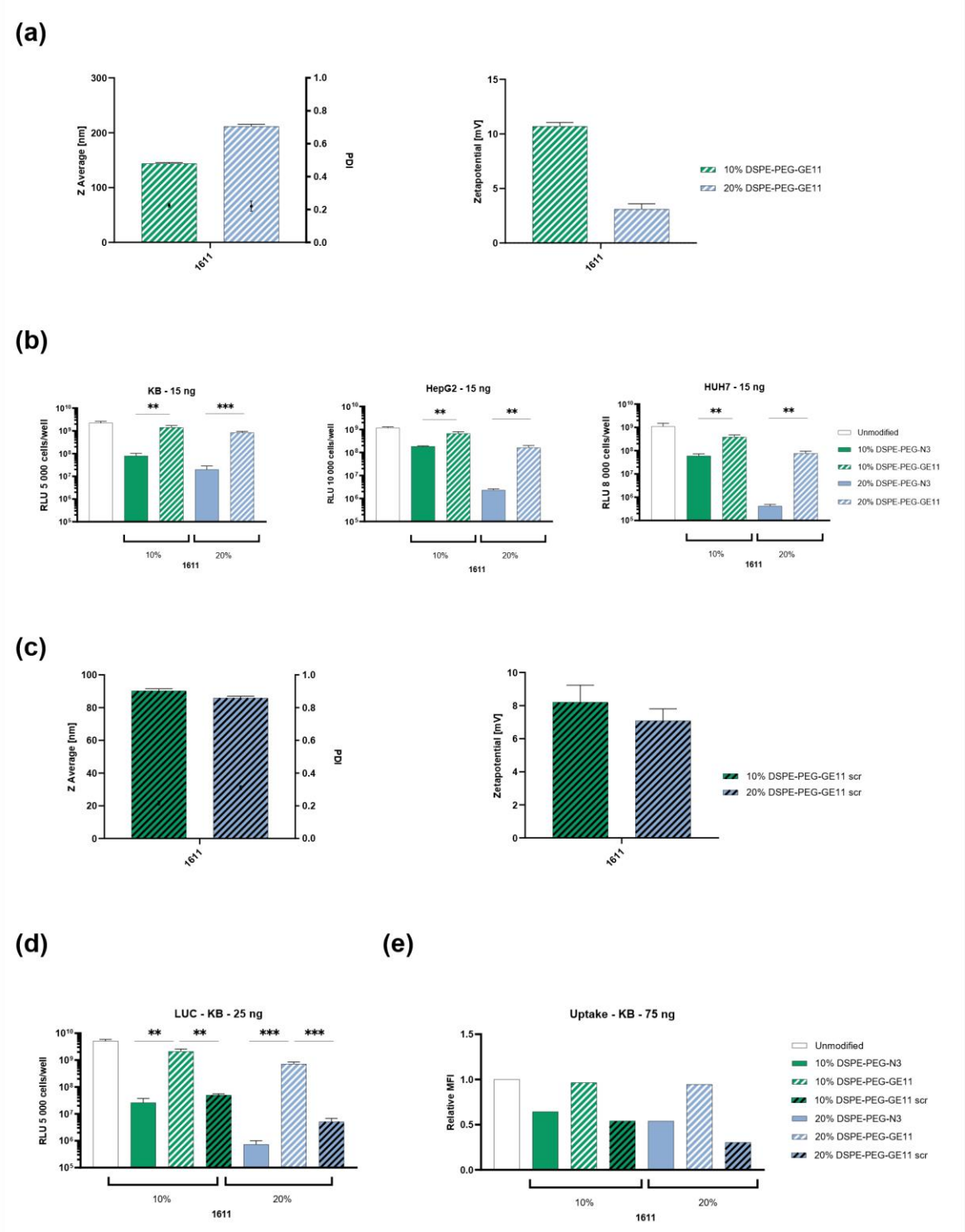

Figure 7. *In vitro evaluation of GE11 and GE11scr functionalized 1611 LAF-XP mRNA polyplexes.* ***(a)*** *and* ***(c)*** *Z average, polydispersity index (PDI) and zeta potential of GE11 and GE11scr functionalized 1611 LAF-polyplexes determined by DLS and ELS.* ***(b)*** *Comparison of luciferase gene expression of unmodified 1611, PEGylated 1611 (10%/20% DSPE-PEG-N3) and GE11 targeted 1611 (10%/20% DSPE-PEG-GE11) LAF-XP polyplexes on KB, HepG2 and HUH7 cells at a dose of 15 ng mRNA-LUC/well after a total incubation time of 24 h (n=3; mean +SD).* ***(d)*** *and* ***(e)*** *Direct comparison of GE11 (EGFR targeting ligand) and scrambled GE11 (negative control ligand) regarding transfection and uptake efficiency on KB cells* ***(d)*** *Luciferase gene expression was determined after a total incubation time of 24 h at a dose of 25 ng mRNA-LUC/well (n=3; mean +SD).* ***(e)*** *Cellular uptake, as determined via flow cytometry (n=1), 2h after transfection at a dose of 75 ng (20% Cy5-labeled mRNA-LUC) per well (50 000 cells). Data presented as mean fluorescence intensity (MFI) in Cy5 positive cells (Cy5-A) normalized to unmodified LAF-XP polyplexes. The statistical significance was determined by unpaired t-test with Welch's correction; ns, not significant; *p ≤ 0.05, **p ≤ 0.01, ***p ≤ 0.001, ****p ≤0.0001. DLS Measurements and luciferase gene expression (HepG2 and HUH7 cells) of GE11-functionalized LAF-XP mRNA nanoparticles were performed by Eric Weidinger, Pharmaceutical Biotechnology, Department of Pharmacy, Center for NanoScience (CeNS), LMU Munich, 80799 Munich, Germany*

4.3 PEGylation and GE11 Targeting of LAF-XP pDNA Polyplexes

For analogue pDNA investigations, U1 U-shapes 1611 and 1719, as well as the B2 bundle 1730 were selected (Scheme 1b, Scheme 1c). Similar trends as for mRNA were observed. DLS measurements revealed that size and PDI remained largely unchanged upon PEGylation, whereas zeta potential was reduced (Figure 8a, Figure 8b). Furthermore, an ethidium bromide (EtBr) assay showed no substantial impact of PEGylation on pDNA binding ability (Figure 8e). LAF–XP pDNA polyplexes are generally more stable than their mRNA counterparts. They tend to aggregate less during particle formation, can be prepared at lower N/P ratios and compact pDNA better than mRNA. These features likely explain why PEGylation has little impact on pDNA compaction, whereas it can affect the compaction of mRNA polyplexes. No considerable differences were detected between DMG-PEG and DSPE-PEG-N_3 in the physicochemical evaluation. However, for transfection efficiency, DSPE-PEG-N_3 led to a stronger reduction than DMG-PEG (Figure 8c). As observed with LAF-XP mRNA polyplexes, this can again be attributed to the differing anchor lengths of the two different PEG lipids.

(a)

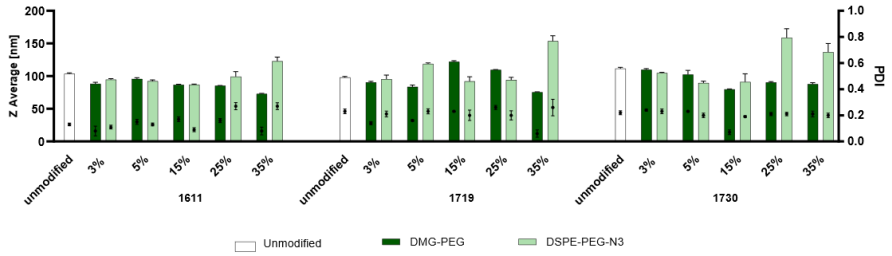
Z Average [nm]
PDI
unmodified
3%
5%
15%
25%
35%
1611
1719
1730
Unmodified
DMG-PEG
DSPE-PEG-N3

(b)

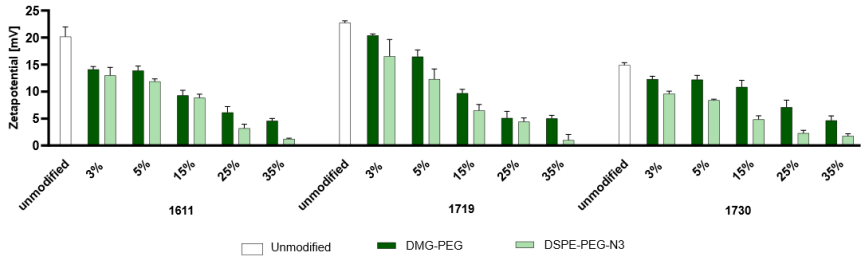
Zetapotential [mV]
unmodified
3%
5%
15%
25%
35%
1611
1719
1730
Unmodified
DMG-PEG
DSPE-PEG-N3

(c)

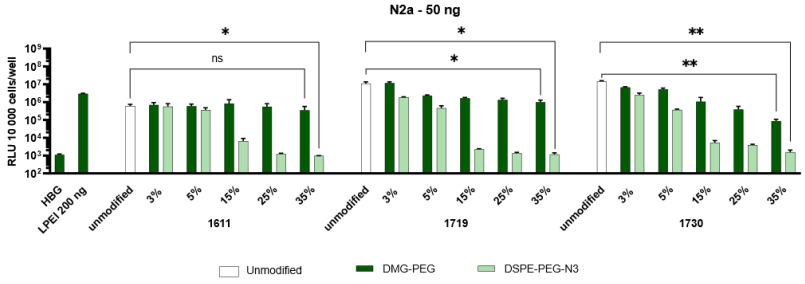
N2a - 50 ng
RLU 10 000 cells/well
ns
*
**
HBG
LPEI 200 ng
unmodified
3%
5%
15%
25%
35%
1611
1719
1730
Unmodified
DMG-PEG
DSPE-PEG-N3

(d)

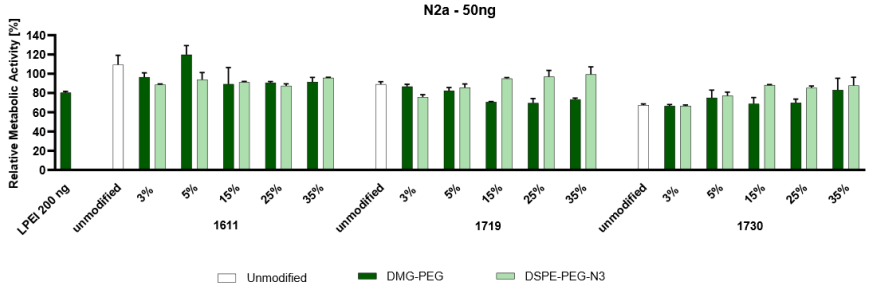
N2a - 50ng
Relative Metabolic Activity [%]
LPEI 200 ng
unmodified
3%
5%
15%
25%
35%
1611
1719
1730
Unmodified
DMG-PEG
DSPE-PEG-N3

(e)

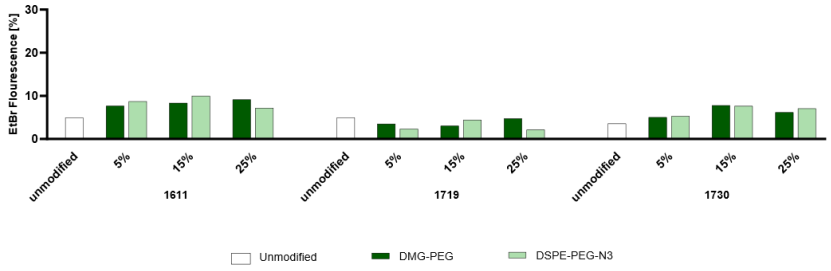
EtBr Flourescence [%]
unmodified
5%
15%
25%
1611
1719
1730
Unmodified
DMG-PEG
DSPE-PEG-N3

Figure 8. *Variation in molar % PEGylation of LAF-XP pDNA polyplexes with DMG-PEG and DSPE-PEG-N_3.* ***(a)*** *Hydrodynamic sizes and polydispersity index (PDI) values of unmodified and PEGylated (different molar %) polyplexes, measured by dynamic light scattering (DLS) and* ***(b)*** *zeta potential analysis determined using electrophoretic light scattering (ELS).* ***(c)*** *Gene transfer activity of LPEI (200 ng pCMVLuc/well), unmodified and PEGylated polyplexes in N2a cells at 24 h after transfection. Comparison of unmodified with PEGylated polyplexes at a dose of 50 ng pCMVLuc/well. Transfection efficacy was determined by luciferase gene expression assay (n = 3, mean + SD).* ***(d)*** *Metabolic activity in relation to HBG treated control cells determined by MTT assay (n = 3, mean + SD).* ***(e)*** *Impact of PEGylation on compaction was determined via an ethidium bromide (EtBr) assay. EtBr fluorescence is proportional to the amount of free, non-compacted pDNA, as only unbound pDNA is accessible for EtBr intercalation. The statistical significance was determined by unpaired t-test with Welch's correction; ns, not significant; *p ≤ 0.05, **p ≤ 0.01.*

For GE11 targeting, unmodified and shielded (25% DSPE-PEG-N_3) 1719 was compared to targeted (25% DSPE-PEG-GE11) 1719. Shielding resulted in a lower transfection efficiency, confirming the results from the initial screening. GE11 functionalization led to the recovery of the transfection efficiency in HepG2 cells and in HUH7 cells it even outperformed the unmodified formulation (Figure 9b).

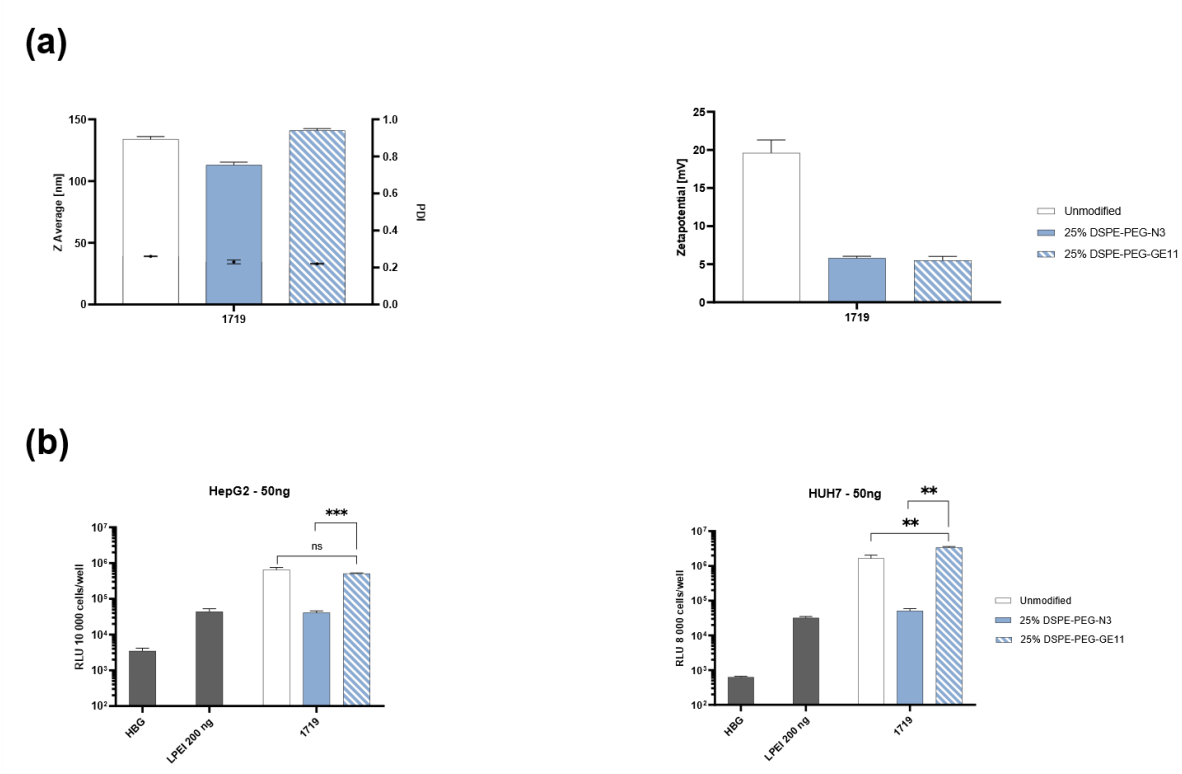

Figure 9. *In vitro evaluation of GE11 functionalized 1611 LAF-XP pDNA polyplexes.* ***(a)*** *Z Average, polydispersity index (PDI) and Zeta potential of GE11 functionalized 1719 polyplexes determined by DLS and ELS.* ***(b)*** *Comparison of luciferase gene expression of LPEI (200 ng pCMVLuc/well), unmodified 1719 and PEGylated 1719 (25% DSPE-PEG-N_3) and GE11 targeted 1719 (25% DSPE-PEG-GE11) polyplexes on HepG2 and HUH7 cells at a dose of 50 ng pCMVLuc/well after a total incubation time of 24 h (n=3; mean +SD). The statistical significance was determined by unpaired t-test with Welch's correction; ns, not significant; **$p \leq 0.01$, ***$p \leq 0.001$.*

4.4 COLLOIDAL STABILITY

In vitro evaluation revealed that DMG-PEG at low molar ratios does not considerably reduce transfection efficiency. Previous work has shown that the addition of small amounts of PEG also improves the colloidal stability of cationic polymer delivery systems [133, 188, 189]. In subsequent experiments, we aim to improve colloidal stability with low amounts of DMG-PEG, however, not at the cost of reduced transfection efficiency.

4.4.1 Steric Stabilization of LAF-XP mRNA Polyplexes Against Salt-Induced Aggregation Through PEGylation

The ionic strength of the physiological environment can present a substantial risk to the stability of cationic delivery systems. Salts can interfere with the electrostatic interactions between cationic carrier and the anionic nucleotide backbone, leading to aggregation. [64, 190]. PEG on the surface of polyplexes can provide protection against salt induced aggregation through steric stabilization [131, 191-196]. In a similar manner, we investigated whether PEGylation could sterically stabilize the LAF-XP polyplexes. We chose two molar ratios of DMG-PEG (3% and 10%) and compared them to unmodified carriers. After LAF-XP polyplex formation, an aliquot of phosphate buffered saline (PBS) was added and size was determined at different time points.

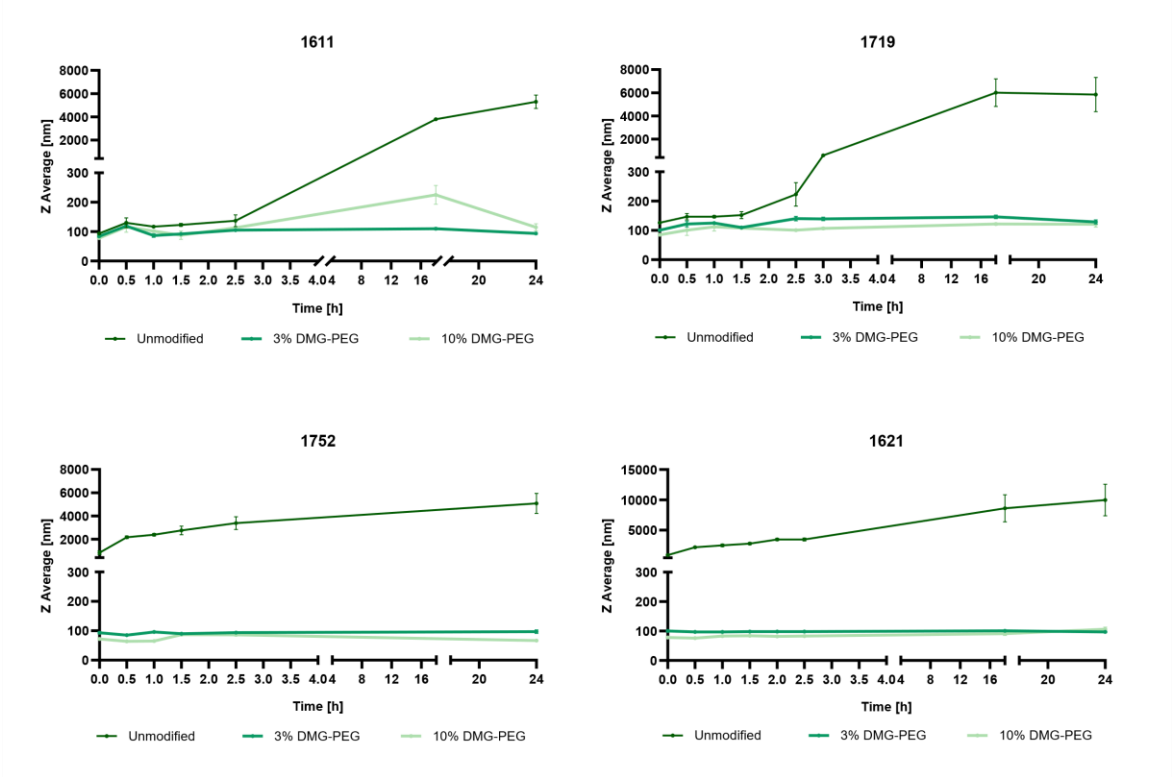

Figure 10. *Stabilization of LAF-XP mRNA polyplexes against salt-induced aggregation via PEGylation with DMG-PEG. Kinetic study of the hydrodynamic size of unmodified and PEGylated (3% and 10% DMG-PEG) LAF-XP polyplexes in the presence of PBS. Following LAF-XP polyplex formulation, PBS was added, and particle size was monitored at the indicated time points via dynamic light scattering (DLS).*

Interestingly, unmodified LAF-XP mRNA polyplexes exhibited topology dependent differences in colloidal stability upon PBS addition. B2 bundles (1752 and 1621) aggregated immediately. U-shapes were more stable, with 1719 aggregating after 150 minutes, and 1611 only after 18 hours (Figure 10). The difference in stability is likely due to the different structural and cationic properties of B2 bundles and U-shapes. The B2 bundles are more hydrophobic and less cationic due to a higher content of LAF residues that are not protonated at physiological pH. In contrast, U-shapes have a lower LAF content and include an additional primary amine in their backbone. This presumably enables stronger electrostatic interactions and compaction of mRNA. A stronger binding in U-shapes is consistent with delayed salt-induced aggregation. PEGylation with both 3% and 10% DMG-PEG prevented aggregation completely in bundles and U-shapes, even after 24 hours (Figure 10). Especially the B2 bundles, with weaker binding, benefit therefore more from PEGylation.

The strong increase in zeta potential under endosomal conditions as observed in section 3.1 suggests that protonation of the LAF carriers leads to dissociation of the PEG lipids from the polyplexes. Consequently, also a functional loss of stability would be predicted in the presence of salt. To verify this, a second PBS stability study was conducted with 1621 polyplexes (Figure 11). Unmodified and PEGylated polyplexes (0.5% and 1% DMG-PEG) were incubated at acidic conditions, before PBS was added for incubation in salt at neutral pH. As a control, standard PEGylated polyplexes (without acidic preincubation) were incubated at pH 7.4. Consistent to the previous findings, unmodified 1621 LAF-XP mRNA polyplexes were immediately aggregated with PBS, whereas PEGylated polyplexes remained stable upon incubation with PBS at pH 7.4. In contrast, PEGylated polyplexes pre-exposed to acidic conditions exhibited aggregation in PBS pH 7.4. The deshielded PEGylated polyplexes aggregated at a markedly slower rate than their unmodified counterpart (Figure S9).

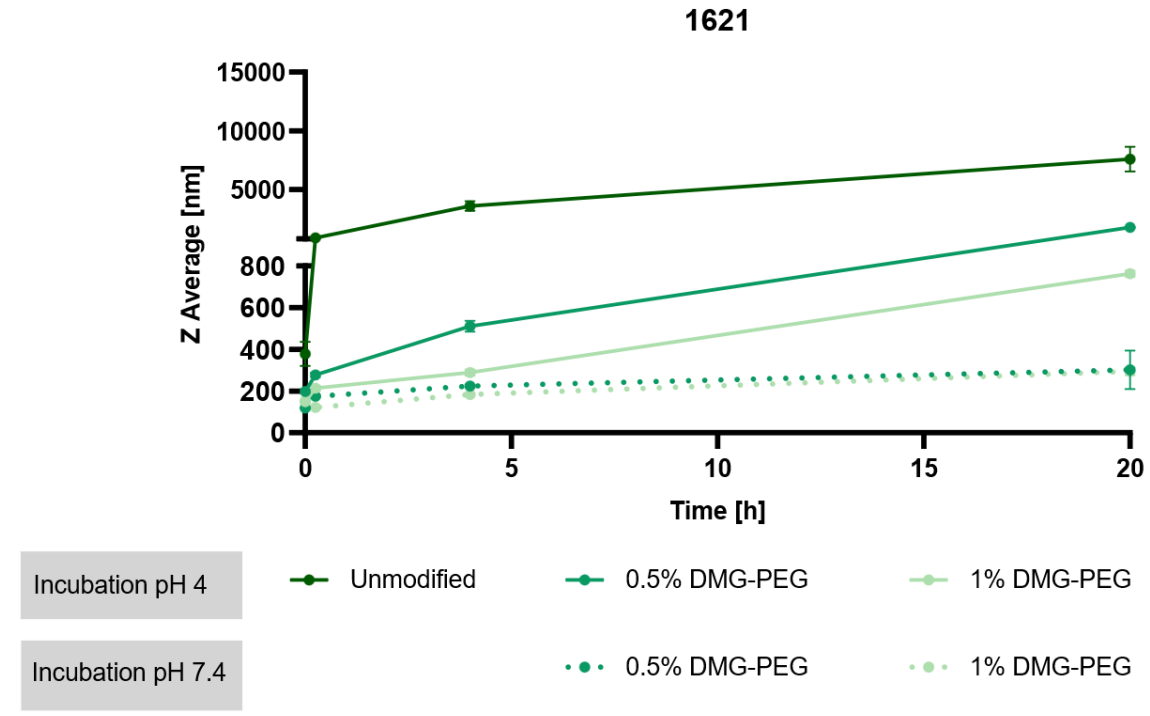

Figure 11. *Kinetic study of the hydrodynamic size of unmodified and PEGylated (0.5% and 1% DMG-PEG) LAF-XP mRNA polyplexes in the presence of PBS. Prior to PBS addition, LAF-XP mRNA polyplexes were preincubated for 30 min under either acidic (pH 4) or physiological (pH 7.4) conditions at 37°C and shaking (300 rpm).*

This suggests that PEG lipids are only partially released under acidic conditions. Nevertheless, this partial deshielding is apparently sufficient for restored high transfection efficiency (Scheme 2, Figure 2).

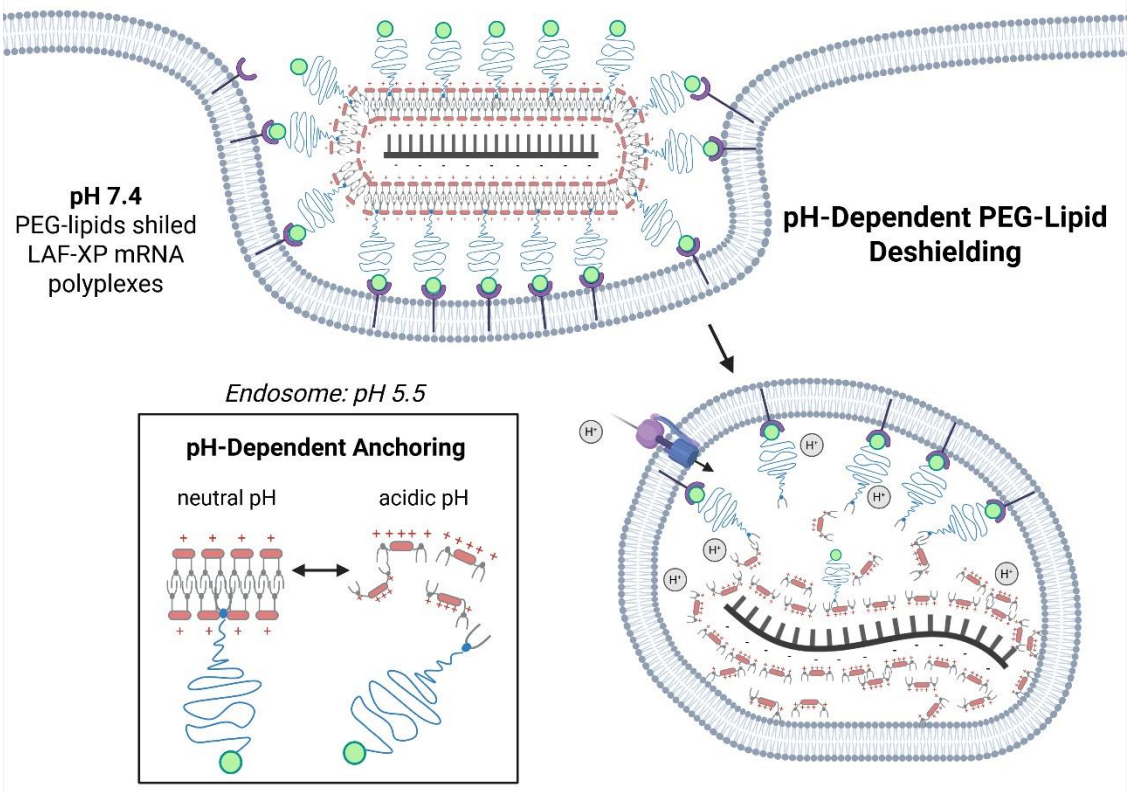

Scheme 2. *Hypothetic model of receptor-targeted delivery and endosomal deshielding. At physiological pH, the PEG-lipids are well anchored within the hydrophobic LAF domains of the carriers and shield the LAF-XP mRNA polyplexes. Cell membrane interactions and subsequent uptake occurs predominantly through ligand-receptor interactions. Endosomal acidification leads to the protonation of the LAF domain, resulting in a polarity shift, solubilization of the nanoparticle and dissociation of PEG-lipids from the polyplex. As a result, interactions of the LAF carriers with the endosomal membrane is restored, enhancing endosomal escape.*

4.4.2 Reduction of the N/P ratio Through PEGylation

Bundles 1621 and 1752 require a higher N/P ratio (N/P 24) to form small and stable particles. At lower N/P ratios, these carriers tend to aggregate, especially at higher concentrations. We investigated whether the bundles 1621 and 1752 could be formulated at half of the standard

N/P ratio (N/P 12 instead of N/P 24) by incorporation of low molar amounts of DMG-PEG (1.5% and 3%) at *in vivo* concentration 33.3 µg/mL (5µg mRNA in 150 µL).

As expected unmodified 1752 and 1621 aggregated at N/P 12. The incorporation of low molar amounts of DMG-PEG led to the formation of small and stable particles with low PDIs and successfully prevented aggregation (Figure 12).

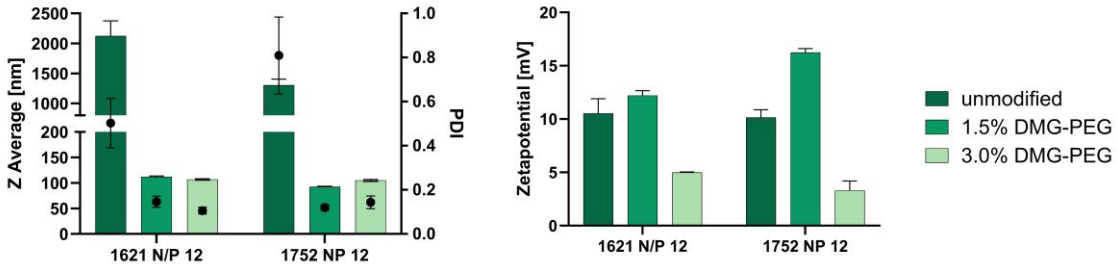

Figure 12. *Stabilization of B2 bundles 1621 and 1752 LAF-XP mRNA polyplexes at low NP ratio. Z average, polydispersity index (PDI) and zeta potential of unmodified and PEGylated (1.5% and 3% DMG-PEG) 1621 and 1752 polyplexes at an N/P ratio of 12, determined by dynamic light scattering (DLS) and electrophoretic light scattering (ELS).*

4.4.3 Overcoming mRNA LAF-XP mRNA Polyplex Instability Through PEGylation

Encouraged by the successful reduction of the N/P ratio in 1752 and 1621, we hypothesized that the PEGylation strategy could be applied to carriers that previously could not be formulated. Thalmayr et al. reported that carriers 1716 and 1613 failed to form stable particles due to severe aggregation [143]. Structurally, 1716 and 1613 are highly similar. Both contain 12Oc as their LAF unit and have nearly identical molecular weights. They only differ in their topology. 1613 is a B2 bundle, while 1716 is a U4 U-shape. The combination of four LAF 12Oc motifs with a single Stp unit appears to result in highly unstable structures. However, both carriers were successfully formulated as LNPs, with 1716 demonstrating a particularly high transfection efficiency [146]. The carriers were PEGylated (1.5% and 3% DMG-PEG) at the N/P ratios of 12 and 18 (Figure 13a). At N/P 12, both unmodified carriers underwent aggregation. However, PEGylation significantly improved size and uniformity. 1.5% DMG-PEG successfully prevented aggregation, although it resulted in larger particles. Nevertheless, the formulations exhibited good uniformity with favorable PDIs. 3% DMG-PEG facilitated optimal particle formation for both 1613 and 1716. Notably, these

formulations exhibited very low zeta potential, approaching near-neutral values. At N/P 18, both 1.5% and 3% DMG-PEG modification resulted in the formation of small particles with low PDI and positive zeta potential.

Subsequently, the different formulations were tested regarding their transfection efficiency in N2a and KB cells. They were compared to 1611 and 1719, which represent the current gold standard for mRNA transfection within the U-shape class. 1716 with 1.5% DMG-PEG outperformed both unmodified 1611 and 1719 in transfection. In contrast, unmodified 1716 aggregates exhibited poor transfection efficiency, emphasizing the positive impact of PEGylation. 1613 demonstrated limited transfection efficiency compared to the other carriers. Here, PEGylation only had a positive effect on transfection efficiency in KB cells where a slight increase in transfection efficiency was observed (Figure 13b).

Our previous work demonstrated, that 1719 had a lower transfection efficiency *in vivo* compared to 1611, 1621, and 1752 [143]. Therefore, the focus in subsequent experiments was placed on these three *in vivo* best performing carriers.

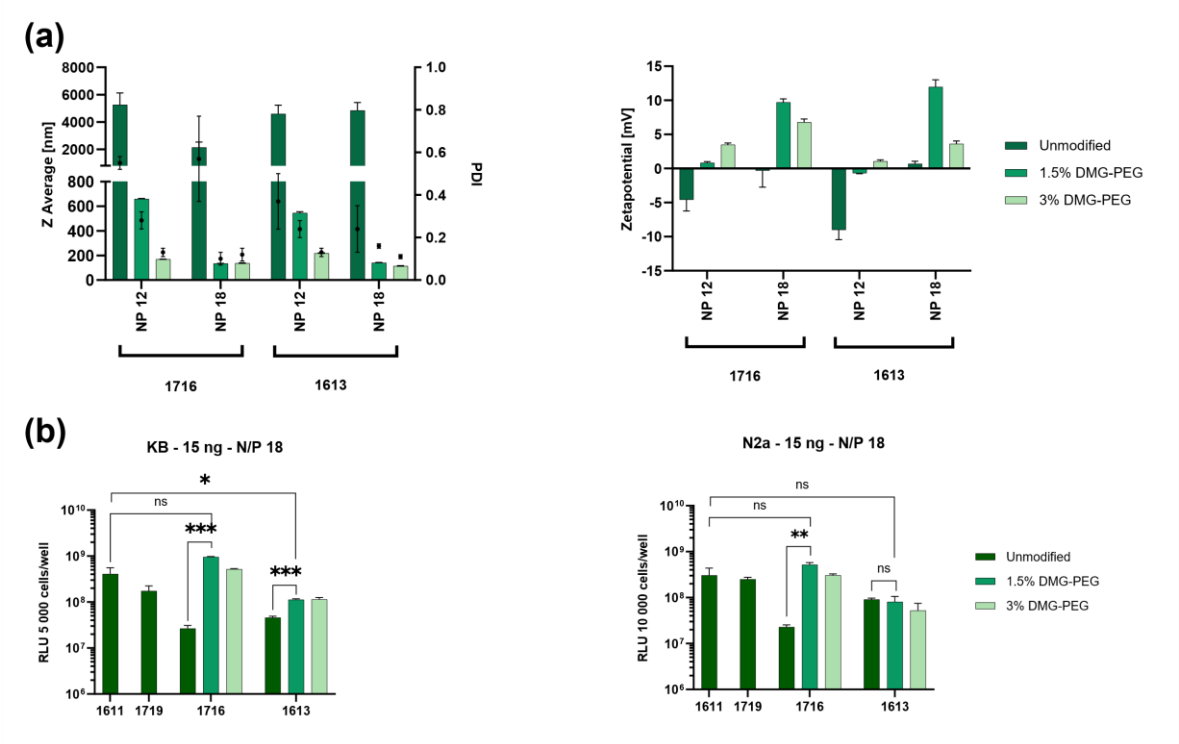

Figure 13. *Stabilization of LAF-XP mRNA polyplexes with aggregation-prone carriers 1613 and 1713 and reduction of N/P ratio.* ***(a)*** *Z Average, polydispersity index (PDI) and zeta potential of unmodified and PEGylated (1.5% and 3% DMG-PEG) 1716 and 1613 polyplexes at N/P ratios of 12 and 18, determined by dynamic light scattering (DLS) and electrophoretic light scattering (ELS).* ***(b)*** *The transfection efficiency of unmodified, aggregation-prone 1716 and 1613 carriers was compared to their stabilized PEGylated counterparts (1.5% and 3% DMG-PEG), at N/P 18. 1611 (N/P 18) and 1719 (N/P 12) polyplexes were included as a control group and represent the current gold standard for mRNA transfection in the U-shape class. Luciferase gene expression was measured at 15 ng mRNA-LUC/well (n = 3, mean ± SD). The statistical significance was determined by unpaired t-test with Welch's correction; ns, not significant; *p ≤ 0.05, **p ≤ 0.01, ***p ≤ 0.001, ****p ≤0.0001.*

4.5 PROTEIN CORONA

In vitro transfection activity often does not match *in vivo* activity [197-199]. Upon exposure of nanoparticles with biological fluids a protein corona forms on the surface that strongly influences further distribution and biological efficacy [200-212]. The novel LAF-XP mRNA polyplexes exhibit unexpectedly high transfection efficiency in the presence of full serum even at very low dose [143, 144]. This is in sharp contrast to classic cationic polymer delivery systems, where serum typically impairs the transfection efficiency [213]. The zwitterionic nature of the LAF-XP carriers at physiological pH suggests that they exhibit a different protein corona compared to purely polycationic delivery systems. In case of LPEI, plasma proteins such as IgM, fibrinogen, fibronectin and complement C3 were found to bind to non-PEGylated polyplexes; [131] furthermore it has been demonstrated that PEG shielding significantly reduced protein adsorption and improves *in vivo* performance of DNA polyplexes. To assess the effect of PEGylation on the protein corona composition of mRNA LAF-XP polyplexes, unmodified and PEGylated 1611 and 1752 (10% DSPE-PEG-N_3) were incubated in serum and unbound proteins were removed via centrifugation. Finally, an SDS-PAGE with subsequent coomassie staining was performed (imperial protein stain) (Figure 14a).

(a)

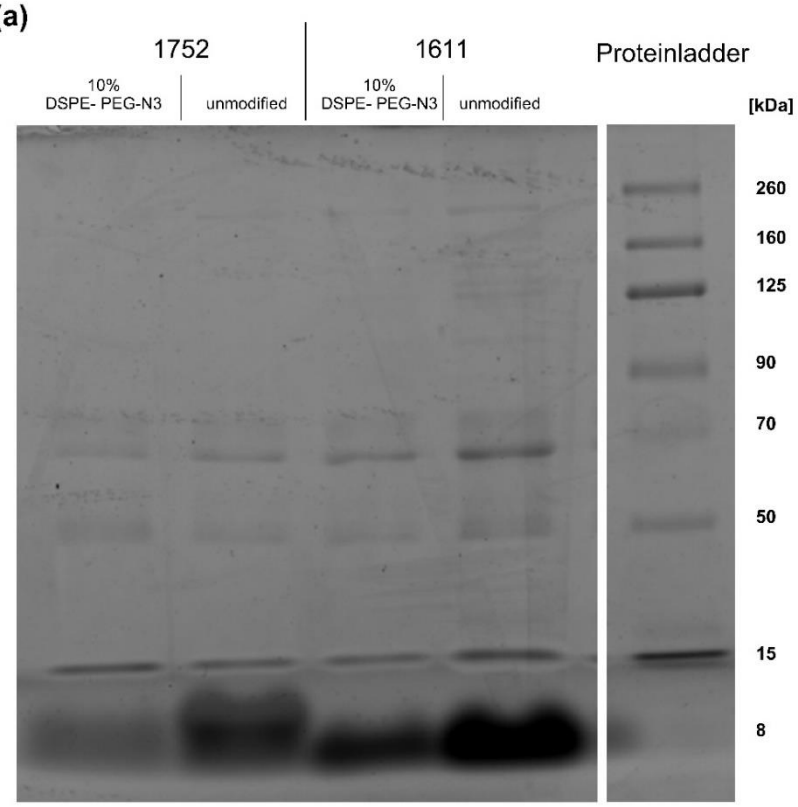

(b)

Unmodified 1611 vs. unmodified 1752

kDa	% Change
70	15.43
15	6.68
8	15.38

Unmodified 1611 vs. 1611 - 10% DSPE-PEG-N_3

kDa	% Change
70	10.33
15	6.38
8	8.87

Unmodified 1752 vs. 1752 - 10% DSPE-PEG-N_3

kDa	% Change
70	3.59
15	-4.46
8	16.36

Figure 14. (a) *SDS-PAGE with subsequent coomassie blue staining (imperial protein stain) of mouse serum incubated unmodified and PEGylated (10% DSPE-PEG-N_3) LAF-XP mRNA polyplexes.* ***(b)*** *Band intensities were quantified using ImageJ. Quantification for the comparison of unmodified 1611 to unmodified 1752 is displayed as percentage change (% change) using the formula* $\%\ change = 100\ x \left(1 - \frac{Intensity\ 1752}{Intensity\ 1611}\right)$ *and for the comparison of PEGylated polyplexes against unmodified polyplexes the formula* $\%\ change = 100\ x \left(1 - \frac{Intensity\ PEGylated}{Intensity\ unmodified}\right)$ *was used. Three protein bands were quantified at approximately 70, 15 and 8 kDa.*

1611 and 1752 polyplexes exhibited distinct differences in protein adsorption. Unmodified 1611 showed higher protein adsorption compared to unmodified 1752. For both carriers, PEGylation with 10% DSPE-PEG-N_3 visibly reduced protein adsorption. To quantify these differences, the intensities of the three most prominent protein bands (~70 kDa, 15 kDa and 8 kDa) were analyzed using Image J. Quantitative analysis revealed, that unmodified 1752 adsorbed less protein than 1611 across all bands. These difference likely comes from their distinct chemical composition. 1752, rich in LAF motifs is less cationic, whereas 1611 has less LAF moieties and resembles more to classical cationic delivery systems such as LPEI. The reduced protein adsorption of the 1752 LAF-XP mRNA polyplexes suggests that the LAF motif already exerts a shielding effect. PEGylation further reduced protein adsorption in both carriers (Figure 14b).

Subsequently, the protein corona of 1611 and 1752 mRNA polyplexes without or with PEGylation (3% DMG-PEG) was investigated in more detail using proteomic methods. This methodological approach allowed the detection of differences in the composition of the protein corona, whereas quantitative changes in the total amount of protein cannot be resolved.

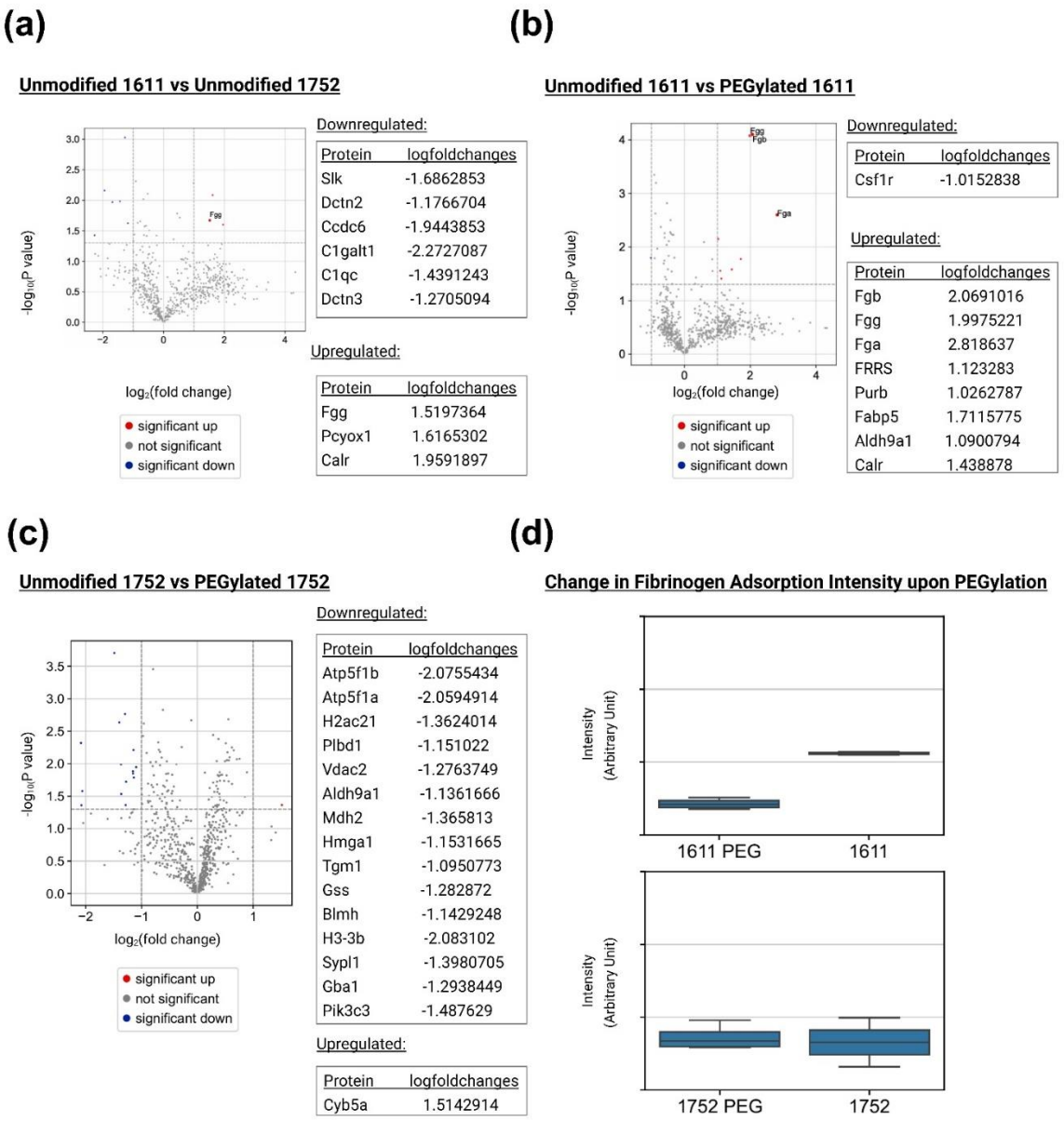

Figure 5. *Proteomic analysis on the protein corona of LAF-XP mRNA polyplexes. PEGylated 1611 (1611 PEG) and 1752 (1752 PEG) refers to formulations containing 3% DMG-PEG. Volcano plots of* ***(a)*** *unmodified 1611 compared to unmodified 1752, displaying proteins up and down regulated for 1611 relative to 1752,* ***(b)*** *unmodified 1611 compared to PEGylated 1611, displaying proteins up and down regulated for 1611 relative to PEGylated 1611 and* ***(c)*** *unmodified 1752 compared to PEGylated 1752, displaying proteins up and down regulated for 1752 relative to PEGylated 1752.* ***(d)*** *Intensity of fibrinogen adsorption of unmodified and PEGylated 1611 and 1752 mRNA LAF-XP polyplexes. Measurement, analysis, and statistical evaluation was performed by Dr. Ceren Kimna, Dr. David-Paul*

Minde and Dr. Mayar Ali. Institute for Intelligent Biotechnologies (iBIO), Helmholtz Center Munich, 85764 Neuherberg, Germany.

Initial analysis of the unmodified carrier polplexes suggests that fibrinogen (Fgg) was upregulated in 1611 compared to 1752 (Figure 15a). Fibrinogen is a large negatively charged glycoprotein. It is known to bind strongly to positively charged particles. 1611 exhibits a zeta potential of 25 - 35 mV, whereas 1752 shows a markedly lower zeta potential of approximately 10 (Figure 1a). Upon PEGylation with 3% DMG-PEG, the zeta potential of 1611 is decreased to ~13. PEGylated 1611 polyplexes thus show a zeta potential comparable to unmodified 1752 polyplexes (Figure 1a). As a result, PEGylated 1611 nanoparticles exhibit significantly reduced fibrinogen adsorption (Figure 15b, Figure 15d). In contrast, 1752 polyplexes inherently adsorb less fibrinogen. Here PEGylation did not further decrease fibrinogen adsorption (Figure 15c, Figure 15d). This difference is likely attributed to the distinct structural composition of the carriers. 1752 contains an Stp/LAF ratio of 1:4 whereas 1611 has a ratio of 1:2. The higher Stp content in 1611 likely contributes to its higher zeta potential. The cationic polar Stp unit is structural derivative of LPEI, which is also known to strongly adsorb fibrinogen. PEGylation of highly cationic LPEI polyplexes likewise resulted in less fibrinogen adsorption [131]. In contrast, the amphiphilic LAF domain behaves differently. It is largely neutral and hydrophobic at physiological pH. In 1752, it likely accounts for its reduced zeta potential by partially neutralizing its surface charge. The decrease in fibrinogen adsorption implies that the LAF motif may provide a shielding effect.

4.6 Steric Stabilization of LAF-XP mRNA Polyplexes Against Protein and Serum Induced Aggregation Through PEGylation

Extensive research especially on cationic carrier systems have shown aggregation after intravenous application resulting in toxicity [214]. Moreover, organ specific targeting can be hampered. For instance, LPEI/DNA polyplexes at high doses aggregates with blood components, which passively accumulate in the lung, predominantly leading to high transfection of pulmonary tissue. This also poses a serious threat to biosafety. In case of PEI, conjugation with PEG evaded these problems [43, 131, 215].

Initially, the stability of unmodified polyplexes with carriers 1611, 1752, and 1621 was investigated in the presence of negatively charged human transferrin (Figure 16a). Unmodified LAF-XP polyplexes were formulated according to the standard preparation protocol, followed by the addition of varying molar amounts of human transferrin (molar equivalent refers to the molar ratio of human transferrin to the carrier). Interestingly, contrary to the PBS results, 1611 appeared to be less stable than the bundles. It failed to form stable particles at any molar ratio of human transferrin. 1621 and 1752 already formed stable particles at a molar equivalent of 0.25. As all carriers underwent aggregation at a molar ratio of 0.1 eq hTF, this ratio was chosen to investigate the impact of PEGylation.

The results were consistent with all carriers. PEGylation effectively prevented aggregation. Particles were slightly larger at 1.5% DMG-PEG compared to 3% DMG-PEG (Figure 16b). Minimal PEGylation again showed a great improvement in colloidal stability.

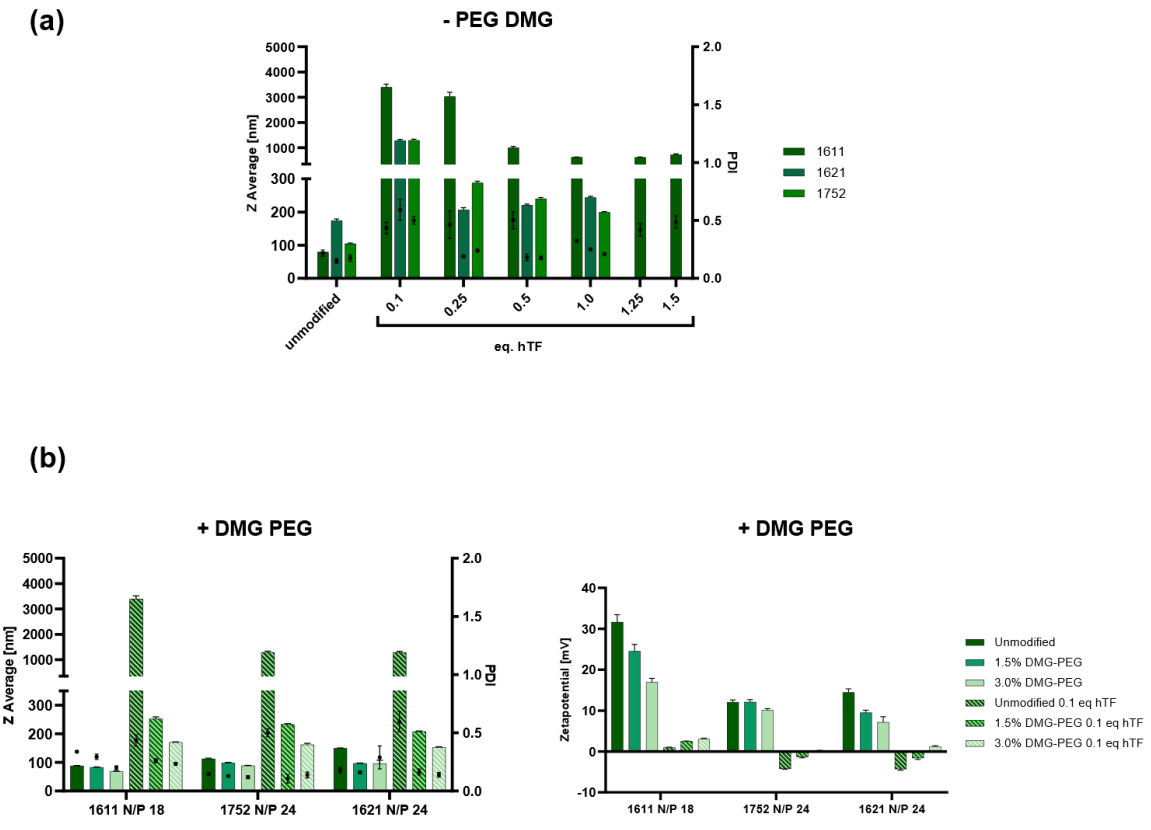

Figure 16. *Stabilization of LAF-XP polyplexes against human transferrin (hTF) induced aggregation with DMG-PEG.* ***(a)*** *Z-average and PDI of 1611, 1621, and 1752 in the presence*

of varying molar equivalents (carrier/hTF molar ratio) of human transferrin, measured by DLS. ***(b)*** *Z-average, polydispersity index (PDI), and zeta potential of unmodified and PEGylated (1.5% and 3% DMG-PEG) carriers, both in the presence and absence of 0.1 eq hTF.*

After intravenous application, besides ionic stress and protein adsorption, higher body temperature and shear forces may challenge the stability of the carriers even further [41, 42, 46, 200]. Therefore a serum assay was conducted. Here, LAF-XP polyplexes are tested in the presence of electrolytes, proteins, higher temperature and shear forces all at once. Unmodified and PEGylated (3% and 10% DSPE-PEG-N_3/DMG-PEG) LAF-XP mRNA polyplexes, formulated at *in vivo* concentration (10µg/150µL), were incubated in 90% fetal bovine serum for 2h under continuous shaking at 300 rpm at 37°C. Subsequently, serum incubated LAF-XP polyplexes were tested regarding their size and transfection efficiency.

First DLS measurements were conducted. Prior to measurement, serum incubated polyplexes were further diluted with HBG resulting in a final serum concentration of 45%. Subsequently DLS measurements were performed. Unmodified carriers showed aggregation after 2h (Figure 17b). Especially the bundles 1621 and 1752 benefitted from PEGylation. Both PEG lipids, DMG-PEG and DSPE-PEG-N_3, at molar ratios of 3% and 10%, effectively prevented aggregation. Interestingly, just like in the stability study with human transferrin, 1611 polyplexes appeared to be less stable. In that case, DMG-PEG at any molar ratio failed to improve stability. Only DSPE-PEG-N_3 prevented aggregation (Figure 17b).

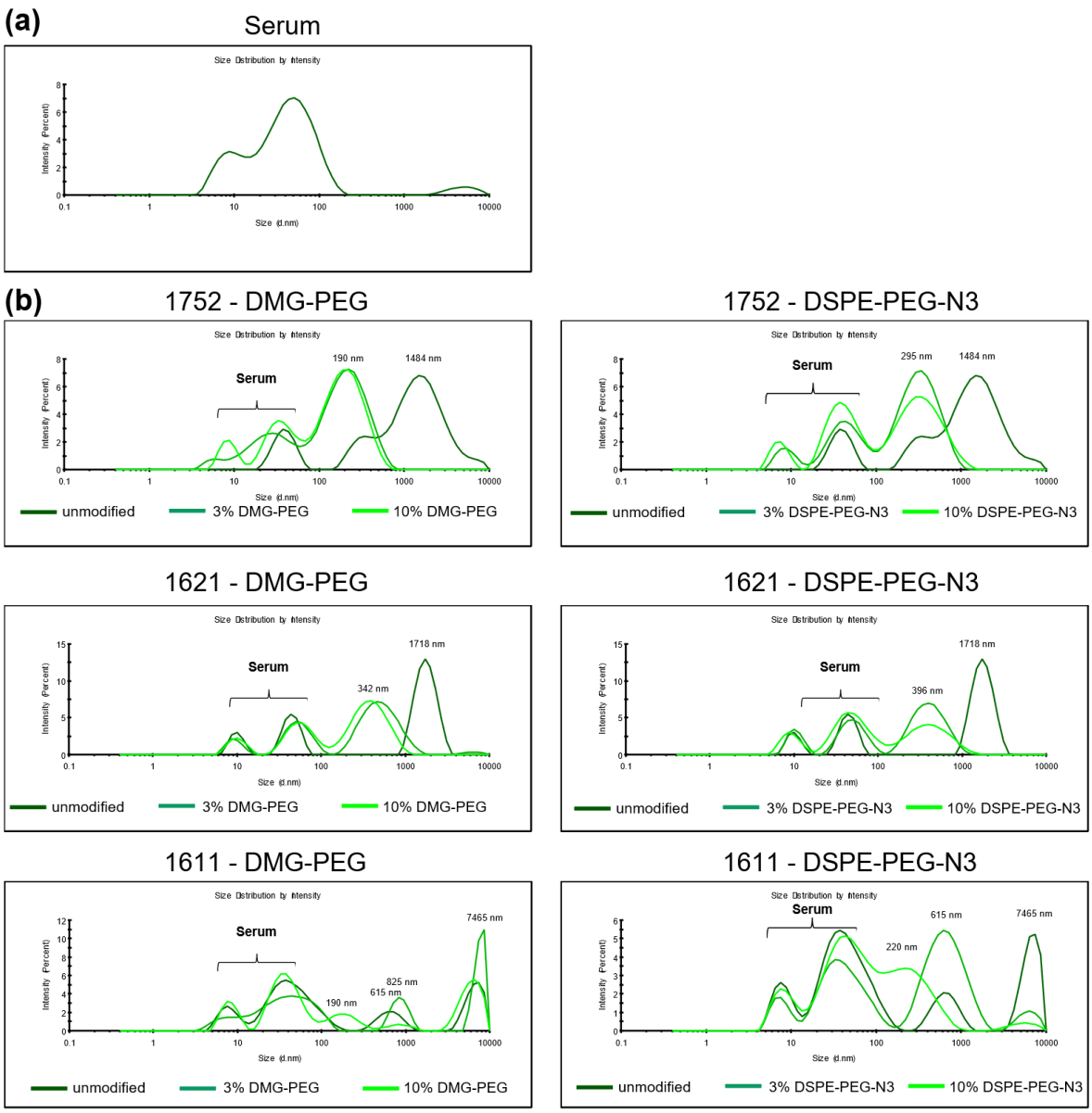

Figure 17. *Assessment of particle stability in the presence of serum. Unmodified and PEGylated LAF-XP mRNA polyplexes were diluted and incubated in 90% fetal bovine serum (FBS) for 2 hours at 37°C under continuous shaking at 300 rpm.* ***(a)*** *and* ***(b)*** *Z average of serum, unmodified and PEGylated LAF-XP polyplexes (3% and 10% DMG-PEG/DSPE) was determined using DLS. For DLS measurements, 40 µL of the FBS-incubated samples were further diluted with 40 µL of HBG, resulting in a final volume of 80 µL, and transferred to a folded capillary cell.*

DLS measurements have limitations in polydisperse samples. Big aggregates might mask smaller particles, leading to underrepresentation of the smaller particle populations. Therefore, to further support these findings, Nanoparticle Tracking analysis (NTA) was performed. In order to distinguish serum background from LAF-XP polyplexes, a serum blank was measured prior to the polyplex measurements (Figure 18). The observed trends were very similar to the DLS results. The unmodified carriers exhibited aggregation after 2h. They formed large, bright particles, that prevented precise NTA quantification (Figure 18). For 1621, PEGylation greatly improved colloidal stability, with already 3% DMG-PEG effectively preventing aggregation. Both PEG lipids, DMG-PEG and DSPE-PEG, enhanced particle stability (Figure 18b, Figure 19a). 1611 polyplexes again appeared to be less stable. For DMG-PEG particle stabilization was achieved only at a molar ratio of 10% whereas 3% was insufficient (Figure 19b). In contrast, for DSPE-PEG-N_3, 3% already improved stability and prevented aggregation (Figure 18b).

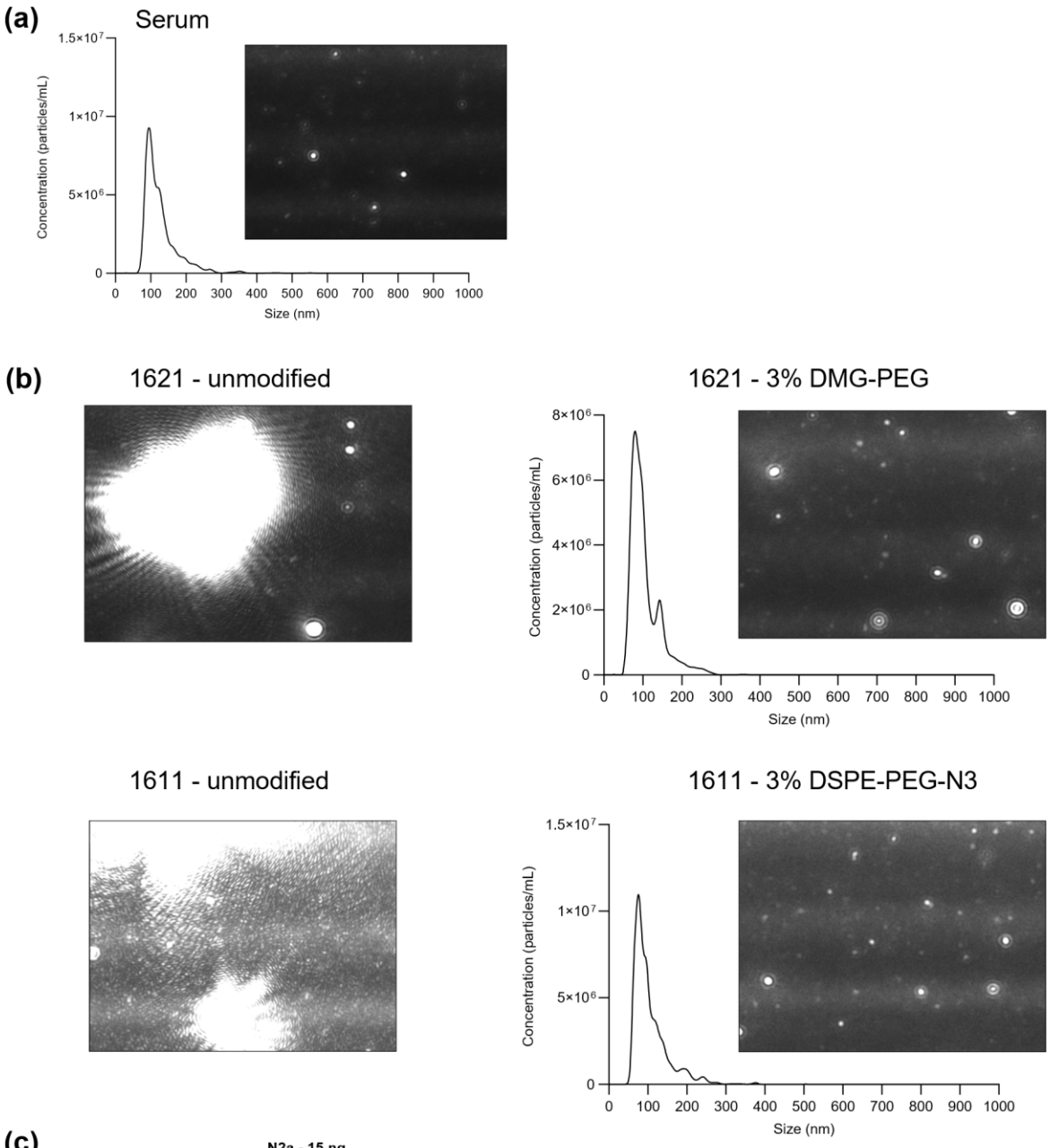
(a)
Serum
Concentration (particles/mL)
Size (nm)
(b)
1621 - unmodified
1621 - 3% DMG-PEG
1611 - unmodified
1611 - 3% DSPE-PEG-N3
(c)
N2a - 15 ng
RLU 10 000 cells/well
Unmodified
3% DMG-PEG
3% DSPE-PEG-N3
1611
1752
1621

Figure 18. *Assessment of stability and functionality in the presence of serum. Unmodified and PEGylated LAF-XP mRNA polyplexes were diluted and incubated in 90% fetal bovine serum (FBS) (1:10) for 2 hours at 37°C under continuous shaking at 300 rpm.* ***(a)*** *and* ***(b)*** *NTA measurements with the corresponding NTA video frame of serum, unmodified and PEGylated 1621 and 1611 LAF-XP mRNA polyplexes (3% DMG-PEG/DSPE-PEG-N_3). For NTA measurements, FBS-incubated samples were further diluted 1:200 in Hepes 7.4* ***(c)*** *Transfection efficiency of unmodified and PEGylated LAF-XP polyplexes (3% DMG-PEG/DSPE) following dilution and incubation in 90% serum was compared to the corresponding LAF-XP polyplexes diluted in HBG (-) in N2a cells. Luciferase gene expression was determined after 24 hours at a dose of 15 ng mRNA-LUC per well (10 000 cells/well) (n = 3; mean ± SD). The statistical significance was determined by unpaired t-test with Welch's correction; ns, not significant; *p ≤ 0.05, **p ≤ 0.01, ***p ≤ 0.001, ****p ≤0.0001.*

These results indicate that bundle carriers 1621 and 1752 benefit from PEGylation to a greater extent than the U shape 1611. This is likely due to their higher number in apolar LAF domains (1621 and 1752 B2 bundles - 4 LAF domains, 1611 U-shape - 2 LAF domains), in which the PEG lipids may be better anchored. This would also explain the superior stabilizing effect of DSPE-PEG-N_3 compared to DMG-PEG in 1611 LAF-XP polyplexes.

Furthermore, transfection efficiency upon serum incubation was assessed. As a control, LAF-XP polyplexes were diluted in HBG instead of serum prior to transfection

(Figure 18b). The DSL measurement has shown that 3% PEG already resulted in stabilization. Therefore, only LAF-XP polyplexes, PEGylated at a molar ratio of 3% PEG-DSPE/DMG were examined.

The luciferase expression assay revealed that the unmodified carriers were not negatively affected by serum incubation. In fact, for the bundles 1621 and 1752, serum incubation even enhanced transfection efficiency compared to their HBG diluted counterparts. On the other hand, the transfection efficiency of 1611 remained largely unchanged.

(a)

1621 - 10% DMG-PEG

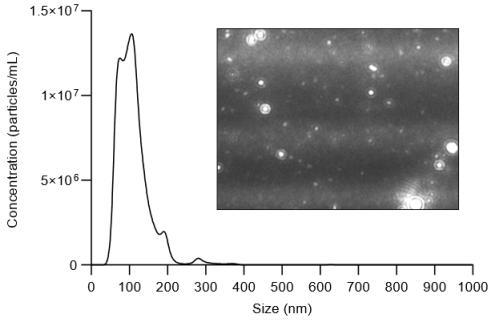

1621 - 3% DSPE-PEG-N3

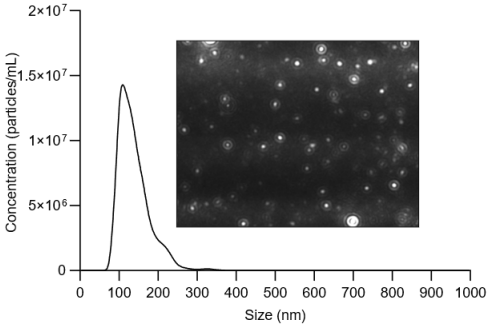

1621 - 10% DSPE-PEG-N3

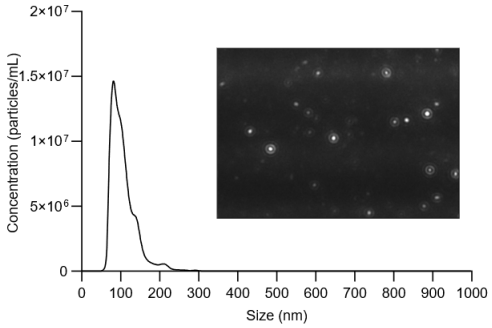

(b)

1611 - 10% DMG-PEG

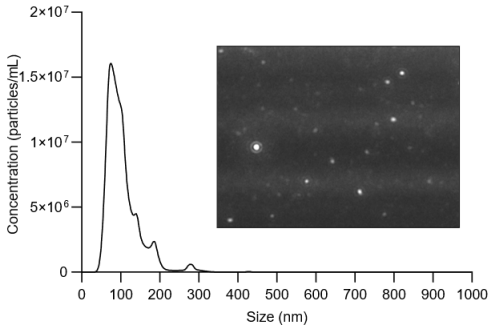

1611 - 3% DMG-PEG

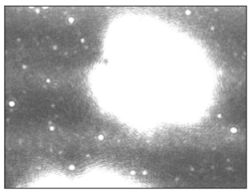

1611 - 10% DSPE-PEG-N3

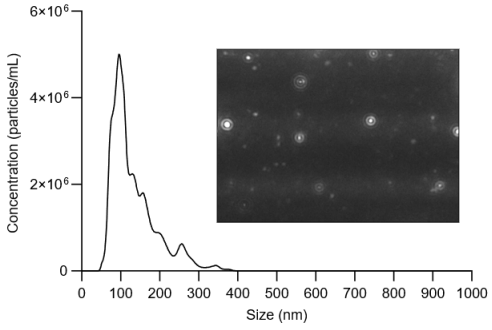

Figure 19. *Assessment of stability and functionality in the presence of serum. Unmodified and PEGylated LAF-XP mRNA polyplexes were diluted and incubated in 90% fetal bovine serum (FBS) for 2 hours at 37°C under continuous shaking at 300 rpm. FBS-incubated samples were further diluted 1:200 in Hepes (7.4).* ***(a)*** *and* ***(b)*** *NTA measurements with the corresponding NTA video frame of unmodified and PEGylated 1621 and 1611 LAF-XP mRNA polyplexes (3% and 10% DMG-PEG/DSPE-PEG-N_3).*

For bundle carriers 1621 and 1752, PEGylation under serum free conditions resulted in a decrease in transfection efficiency with DSPE-PEG-N_3 again having a stronger effect. In the presence of serum, however, this reduction in transfection efficiency was less pronounced. In fact, for 1621, 3% DMG-PEG enhanced the transfection efficiency.

Similarly, for 1611 under serum free conditions, PEGylation led to a decrease in transfection efficiency. However, in the presence of serum the trends were opposite. PEGylation led to an increase in transfection efficiency. DSPE-PEG-N_3 (containing a larger lipid anchor) outperformed DMG-PEG. This reversed trend might be explained by the prior DLS measurement, which revealed that DSPE-PEG-N_3 at 3% managed to better stabilize the particles, which ultimately leads to enhanced transfection efficiency. Besides the different Stp/LAF ratio, the topology may also have a big impact on PEG anchoring. In the bundles, the LAF domains are forced to stay in close proximity, as they are connected via lysine residues. In contrast, in 1611 the two LAF moieties are separated by the Stp unit. Bundles may more easily form more localized lipophilic regions in which PEG lipids are more stably anchored. Moreover, 1611 contains a primary amine in its backbone, which might interfere with lipophilic interactions between the LAF unit and the lipid anchors.

4.7 IN VIVO DOSE STUDY: 1621 AND 1752

1621 and 1752 greatly benefit from PEGylation and were therefore selected for intravenous application. A dose escalation study was conducted to evaluate whether minimal PEGylation (3% DMG-PEG) would allow the injection of a higher mRNA dose. Specifically, for 1621, a starting dose of 5 µg mRNA was selected (A/J mice) and for 1752, the starting dose was 6 µg mRNA (N2a tumor-bearing NMRI mice).

Upon injection of the high dose of unmodified 1621 and 1752 LAF-XP mRNA polyplexes, mice suffered from severe toxicity symptoms and had to be euthanized. The dose had to be reduced for the remaining animals, which was then well tolerated. In contrast, the higher doses were tolerated with the PEGylated formulations, which exhibited no signs of toxicity.

These observations indicate that PEGylation may contribute to biosafety, as its ability to prevent aggregation thus improving stability made it possible to increase the dose. Regarding transfection efficiency, there were no notable differences between the unmodified and the PEGylated formulations (Figure 20a, Figure 20b).

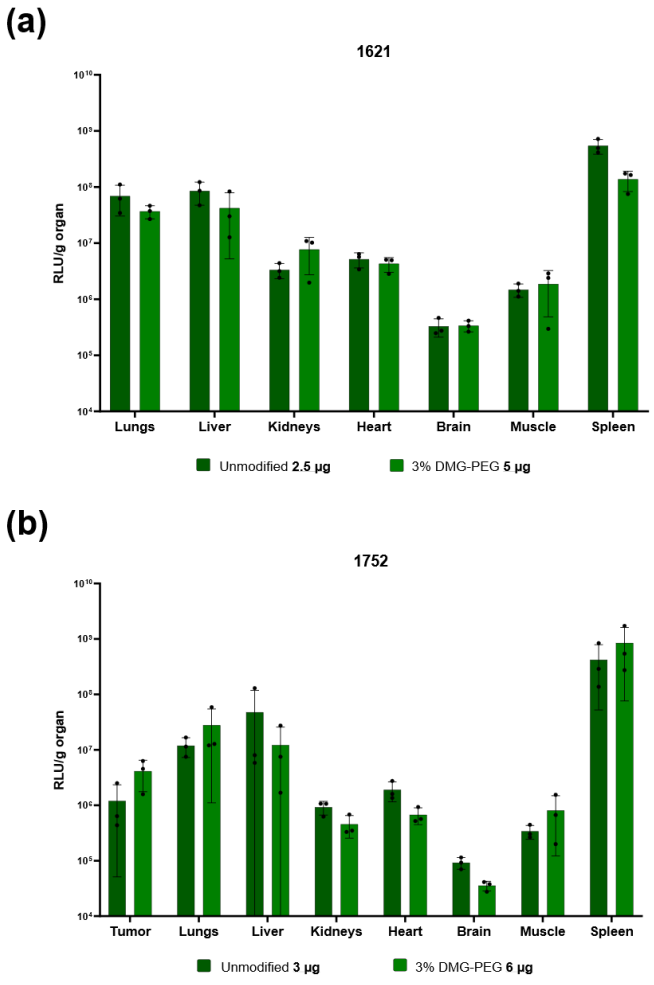

Figure 20. *Dose study of 1621 and 1752 LAF-XP mRNA polyplexes. Ex vivo luciferase (LUC) assay of organs from A/J mice (1621)* ***(a)*** *and N2a tumor-bearing NMRI mice (1752)* ***(b),*** *24 h post-administration (n = 3; mean + SD). Comparison of unmodified 1621 and 1752 polyplexes, both at NP 24, administered at doses of 2.5 µg (1621) and 3 µg (1752), to*

PEGylated 1621 (NP 24; 3% DMG-PEG) or 1752 (NP 24, 3% DMG-PEG) polyplexes at doses of 5 µg or 6 µg mRNA. Unmodified 1621 NP 24 and 1752 NP 24 at doses of 5 µg (1621) or 6 µg mRNA (1752) caused severe toxicity, resulting in indicated euthanasia shortly after administration. Animal experiments (i.v. application and organ harvesting) were performed by veterinarians Dr. Mina Yazid and Dr. Jana Pöhmerer. Pharmaceutical Biotechnology, Department of Pharmacy, Ludwig-Maximilians-Universitätm (LMU) Munich, 81377, Germany.

To explore any effect of PEGylation on tumor accumulation, polyplexes of unmodified 1621 (at the low dose 2.5 µg mRNA) and PEGylated 1621 (at low and high dose 2.5 µg and 5 µg mRNA) were intravenously injected into N2a tumor bearing A/J Mice. The higher dose of 5 µg mRNA of the PEGylated formulation was again well tolerated, confirming the results from the initial dosing study (Figure 21). A comparison between the PEGylated and the unmodified formulation did not show notable differences in tumor expression signal nor in other organs. These findings suggest that minimal PEGylation without targeting does not influence transfection efficiency, but enhances biocompatibility.

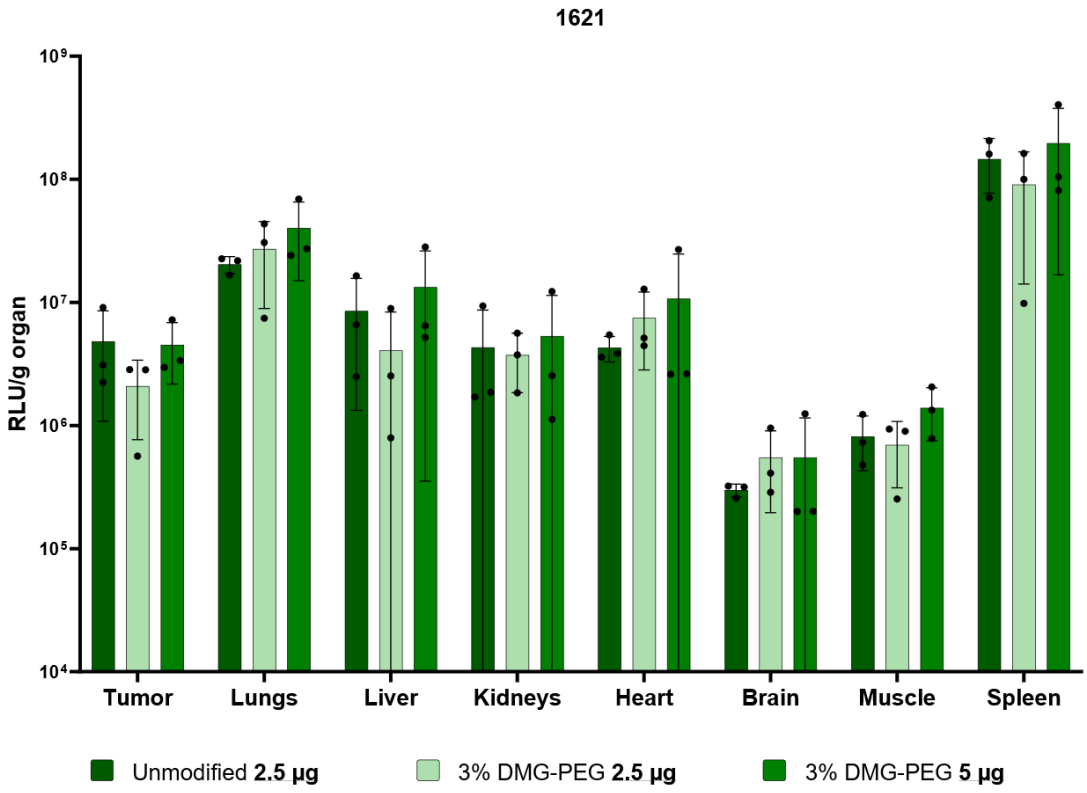

Figure 21. *In vivo transfection efficiency assessment of unmodified 1621 vs. PEGylated 1621 LAF-XP mRNA polyplexes in N2a tumor-bearing A/J mice. Ex vivo luciferase (LUC) assay of organs comparing unmodified 1621 polyplexes at a dose of 2.5 µg mRNA with PEGylated (3% DMG-PEG) 1621 polyplexes at doses of 2.5 µg and 5 µg mRNA, 24 hours post-administration (n = 3; mean ± SD). Animal experiments (i.v. application and organ harvesting) were performed by veterinarians Dr. Mina Yazid and Dr. Jana Pöhmerer. Pharmaceutical Biotechnology, Department of Pharmacy, Ludwig-Maximilians-Universitätm (LMU) Munich, 81377, Germany.*

5 SUMMARY

mRNA has emerged as a powerful therapeutic modality, with lipo amino fatty acid (LAF) - xenopeptides (XPs) representing a promising delivery platform. However, for successful clinical translation challenges in formulation, in vivo stability and targeted delivery must be addressed.

The first challenge lies in the formulation of mRNA nanoparticles, where efficient mRNA complexation must be combined with high colloidal stability. Several LAF-XP carriers, particularly those with a high content of lipophilic LAF motifs, suffer from aggregation during or after particle formation. Some carriers could previously be formulated only as LNPs or required high N/P ratios to achieve stable formulations. To overcome these limitations, a PEGylation strategy was successfully applied to LAF-XP polyplexes. By co-diluting PEG lipids (DMG-PEG or DSPE-PEG-N_3) with LAF-XP carriers in water and subsequent turbulent mixing with mRNA, a simple, aqueous, and dialysis-free formulation protocol was established. Already low molar ratios of DMG-PEG effectively provided colloidal stabilization of polyplexes. mRNA could be formulated with XP 1621 and XP 1752 at an N/P 12 instead of 24. Previously non-formulatable carriers XP 1716 and XP 1613 could be successfully used in mRNA polyplexes.

Upon intravenous administration, nanoparticles are exposed to ionic stress, shear forces, elevated temperatures and extensive interactions with serum proteins. Aggregation of LAF-XP polyplexes under these conditions not only reduces delivery efficiency but also poses a serious biosafety risk. PEGylation effectively mitigated this instability. Regarding serum stability, the U-shape XP 1611 required stronger PEG anchoring, with 3% DSPE-PEG-N_3 providing robust stabilization. In contrast, for bundles XP 1621 and XP 1752, 3% DMG-PEG was sufficient to prevent aggregation and significantly reduce toxicity after intravenous administration.

Protein adsorption studies revealed that unmodified XP 1752 polyplexes bound substantially less serum protein than XP 1611, most likely due to their higher LAF content and lower surface charge. For both carriers, subsequent PEGylation quantitatively reduced protein adsorption. Further proteomic analysis identified fibrinogen as a key discriminating

protein, showing strong association with the more positively charged XP 1611 compared to XP 1752. PEGylation reduced the zeta potential and fibrinogen adsorption of XP 1611 to levels to unmodified XP 1752. However, PEGylation had little effect on fibrinogen adsorption of XP 1752, indicating that the LAF motif already provides an intrinsic shielding effect.

While PEGylation improves stability and biocompatibility, cellular uptake and endosomal escape can be impaired. In order to restore uptake and enable targeted delivery, DSPE-PEG-N_3 was used as a stable anchor for ligand conjugation via copper-free click chemistry. Conjugation of the EGFR-targeting peptide GE11 restored uptake and transfection of EGFR-expressing cells. Finally, the anchoring behavior of PEG lipids under physiological and endosomal conditions was investigated. Upon acidification, a sharp increase in zeta potential was observed, suggesting PEG lipid dissociation due to protonation of the LAF domain. This pH-triggered deshielding mechanism was further confirmed in stability assays, where PEGylated polyplexes pre-exposed to acidic conditions lost salt stability at neutral pH. Together, these results demonstrate that the PEG lipids remain stably anchored in the extracellular neutral environment, but are released under endosomal conditions.

6 APPENDIX

Abbreviations: The following abbreviations are used in this manuscript:

mRNA	Messenger ribonucleic acid
pDNA	Plasmid deoxyribonucleic acid
siRNA	Small interfering ribonucleic acid
DMG-PEG	1,2-dimyristoyl-rac-glycero-3-methoxypolyethylene glycol-2k
DSPE-PEG-N_3	1,2-distearoyl-sn-glycero-3-phosphoethanolamine-N [azido (polyethylene glycol)-2k]
DOPE	1,2-di-(9Z-octadecenoyl)-sn-glycero-3-phosphoethanolamine
DSPC	1,2-dioctadecanoyl-sn-glycero-3-phosphocholine
DLVO	Derjaguin–Landau–Verwey–Overbeek
i.v.	Intravenous
(SPAAC)	Strain-promoted azide-alkyne cycloaddition
DBCO	Dibenzocyclooctyne
AAV	adeno-associated viruses
LNP	Lipid nanoparticle
FDA	Food and drug administration
COVID-19	Coronavirus disease 2019
pHPMA	Poly(N-(2-hydroxypropyl)methacrylamide)
pOx	Poly(2-oxazoline)
apoE	Apolipoprotein E
LAF	Lipo-amino fatty acid
LAF-XP	Lipo-amino fatty acid- xenopeptide
SPPS	Solid-phase-assisted-peptide synthesis
Stp	Succinoyl tetraethylene pentamine
EGFR	Epidermal growth factor receptor
HEPES	4-(2-hydroxyethyl)-1-piperazineethansulfonic acid
HBG	HEPES-buffered glucose
PBS	Phosphate buffered saline
DLS	Dynamic light scattering
N2A	Neuro-2a cell line
HEPG2	Human hepatocellular carcinoma cell line
HUH7	Human hepatoma cell line
PDI	Polydispersity index
MTT	3-(4,5-dimethylthiazol-2-yl)-2,5-diphenyltetrazolium bromide
HPLC	High performance liquid chromatography

MALDI-TOF-MS	Matrix-assisted Laser Desorption/Ionization - time of flight – mass spectrometry
EtBr	Ethidium bromide
FGG	Fibrinogen
Csf1r	Colony stimulating factor 1 receptor
LDL	Low-density lipoprotein
ApoE	Apolipoprotein E
PEI	Polyethylenimine
NTA	Nanoparticle Tracking Analysis

7 REFERENCES

1. Pertea, M. and S. L. Salzberg. "Between a chicken and a grape: Estimating the number of human genes." *Genome Biology* 11 (2010): 206. 10.1186/gb-2010-11-5-206. https://doi.org/10.1186/gb-2010-11-5-206.
2. Amaral, P., S. Carbonell-Sala, F. M. De La Vega, T. Faial, A. Frankish, T. Gingeras, R. Guigo, J. L. Harrow, A. G. Hatzigeorgiou, R. Johnson, *et al.* "The status of the human gene catalogue." *Nature* 622 (2023): 41-47. 10.1038/s41586-023-06490-x.
3. Buccitelli, C. and M. Selbach. "Mrnas, proteins and the emerging principles of gene expression control." *Nature Reviews Genetics* 21 (2020): 630-44. 10.1038/s41576-020-0258-4. https://doi.org/10.1038/s41576-020-0258-4.
4. Cowling, V. H. "Regulation of mrna cap methylation." *Biochem J* 425 (2009): 295-302. 10.1042/BJ20091352. https://www.ncbi.nlm.nih.gov/pubmed/20025612.
5. Licatalosi, D. D. and R. B. Darnell. "Rna processing and its regulation: Global insights into biological networks." *Nat Rev Genet* 11 (2010): 75-87. 10.1038/nrg2673.
6. Hocine, S., R. H. Singer and D. Grunwald. "Rna processing and export." *Cold Spring Harb Perspect Biol* 2 (2010): a000752. 10.1101/cshperspect.a000752. https://www.ncbi.nlm.nih.gov/pubmed/20961978.
7. Tahmasebi, S., N. Sonenberg, J. W. B. Hershey and M. B. Mathews. "Protein synthesis and translational control: A historical perspective." *Cold Spring Harb Perspect Biol* 11 (2019): 10.1101/cshperspect.a035584. https://www.ncbi.nlm.nih.gov/pubmed/30082466.
8. Wang, Y. S., M. Kumari, G. H. Chen, M. H. Hong, J. P. Yuan, J. L. Tsai and H. C. Wu. "Mrna-based vaccines and therapeutics: An in-depth survey of current and upcoming clinical applications." *J Biomed Sci* 30 (2023): 84. 10.1186/s12929-023-00977-5. https://www.ncbi.nlm.nih.gov/pubmed/37805495.
9. Polack, F. P., S. J. Thomas, N. Kitchin, J. Absalon, A. Gurtman, S. Lockhart, J. L. Perez, G. Perez Marc, E. D. Moreira, C. Zerbini, *et al.* "Safety and efficacy of the bnt162b2 mrna covid-19 vaccine." *N Engl J Med* 383 (2020): 2603-15. 10.1056/NEJMoa2034577. https://www.ncbi.nlm.nih.gov/pubmed/33301246.
10. Administration, U. S. F. a. D. "Fda approval of moderna's mnexspike (mrna-1283)https://www.Fda.Gov/vaccines-blood-biologics/mnexspike?Utm_source=chatgpt.Com."
11. (EMA), E. M. A. "Mresvia: Epar, https://www.Ema.Europa.Eu/en/medicines/human/epar/mresvia?Utm_source=chatgpt.Com." 2025.
12. BioNTech. "Pipeline and products: Pipeline. N.D. ." https://www.biontech.com/int/en/home/pipeline-and-products/pipeline.html?search=bnt122.
13. Gillmore, J. D., E. Gane, J. Taubel, B. Pilebro, A. Echaniz-Laguna, J. Kao, W. Litchy, S. Shahda, A. Haagensen, L. Walsh, *et al.* "Nexiguran ziclumeran gene editing in hereditary attr with polyneuropathy." *N Engl J Med* (2025): 10.1056/NEJMoa2510209. https://www.ncbi.nlm.nih.gov/pubmed/41002250.
14. Therapy, A. S. o. G. C. "Landscape report 2025, q2. 2025, https://www.Asgct.Org/uploads/files/general/landscape-report-2025-q2.Pdf."
15. Pardi, N., M. J. Hogan, F. W. Porter and D. Weissman. "Mrna vaccines - a new era in vaccinology." *Nat Rev Drug Discov* 17 (2018): 261-79. 10.1038/nrd.2017.243. https://www.ncbi.nlm.nih.gov/pubmed/29326426.
16. Beckert, B. and B. Masquida. "Synthesis of rna by in vitro transcription." *Methods Mol Biol* 703 (2011): 29-41. 10.1007/978-1-59745-248-9_3.
17. O'Flaherty, R., A. Bergin, E. Flampouri, L. M. Mota, I. Obaidi, A. Quigley, Y. Xie and M. Butler. "Mammalian cell culture for production of recombinant proteins: A review of the

critical steps in their biomanufacturing." *Biotechnology Advances* 43 (2020): 107552. https://doi.org/10.1016/j.biotechadv.2020.107552.

18. Jayakrishnan, A., W. R. Wan Rosli, A. R. M. Tahir, F. S. A. Razak, P. E. Kee, H. S. Ng, Y.-L. Chew, S.-K. Lee, M. Ramasamy, C. S. Tan, *et al.* "Evolving paradigms of recombinant protein production in pharmaceutical industry: A rigorous review." *Sci* 6 (2024): 9. https://www.mdpi.com/2413-4155/6/1/9.
19. Brenner, S., F. Jacob and M. Meselson. "An unstable intermediate carrying information from genes to ribosomes for protein synthesis." *Nature* 190 (1961): 576-81. 10.1038/190576a0. https://www.ncbi.nlm.nih.gov/pubmed/20446365.
20. Wolff, J. A., R. W. Malone, P. Williams, W. Chong, G. Acsadi, A. Jani and P. L. Felgner. "Direct gene transfer into mouse muscle in vivo 726." *Science* 247 (1990): 1465-68.
21. Sahin, U., K. Kariko and O. Tureci. "Mrna-based therapeutics--developing a new class of drugs." *Nat Rev Drug Discov* 13 (2014): 759-80. 10.1038/nrd4278. https://www.ncbi.nlm.nih.gov/pubmed/25233993.
22. Alexopoulou, L., A. C. Holt, R. Medzhitov and R. A. Flavell. "Recognition of double-stranded rna and activation of nf-kappab by toll-like receptor 3." *Nature* 413 (2001): 732-8. 10.1038/35099560. https://www.ncbi.nlm.nih.gov/pubmed/11607032.
23. Heil, F., H. Hemmi, H. Hochrein, F. Ampenberger, C. Kirschning, S. Akira, G. Lipford, H. Wagner and S. Bauer. "Species-specific recognition of single-stranded rna via toll-like receptor 7 and 8." *Science* 303 (2004): 1526-9. 10.1126/science.1093620. https://www.ncbi.nlm.nih.gov/pubmed/14976262.
24. Kariko, K., M. Buckstein, H. Ni and D. Weissman. "Suppression of rna recognition by toll-like receptors: The impact of nucleoside modification and the evolutionary origin of rna." *Immunity* 23 (2005): 165-75. 10.1016/j.immuni.2005.06.008. https://www.ncbi.nlm.nih.gov/pubmed/16111635.
25. Kato, H., O. Takeuchi, S. Sato, M. Yoneyama, M. Yamamoto, K. Matsui, S. Uematsu, A. Jung, T. Kawai, K. J. Ishii, *et al.* "Differential roles of mda5 and rig-i helicases in the recognition of rna viruses." *Nature* 441 (2006): 101-5. 10.1038/nature04734. https://www.ncbi.nlm.nih.gov/pubmed/16625202.
26. Yoneyama, M., M. Kikuchi, T. Natsukawa, N. Shinobu, T. Imaizumi, M. Miyagishi, K. Taira, S. Akira and T. Fujita. "The rna helicase rig-i has an essential function in double-stranded rna-induced innate antiviral responses." *Nat Immunol* 5 (2004): 730-7. 10.1038/ni1087. https://www.ncbi.nlm.nih.gov/pubmed/15208624.
27. Houseley, J. and D. Tollervey. "The many pathways of rna degradation." *Cell* 136 (2009): 763-76. 10.1016/j.cell.2009.01.019. https://www.ncbi.nlm.nih.gov/pubmed/19239894.
28. Kariko, K., H. Muramatsu, F. A. Welsh, J. Ludwig, H. Kato, S. Akira and D. Weissman. "Incorporation of pseudouridine into mrna yields superior nonimmunogenic vector with increased translational capacity and biological stability." *Mol Ther* 16 (2008): 1833-40. 10.1038/mt.2008.200. https://www.ncbi.nlm.nih.gov/pubmed/18797453.
29. Shanmugasundaram, M., A. Senthilvelan and A. R. Kore. "Recent advances in modified cap analogs: Synthesis, biochemical properties, and mrna based vaccines." *Chem Rec* 22 (2022): e202200005. 10.1002/tcr.202200005.
30. Galloway, A. and V. H. Cowling. "Mrna cap regulation in mammalian cell function and fate." *Biochim Biophys Acta Gene Regul Mech* 1862 (2019): 270-79. 10.1016/j.bbagrm.2018.09.011. https://www.ncbi.nlm.nih.gov/pubmed/30312682.
31. Devarkar, S. C., C. Wang, M. T. Miller, A. Ramanathan, F. Jiang, A. G. Khan, S. S. Patel and J. Marcotrigiano. "Structural basis for m7g recognition and 2'-o-methyl discrimination in capped rnas by the innate immune receptor rig-i." *Proc Natl Acad Sci U S A* 113 (2016): 596-601. 10.1073/pnas.1515152113. https://www.ncbi.nlm.nih.gov/pubmed/26733676.

32. Szabó, G. T., A. J. Mahiny and I. Vlatkovic. "Covid-19 mrna vaccines: Platforms and current developments." *Molecular Therapy* 30 (2022): 1850-68. https://doi.org/10.1016/j.ymthe.2022.02.016.
33. Jalkanen, A. L., S. J. Coleman and J. Wilusz. "Determinants and implications of mrna poly(a) tail size--does this protein make my tail look big?" *Semin Cell Dev Biol* 34 (2014): 24-32. 10.1016/j.semcdb.2014.05.018. https://www.ncbi.nlm.nih.gov/pubmed/24910447.
34. Park, J. E., H. Yi, Y. Kim, H. Chang and V. N. Kim. "Regulation of poly(a) tail and translation during the somatic cell cycle." *Mol Cell* 62 (2016): 462-71. 10.1016/j.molcel.2016.04.007. https://www.ncbi.nlm.nih.gov/pubmed/27153541.
35. Schlake, T., A. Thess, M. Fotin-Mleczek and K. J. Kallen. "Developing mrna-vaccine technologies." *RNA Biol* 9 (2012): 1319-30. 10.4161/rna.22269. https://www.ncbi.nlm.nih.gov/pubmed/23064118.
36. Bulcha, J. T., Y. Wang, H. Ma, P. W. L. Tai and G. Gao. "Viral vector platforms within the gene therapy landscape." *Signal Transduct Target Ther* 6 (2021): 53. 10.1038/s41392-021-00487-6. https://www.ncbi.nlm.nih.gov/pubmed/33558455.
37. Wang, J. H., D. J. Gessler, W. Zhan, T. L. Gallagher and G. Gao. "Adeno-associated virus as a delivery vector for gene therapy of human diseases." *Signal Transduct Target Ther* 9 (2024): 78. 10.1038/s41392-024-01780-w. https://www.ncbi.nlm.nih.gov/pubmed/38565561.
38. Yuan, M., Z. Han, Y. Liang, Y. Sun, B. He, W. Chen and F. Li. "Mrna nanodelivery systems: Targeting strategies and administration routes." *Biomater Res* 27 (2023): 90. 10.1186/s40824-023-00425-3. https://www.ncbi.nlm.nih.gov/pubmed/37740246.
39. Gautam, M., A. Jozic, G. L. Su, M. Herrera-Barrera, A. Curtis, S. Arrizabalaga, W. Tschetter, R. C. Ryals and G. Sahay. "Lipid nanoparticles with peg-variant surface modifications mediate genome editing in the mouse retina." *Nat Commun* 14 (2023): 6468. 10.1038/s41467-023-42189-3. https://www.ncbi.nlm.nih.gov/pubmed/37833442.
40. Yong, H., Y. Tian, Z. Li, C. Wang, D. Zhou, J. Liu, X. Huang and J. Li. "Highly branched poly(β-amino ester)s for efficient mrna delivery and nebulization treatment of silicosis." *Advanced Materials* 37 (2025): 2414991. https://doi.org/10.1002/adma.202414991. https://advanced.onlinelibrary.wiley.com/doi/abs/10.1002/adma.202414991.
41. Wen, H., Q. Yu, Y. Yin, W. Pan, S. Yang and D. Liang. "Shear effects on stability of DNA complexes in the presence of serum." *Biomacromolecules* 18 (2017): 3252-59. 10.1021/acs.biomac.7b00900. https://www.ncbi.nlm.nih.gov/pubmed/28826209.
42. Yin, D., H. Wen, G. Wu, S. Li, C. Liu, H. Lu and D. Liang. "Pegylated gene carriers in serum under shear flow." *Soft Matter* 16 (2020): 2301-10. 10.1039/c9sm02397f. https://www.ncbi.nlm.nih.gov/pubmed/32052004.
43. Chollet, P., M. C. Favrot, A. Hurbin and J. L. Coll. "Side-effects of a systemic injection of linear polyethylenimine-DNA complexes." *J Gene Med* 4 (2002): 84-91. 10.1002/jgm.237 [pii]. http://www.ncbi.nlm.nih.gov/entrez/query.fcgi?cmd=Retrieve&db=PubMed&dopt=Citation&list_uids=11828391.
44. Agmo Hernández, V. "An overview of surface forces and the dlvo theory." *ChemTexts* 9 (2023): 10. 10.1007/s40828-023-00182-9. https://doi.org/10.1007/s40828-023-00182-9.
45. Stern, O. "Zur theorie der elektrolytischen doppelschicht." *Zeitschrift für Elektrochemie und angewandte physikalische Chemie* (1924): https:// doi. org/ 10.1002/ bbpc. 19240 0182.
46. Takeda, K. M., Y. Yamasaki, A. Dirisala, S. Ikeda, T. A. Tockary, K. Toh, K. Osada and K. Kataoka. "Effect of shear stress on structure and function of polyplex micelles from poly(ethylene glycol)-poly(l-lysine) block copolymers as systemic gene delivery carrier." *Biomaterials* 126 (2017): 31-38. 10.1016/j.biomaterials.2017.02.012. https://www.ncbi.nlm.nih.gov/pubmed/28254691.

47. De Gennes, P. G. "Polymer solutions near an interface. Adsorption and depletion layers." *Macromolecules* 14 (1981): 1637-44. 10.1021/ma50007a007. https://doi.org/10.1021/ma50007a007.
48. Ahsan, S. M., C. M. Rao and M. F. Ahmad. "Nanoparticle-protein interaction: The significance and role of protein corona." *Adv Exp Med Biol* 1048 (2018): 175-98. 10.1007/978-3-319-72041-8_11. https://www.ncbi.nlm.nih.gov/pubmed/29453539.
49. Corbo, C., R. Molinaro, A. Parodi, N. E. Toledano Furman, F. Salvatore and E. Tasciotti. "The impact of nanoparticle protein corona on cytotoxicity, immunotoxicity and target drug delivery." *Nanomedicine (Lond)* 11 (2016): 81-100. 10.2217/nnm.15.188. https://www.ncbi.nlm.nih.gov/pubmed/26653875.
50. Treuel, L. and G. U. Nienhaus. "Toward a molecular understanding of nanoparticle-protein interactions." *Biophys Rev* 4 (2012): 137-47. 10.1007/s12551-012-0072-0. https://www.ncbi.nlm.nih.gov/pubmed/28510093.
51. Barz, M., W. J. Parak and R. Zentel. "Concepts and approaches to reduce or avoid protein corona formation on nanoparticles: Challenges and opportunities." *Adv Sci (Weinh)* 11 (2024): e2402935. 10.1002/advs.202402935. https://www.ncbi.nlm.nih.gov/pubmed/38976560.
52. Ahmadi, M., S. M. Ayyoubzadeh, S. A. Ardekani, Z. Ghaedrahmat, N. Masoumi, M. M. Farnia and F. Ghorbani-Bidkorpeh. "A review on protein corona formation on nanoparticles and prediction of its composition using artificial intelligence tools." *Int J Pharm* 683 (2025): 126094. 10.1016/j.ijpharm.2025.126094. https://www.ncbi.nlm.nih.gov/pubmed/40840810.
53. Dawson, K. A. and Y. Yan. "Current understanding of biological identity at the nanoscale and future prospects." *Nat Nanotechnol* 16 (2021): 229-42. 10.1038/s41565-021-00860-0. https://www.ncbi.nlm.nih.gov/pubmed/33597736.
54. Vroman, L. and A. L. Adams. "Identification of rapid changes at plasma-solid interfaces." *J Biomed Mater Res* 3 (1969): 43-67. 10.1002/jbm.820030106. https://www.ncbi.nlm.nih.gov/pubmed/5784967.
55. Elechalawar, C. K., M. N. Hossen, L. McNally, R. Bhattacharya and P. Mukherjee. "Analysing the nanoparticle-protein corona for potential molecular target identification." *J Control Release* 322 (2020): 122-36. 10.1016/j.jconrel.2020.03.008. https://www.ncbi.nlm.nih.gov/pubmed/32165239.
56. Lee, Y. K., E. J. Choi, T. J. Webster, S. H. Kim and D. Khang. "Effect of the protein corona on nanoparticles for modulating cytotoxicity and immunotoxicity." *Int J Nanomedicine* 10 (2015): 97-113. 10.2147/IJN.S72998. https://www.ncbi.nlm.nih.gov/pubmed/25565807.
57. Panico, S., S. Capolla, S. Bozzer, G. Toffoli, M. Dal Bo and P. Macor. "Biological features of nanoparticles: Protein corona formation and interaction with the immune system." *Pharmaceutics* 14 (2022): 10.3390/pharmaceutics14122605. https://www.ncbi.nlm.nih.gov/pubmed/36559099.
58. Tirosh, O., Y. Barenholz, J. Katzhendler and A. Priev. "Hydration of polyethylene glycol-grafted liposomes." *Biophys J* 74 (1998): 1371-9. 10.1016/S0006-3495(98)77849-X. https://www.ncbi.nlm.nih.gov/pubmed/9512033.
59. Abuchowski, A., J. R. McCoy, N. C. Palczuk, T. van Es and F. F. Davis. "Effect of covalent attachment of polyethylene glycol on immunogenicity and circulating life of bovine liver catalase." *J Biol Chem* 252 (1977): 3582-6. https://www.ncbi.nlm.nih.gov/pubmed/16907.
60. Owens, D. E., 3rd and N. A. Peppas. "Opsonization, biodistribution, and pharmacokinetics of polymeric nanoparticles." *Int J Pharm* 307 (2006): 93-102. 10.1016/j.ijpharm.2005.10.010. https://www.ncbi.nlm.nih.gov/pubmed/16303268.

61. Gref, R., M. Luck, P. Quellec, M. Marchand, E. Dellacherie, S. Harnisch, T. Blunk and R. H. Muller. "'Stealth' corona-core nanoparticles surface modified by polyethylene glycol (peg): Influences of the corona (peg chain length and surface density) and of the core composition on phagocytic uptake and plasma protein adsorption." *Colloids Surf B Biointerfaces* 18 (2000): 301-13. 10.1016/s0927-7765(99)00156-3. https://www.ncbi.nlm.nih.gov/pubmed/10915952.
62. Heyes, C. D., A. Y. Kobitski, E. V. Amirgoulova and G. U. Nienhaus. "Biocompatible surfaces for specific tethering of individual protein molecules." *The Journal of Physical Chemistry B* 108 (2004): 13387-94. 10.1021/jp049057o. https://doi.org/10.1021/jp049057o.
63. Vonarbourg, A., C. Passirani, P. Saulnier and J. P. Benoit. "Parameters influencing the stealthiness of colloidal drug delivery systems." *Biomaterials* 27 (2006): 4356-73. 10.1016/j.biomaterials.2006.03.039. https://www.ncbi.nlm.nih.gov/pubmed/16650890.
64. Kumar, R., C. F. Santa Chalarca, M. R. Bockman, C. V. Bruggen, C. J. Grimme, R. J. Dalal, M. G. Hanson, J. K. Hexum and T. M. Reineke. "Polymeric delivery of therapeutic nucleic acids." *Chem Rev* 121 (2021): 11527-652. 10.1021/acs.chemrev.0c00997. https://www.ncbi.nlm.nih.gov/pubmed/33939409.
65. Papahadjopoulos, D., T. M. Allen, A. Gabizon, E. Mayhew, K. Matthay, S. K. Huang, K. D. Lee, M. C. Woodle, D. D. Lasic, C. Redemann, *et al.* "Sterically stabilized liposomes: Improvements in pharmacokinetics and antitumor therapeutic efficacy." *Proc Natl Acad Sci U S A* 88 (1991): 11460-4. 10.1073/pnas.88.24.11460. https://www.ncbi.nlm.nih.gov/pubmed/1763060.
66. Gabizon, A. and D. Papahadjopoulos. "Liposome formulations with prolonged circulation time in blood and enhanced uptake by tumors." *Proc Natl Acad Sci U S A* 85 (1988): 6949-53. 10.1073/pnas.85.18.6949. https://www.ncbi.nlm.nih.gov/pubmed/3413128.
67. Allen, T. M. "Long-circulating (sterically stabilized) liposomes for targeted drug delivery." *Trends Pharmacol Sci* 15 (1994): 215-20. 10.1016/0165-6147(94)90314-x. https://www.ncbi.nlm.nih.gov/pubmed/7940982.
68. Philipp, J., A. Dabkowska, A. Reiser, K. Frank, R. Krzyszton, C. Brummer, B. Nickel, C. E. Blanchet, A. Sudarsan, M. Ibrahim, *et al.* "Ph-dependent structural transitions in cationic ionizable lipid mesophases are critical for lipid nanoparticle function." *Proc Natl Acad Sci U S A* 120 (2023): e2310491120. 10.1073/pnas.2310491120. https://www.ncbi.nlm.nih.gov/pubmed/38055742.
69. Yanez Arteta, M., T. Kjellman, S. Bartesaghi, S. Wallin, X. Wu, A. J. Kvist, A. Dabkowska, N. Szekely, A. Radulescu, J. Bergenholtz, *et al.* "Successful reprogramming of cellular protein production through mrna delivered by functionalized lipid nanoparticles." *Proc Natl Acad Sci U S A* 115 (2018): E3351-E60. 10.1073/pnas.1720542115. https://www.ncbi.nlm.nih.gov/pubmed/29588418.
70. Tockary, T. A., K. Osada, Q. Chen, K. Machitani, A. Dirisala, S. Uchida, T. Nomoto, K. Toh, Y. Matsumoto, K. Itaka, *et al.* "Tethered peg crowdedness determining shape and blood circulation profile of polyplex micelle gene carriers." *Macromolecules* 46 (2013): 6585-92. 10.1021/ma401093z. https://doi.org/10.1021/ma401093z.
71. Walker, G. F., C. Fella, J. Pelisek, J. Fahrmeir, S. Boeckle, M. Ogris and E. Wagner. "Toward synthetic viruses: Endosomal ph-triggered deshielding of targeted polyplexes greatly enhances gene transfer in vitro and in vivo." *Mol Ther* 11 (2005): 418-25. 10.1016/j.ymthe.2004.11.006.
72. Hatakeyama, H., H. Akita and H. Harashima. "A multifunctional envelope type nano device (mend) for gene delivery to tumours based on the epr effect: A strategy for overcoming the peg dilemma." *Adv Drug Deliv Rev* 63 (2011): 152-60. 10.1016/j.addr.2010.09.001.
73. Wang, T., J. R. Upponi and V. P. Torchilin. "Design of multifunctional non-viral gene vectors to overcome physiological barriers: Dilemmas and strategies." *Int J Pharm* 427

(2012): 3-20. 10.1016/j.ijpharm.2011.07.013. https://www.ncbi.nlm.nih.gov/pubmed/21798324.

74. Hatakeyama, H., H. Akita, K. Kogure, M. Oishi, Y. Nagasaki, Y. Kihira, M. Ueno, H. Kobayashi, H. Kikuchi and H. Harashima. "Development of a novel systemic gene delivery system for cancer therapy with a tumor-specific cleavable peg-lipid." *Gene Ther* 14 (2007): 68-77. PM:16915290.
75. Takae, S., K. Miyata, M. Oba, T. Ishii, N. Nishiyama, K. Itaka, Y. Yamasaki, H. Koyama and K. Kataoka. "Peg-detachable polyplex micelles based on disulfide-linked block catiomers as bioresponsive nonviral gene vectors." *J Am Chem Soc* 130 (2008): 6001-09. PM:18396871.
76. Guo, X., J. A. MacKay and F. C. Szoka, Jr. "Mechanism of ph-triggered collapse of phosphatidylethanolamine liposomes stabilized by an ortho ester polyethyleneglycol lipid." *Biophys J* 84 (2003): 1784-95. 10.1016/s0006-3495(03)74986-8. https://www.ncbi.nlm.nih.gov/pubmed/12609880.
77. Murthy, N., J. Campbell, N. Fausto, A. S. Hoffman and P. S. Stayton. "Design and synthesis of ph-responsive polymeric carriers that target uptake and enhance the intracellular delivery of oligonucleotides." *J.Control Release* 89 (2003): 365-74. PM:12737839.
78. Fella, C., G. F. Walker, M. Ogris and E. Wagner. "Amine-reactive pyridylhydrazone-based peg reagents for ph-reversible pei polyplex shielding." *Eur J Pharm Sci* 34 (2008): 309-20. 10.1016/j.ejps.2008.05.004.
79. Nie, Y., M. Günther, Z. Gu and E. Wagner. "Pyridylhydrazone-based pegylation for ph-reversible lipopolyplex shielding." *Biomaterials* 32 (2011): 858-69. https://doi.org/10.1016/j.biomaterials.2010.09.032.
80. Chaudhary, N., L. N. Kasiewicz, A. N. Newby, M. L. Arral, S. S. Yerneni, J. R. Melamed, S. T. LoPresti, K. C. Fein, D. M. Strelkova Petersen, S. Kumar, *et al.* "Amine headgroups in ionizable lipids drive immune responses to lipid nanoparticles by binding to the receptors tlr4 and cd1d." *Nat Biomed Eng* 8 (2024): 1483-98. 10.1038/s41551-024-01256-w. https://www.ncbi.nlm.nih.gov/pubmed/39363106.
81. Dash, P. R., M. L. Read, K. D. Fisher, K. A. Howard, M. Wolfert, D. Oupicky, V. Subr, J. Strohalm, K. Ulbrich and L. W. Seymour. "Decreased binding to proteins and cells of polymeric gene delivery vectors surface modified with a multivalent hydrophilic polymer and retargeting through attachment of transferrin." *J.Biol.Chem.* 275 (2000): 3793-802. PM:0010660529.
82. Burke, R. S. and S. H. Pun. "Synthesis and characterization of biodegradable hpma-oligolysine copolymers for improved gene delivery." *Bioconjug Chem* 21 (2010): 140-50. 10.1021/bc9003662. https://www.ncbi.nlm.nih.gov/pubmed/19968270.
83. Gaspar, V. M., C. Goncalves, D. de Melo-Diogo, E. C. Costa, J. A. Queiroz, C. Pichon, F. Sousa and I. J. Correia. "Poly(2-ethyl-2-oxazoline)-pla-g-pei amphiphilic triblock micelles for co-delivery of minicircle DNA and chemotherapeutics." *J Control Release* 189 (2014): 90-104. 10.1016/j.jconrel.2014.06.040. https://www.ncbi.nlm.nih.gov/pubmed/24984013.
84. Yamaleyeva, D. N., N. Makita, D. Hwang, M. J. Haney, R. Jordan and A. V. Kabanov. "Poly(2-oxazoline)-based polyplexes as a peg-free plasmid DNA delivery platform." *Macromol Biosci* 23 (2023): e2300177. 10.1002/mabi.202300177. https://www.ncbi.nlm.nih.gov/pubmed/37466165.
85. Heller, P., A. Birke, D. Huesmann, B. Weber, K. Fischer, A. Reske-Kunz, M. Bros and M. Barz. "Introducing peptoplexes: Polylysine-block-polysarcosine based polyplexes for transfection of hek 293t cells." *Macromol Biosci* 14 (2014): 1380-95. 10.1002/mabi.201400167.

86. Klein, P. M., K. Klinker, W. Zhang, S. Kern, E. Kessel, E. Wagner and M. Barz. "Efficient shielding of polyplexes using heterotelechelic polysarcosines." *Polymers (Basel)* 10 (2018): 10.3390/polym10060689.
87. Bayraktutan, H., R. J. Kopiasz, A. Elsherbeny, M. Martinez Espuga, N. Gumus, U. C. Oz, K. Polra, P. F. McKay, R. J. Shattock, P. Ordóñez-Morán, *et al.* "Polysarcosine functionalised cationic polyesters efficiently deliver self-amplifying mrna." *Polymer Chemistry* 15 (2024): 1862-76. 10.1039/D4PY00064A. http://dx.doi.org/10.1039/D4PY00064A.
88. Felgner, P. L., Y. Barenholz, J. P. Behr, S. H. Cheng, P. Cullis, L. Huang, J. A. Jessee, L. Seymour, F. Szoka, A. R. Thierry, *et al.* "Nomenclature for synthetic gene delivery systems." *Hum Gene Ther* 8 (1997): 511-2. 10.1089/hum.1997.8.5-511.
89. van der Meel, R., P. A. Wender, O. M. Merkel, I. Lostalé-Seijo, J. Montenegro, A. Miserez, Q. Laurent, H. Sleiman and P. Luciani. "Next-generation materials for nucleic acid delivery." *Nature Reviews Materials* 10 (2025): 490-99. 10.1038/s41578-025-00814-1. https://doi.org/10.1038/s41578-025-00814-1.
90. Witten, J., Y. Hu, R. Langer and D. G. Anderson. "Recent advances in nanoparticulate rna delivery systems." *Proc Natl Acad Sci U S A* 121 (2024): e2307798120. 10.1073/pnas.2307798120. https://www.ncbi.nlm.nih.gov/pubmed/38437569.
91. Berger, S., U. Lachelt and E. Wagner. "Dynamic carriers for therapeutic rna delivery." *Proc Natl Acad Sci U S A* 121 (2024): e2307799120. 10.1073/pnas.2307799120. https://www.ncbi.nlm.nih.gov/pubmed/38437544.
92. Freitag, F. and E. Wagner. "Optimizing synthetic nucleic acid and protein nanocarriers: The chemical evolution approach." *Adv Drug Deliv Rev* 168 (2021): 30-54. 10.1016/j.addr.2020.03.005.
93. Luo, T., H. Liang, R. Jin and Y. Nie. "Virus inspired and mimetic designs in nonviral gene delivery." *J Gene Med* (2019): e3090. 10.1002/jgm.3090.
94. Anderson, D. G., D. M. Lynn and R. Langer. "Semi-automated synthesis and screening of a large library of degradable cationic polymers for gene delivery." *Angew.Chem.Int.Ed Engl.* 42 (2003): 3153-58. PM:12866105.
95. Itaka, K., A. Harada, Y. Yamasaki, K. Nakamura, H. Kawaguchi and K. Kataoka. "In situ single cell observation by fluorescence resonance energy transfer reveals fast intra-cytoplasmic delivery and easy release of plasmid DNA complexed with linear polyethylenimine." *J Gene Med* 6 (2004): 76-84. PM:14716679.
96. Pack, D. W., A. S. Hoffman, S. Pun and P. S. Stayton. "Design and development of polymers for gene delivery." *Nat.Rev.Drug Discov.* 4 (2005): 581-93. PM:16052241.
97. Miyata, K., N. Nishiyama and K. Kataoka. "Rational design of smart supramolecular assemblies for gene delivery: Chemical challenges in the creation of artificial viruses." *Chem Soc Rev* 41 (2012): 2562-74. 10.1039/c1cs15258k.
98. Lachelt, U. and E. Wagner. "Nucleic acid therapeutics using polyplexes: A journey of 50 years (and beyond)." *Chem Rev* 115 (2015): 11043-78. 10.1021/cr5006793.
99. Dirisala, A., S. Uchida, J. Li, J. F. R. Van Guyse, K. Hayashi, S. V. C. Vummaleti, S. Kaur, Y. Mochida, S. Fukushima and K. Kataoka. "Effective mrna protection by poly(l-ornithine) synergizes with endosomal escape functionality of a charge-conversion polymer toward maximizing mrna introduction efficiency." *Macromol Rapid Commun* 43 (2022): e2100754. 10.1002/marc.202100754.
100. Nabel, G. J., E. G. Nabel, Z. Y. Yang, B. A. Fox, G. E. Plautz, X. Gao, L. Huang, S. Shu, D. Gordon and A. E. Chang. "Direct gene transfer with DNA-liposome complexes in melanoma: Expression, biologic activity, and lack of toxicity in humans." *Proc Natl Acad Sci U S A* 90 (1993): 11307-11. 10.1073/pnas.90.23.11307.

101. Sakurai, Y., H. Hatakeyama, Y. Sato, M. Hyodo, H. Akita and H. Harashima. "Gene silencing via rnai and sirna quantification in tumor tissue using mend, a liposomal sirna delivery system." *Mol Ther* 21 (2013): 1195-203. 10.1038/mt.2013.57.
102. Cullis, P. R. and P. L. Felgner. "The 60-year evolution of lipid nanoparticles for nucleic acid delivery." *Nat Rev Drug Discov* 23 (2024): 709-22. 10.1038/s41573-024-00977-6.
103. Lin, Y., M. Li, Z. Luo, Y. Meng, Y. Zong, H. Ren, X. Yu, X. Tan, F. Liu, T. Wei, *et al.* "Tissue-specific mrna delivery and prime editing with peptide-ionizable lipid nanoparticles." *Nat Mater* (2025): 10.1038/s41563-025-02320-9. https://www.ncbi.nlm.nih.gov/pubmed/40890498.
104. Verbeke, R., I. Lentacker, S. C. De Smedt and H. Dewitte. "The dawn of mrna vaccines: The covid-19 case." *J Control Release* 333 (2021): 511-20. 10.1016/j.jconrel.2021.03.043. https://www.ncbi.nlm.nih.gov/pubmed/33798667.
105. Schoenmaker, L., D. Witzigmann, J. A. Kulkarni, R. Verbeke, G. Kersten, W. Jiskoot and D. J. A. Crommelin. "Mrna-lipid nanoparticle covid-19 vaccines: Structure and stability." *Int J Pharm* 601 (2021): 120586. 10.1016/j.ijpharm.2021.120586.
106. Han, X., H. Zhang, K. Butowska, K. L. Swingle, M. G. Alameh, D. Weissman and M. J. Mitchell. "An ionizable lipid toolbox for rna delivery." *Nat Commun* 12 (2021): 7233. 10.1038/s41467-021-27493-0. https://www.ncbi.nlm.nih.gov/pubmed/34903741.
107. Cullis, P. R. and M. J. Hope. "Effects of fusogenic agent on membrane structure of erythrocyte ghosts and the mechanism of membrane fusion." *Nature* 271 (1978): 672-4. 10.1038/271672a0. https://www.ncbi.nlm.nih.gov/pubmed/625336.
108. Farhood, H., N. Serbina and L. Huang. "The role of dioleoyl phosphatidylethanolamine in cationic liposome mediated gene transfer." *Biochim Biophys Acta* 1235 (1995): 289-95. 10.1016/0005-2736(95)80016-9. https://www.ncbi.nlm.nih.gov/pubmed/7756337.
109. Hafez, I. M., N. Maurer and P. R. Cullis. "On the mechanism whereby cationic lipids promote intracellular delivery of polynucleic acids." *Gene Ther* 8 (2001): 1188-96. PM:11509950.
110. Cullis, P. R. and B. de Kruijff. "Lipid polymorphism and the functional roles of lipids in biological membranes." *Biochim Biophys Acta* 559 (1979): 399-420. 10.1016/0304-4157(79)90012-1. https://www.ncbi.nlm.nih.gov/pubmed/391283.
111. Pozzi, D., F. Cardarelli, F. Salomone, C. Marchini, H. Amenitsch, G. L. Barbera and G. Caracciolo. "Role of cholesterol on the transfection barriers of cationic lipid/DNA complexes." *Applied Physics Letters* 105 (2014): 10.1063/1.4892915. https://doi.org/10.1063/1.4892915.
112. Cheng, X. and R. J. Lee. "The role of helper lipids in lipid nanoparticles (lnps) designed for oligonucleotide delivery." *Adv Drug Deliv Rev* 99 (2016): 129-37. 10.1016/j.addr.2016.01.022. https://www.ncbi.nlm.nih.gov/pubmed/26900977.
113. Hou, X., T. Zaks, R. Langer and Y. Dong. "Lipid nanoparticles for mrna delivery." *Nat Rev Mater* 6 (2021): 1078-94. 10.1038/s41578-021-00358-0. https://www.ncbi.nlm.nih.gov/pubmed/34394960.
114. Kim, J., Y. Eygeris, M. Gupta and G. Sahay. "Self-assembled mrna vaccines." *Adv Drug Deliv Rev* 170 (2021): 83-112. 10.1016/j.addr.2020.12.014. https://www.ncbi.nlm.nih.gov/pubmed/33400957.
115. Lokugamage, M. P., D. Vanover, J. Beyersdorf, M. Z. C. Hatit, L. Rotolo, E. S. Echeverri, H. E. Peck, H. Ni, J. K. Yoon, Y. Kim, *et al.* "Optimization of lipid nanoparticles for the delivery of nebulized therapeutic mrna to the lungs." *Nat Biomed Eng* 5 (2021): 1059-68. 10.1038/s41551-021-00786-x. https://www.ncbi.nlm.nih.gov/pubmed/34616046.
116. Hald Albertsen, C., J. A. Kulkarni, D. Witzigmann, M. Lind, K. Petersson and J. B. Simonsen. "The role of lipid components in lipid nanoparticles for vaccines and gene

therapy." *Adv Drug Deliv Rev* 188 (2022): 114416. 10.1016/j.addr.2022.114416. https://www.ncbi.nlm.nih.gov/pubmed/35787388.

117. Chen, S., Y. Y. C. Tam, P. J. C. Lin, M. M. H. Sung, Y. K. Tam and P. R. Cullis. "Influence of particle size on the in vivo potency of lipid nanoparticle formulations of sirna." *J Control Release* 235 (2016): 236-44. 10.1016/j.jconrel.2016.05.059. https://www.ncbi.nlm.nih.gov/pubmed/27238441.
118. Harvie, P., F. M. Wong and M. B. Bally. "Use of poly(ethylene glycol)-lipid conjugates to regulate the surface attributes and transfection activity of lipid-DNA particles." *J Pharm Sci* 89 (2000): 652-63. 10.1002/(SICI)1520-6017(200005)89:5<652::AID-JPS11>3.0.CO;2-H. https://www.ncbi.nlm.nih.gov/pubmed/10756331.
119. Mui, B. L., Y. K. Tam, M. Jayaraman, S. M. Ansell, X. Du, Y. Y. Tam, P. J. Lin, S. Chen, J. K. Narayanannair, K. G. Rajeev, *et al.* "Influence of polyethylene glycol lipid desorption rates on pharmacokinetics and pharmacodynamics of sirna lipid nanoparticles." *Mol Ther Nucleic Acids* 2 (2013): e139. 10.1038/mtna.2013.66. https://www.ncbi.nlm.nih.gov/pubmed/24345865.
120. Waggoner, L. E., K. F. Miyasaki and E. J. Kwon. "Analysis of peg-lipid anchor length on lipid nanoparticle pharmacokinetics and activity in a mouse model of traumatic brain injury." *Biomater Sci* 11 (2023): 4238-53. 10.1039/d2bm01846b. https://www.ncbi.nlm.nih.gov/pubmed/36987922.
121. Suzuki, T., Y. Suzuki, T. Hihara, K. Kubara, K. Kondo, K. Hyodo, K. Yamazaki, T. Ishida and H. Ishihara. "Peg shedding-rate-dependent blood clearance of pegylated lipid nanoparticles in mice: Faster peg shedding attenuates anti-peg igm production." *Int J Pharm* 588 (2020): 119792. 10.1016/j.ijpharm.2020.119792. https://www.ncbi.nlm.nih.gov/pubmed/32827675.
122. Zhou, X. H., A. L. Klibanov and L. Huang. "Lipophilic polylysines mediate efficient DNA transfection in mammalian cells." *Biochim Biophys Acta* 1065 (1991): 8-14.
123. Emi, N., S. Kidoaki, K. Yoshikawa and H. Saito. "Gene transfer mediated by polyarginine requires a formation of big carrier-complex of DNA aggregate 1." *Biochem.Biophys.Res.Commun.* 231 (1997): 421-24. PM:9070292.
124. Kichler, A., C. Leborgne, E. Coeytaux and O. Danos. "Polyethylenimine-mediated gene delivery: A mechanistic study." *J Gene Med* 3 (2001): 135-44. PM:11318112.
125. Plank, C., K. Mechtler, F. C. Szoka, Jr. and E. Wagner. "Activation of the complement system by synthetic DNA complexes: A potential barrier for intravenous gene delivery." *Hum Gene Ther* 7 (1996): 1437-46. 10.1089/hum.1996.7.12-1437.
126. Merkel, O. M., R. Urbanics, P. Bedocs, Z. Rozsnyay, L. Rosivall, M. Toth, T. Kissel and J. Szebeni. "In vitro and in vivo complement activation and related anaphylactic effects associated with polyethylenimine and polyethylenimine-graft-poly(ethylene glycol) block copolymers." *Biomaterials* 32 (2011): 4936-42. 10.1016/j.biomaterials.2011.03.035.
127. Mosqueira, V. C. F., P. Legrand, A. Gulik, O. Bourdon, R. Gref, D. Labarre and G. Barratt. "Relationship between complement activation, cellular uptake and surface physicochemical aspects of novel peg-modified nanocapsules." *Biomaterials* 22 (2001): 2967-79. https://doi.org/10.1016/S0142-9612(01)00043-6.
128. Hong, K., W. Zheng, A. Baker and D. Papahadjopoulos. "Stabilization of cationic liposome-plasmid DNA complexes by polyamines and poly(ethylene glycol)-phospholipid conjugates for efficient in vivo gene delivery." *FEBS Lett* 400 (1997): 233-7. 10.1016/s0014-5793(96)01397-x.
129. Wheeler, J. J., L. Palmer, M. Ossanlou, I. MacLachlan, R. W. Graham, Y. P. Zhang, M. J. Hope, P. Scherrer and P. R. Cullis. "Stabilized plasmid-lipid particles: Construction and characterization." *Gene Ther.* 6 (1999): 271-81. PM:10435112.

130. Katayose, S. and K. Kataoka. "Water-soluble polyion complex associates of DNA and poly(ethylene glycol)-poly(l-lysine) block copolymer." *Bioconjug Chem* 8 (1997): 702-7. 10.1021/bc9701306. https://www.ncbi.nlm.nih.gov/pubmed/9327134.
131. Ogris, M., S. Brunner, S. Schuller, R. Kircheis and E. Wagner. "Pegylated DNA/transferrin-pei complexes: Reduced interaction with blood components, extended circulation in blood and potential for systemic gene delivery." *Gene Ther* 6 (1999): 595-605. 10.1038/sj.gt.3300900.
132. Itaka, K., K. Yamauchi, A. Harada, K. Nakamura, H. Kawaguchi and K. Kataoka. "Polyion complex micelles from plasmid DNA and poly(ethylene glycol)-poly(l-lysine) block copolymer as serum-tolerable polyplex system: Physicochemical properties of micelles relevant to gene transfection efficiency." *Biomaterials* 24 (2003): 4495-506. S0142961203003478 [pii]. http://www.ncbi.nlm.nih.gov/entrez/query.fcgi?cmd=Retrieve&db=PubMed&dopt=Citation&list_uids=12922159.
133. Roy, P., N. W. Kreofsky, C. F. Santa Chalarca and T. M. Reineke. "Binary copolymer blending enhances pdna delivery performance and colloidal shelf stability of quinine-based polyplexes." *Bioconjug Chem* (2025): 10.1021/acs.bioconjchem.5c00040. https://www.ncbi.nlm.nih.gov/pubmed/40067683.
134. Katayose, S. and K. Kataoka. "Remarkable increase in nuclease resistance of plasmid DNA through supramolecular assembly with poly(ethylene glycol)-poly(l-lysine) block copolymer." *J Pharm Sci* 87 (1998): 160-3. 10.1021/js970304s. https://www.ncbi.nlm.nih.gov/pubmed/9519147.
135. Erbacher, P., T. Bettinger, P. Belguise-Valladier, S. Zou, J. L. Coll, J. P. Behr and J. S. Remy. "Transfection and physical properties of various saccharide, poly(ethylene glycol), and antibody-derivatized polyethylenimines (pei)." *J Gene Med* 1 (1999): 210-22. PM:10738569.
136. Merdan, T., K. Kunath, H. Petersen, U. Bakowsky, K. H. Voigt, J. Kopecek and T. Kissel. "Pegylation of poly(ethylene imine) affects stability of complexes with plasmid DNA under in vivo conditions in a dose-dependent manner after intravenous injection into mice." *Bioconjug.Chem.* 16 (2005): 785-92. PM:16029019.
137. Wagner, E. "Have we finally found the ideal nucleic acid carrier with lipo-xenopeptides?" *Expert Opin Drug Deliv* (2025): 1-4. 10.1080/17425247.2025.2586170.
138. Schaffert, D., C. Troiber, E. E. Salcher, T. Frohlich, I. Martin, N. Badgujar, C. Dohmen, D. Edinger, R. Klager, G. Maiwald, *et al.* "Solid-phase synthesis of sequence-defined t-, i-, and u-shape polymers for pdna and sirna delivery." *Angew Chem Int Ed Engl* 50 (2011): 8986-9. 10.1002/anie.201102165. http://www.ncbi.nlm.nih.gov/entrez/query.fcgi?cmd=Retrieve&db=PubMed&dopt=Citation&list_uids=21837712.
139. Salcher, E. E., P. Kos, T. Frohlich, N. Badgujar, M. Scheible and E. Wagner. "Sequence-defined four-arm oligo(ethanamino)amides for pdna and sirna delivery: Impact of building blocks on efficacy." *J Control Release* 164 (2012): 380-6. https://doi.org/10.1016/j.jconrel.2012.06.023.
140. Fröhlich, T., D. Edinger, R. Kläger, C. Troiber, E. Salcher, N. Badgujar, I. Martin, D. Schaffert, A. Cengizeroglu, P. Hadwiger, *et al.* "Structure-activity relationships of sirna carriers based on sequence-defined oligo (ethane amino) amides." *J Control Release* (2012): https://doi.org/10.1016/j.jconrel.2012.03.018.
141. Troiber, C., D. Edinger, P. Kos, L. Schreiner, R. Klager, A. Herrmann and E. Wagner. "Stabilizing effect of tyrosine trimers on pdna and sirna polyplexes." *Biomaterials* 34 (2013): 1624-33. https://doi.org/10.1016/j.biomaterials.2012.11.021.

http://www.ncbi.nlm.nih.gov/entrez/query.fcgi?cmd=Retrieve&db=PubMed&dopt=Citation&list_uids=23199743.
142. Lachelt, U., P. Kos, F. M. Mickler, A. Herrmann, E. E. Salcher, W. Rodl, N. Badgujar, C. Brauchle and E. Wagner. "Fine-tuning of proton sponges by precise diaminoethanes and histidines in pdna polyplexes." *Nanomedicine* 10 (2014): 35-44. 10.1016/j.nano.2013.07.008.
143. Thalmayr, S., M. Grau, L. Peng, J. Pöhmerer, U. Wilk, P. Folda, M. Yazdi, E. Weidinger, T. Burghardt, M. Höhn, *et al.* "Molecular chameleon carriers for nucleic acid delivery: The sweet spot between lipoplexes and polyplexes." *Adv Mater* 35 (2023): e2211105. 10.1002/adma.202211105.
144. Germer, J., A. L. Lessl, J. Pöhmerer, M. Grau, E. Weidinger, M. Höhn, M. Yazdi, M. A. Cappelluti, A. Lombardo, U. Lächelt, *et al.* "Lipo-xenopeptide polyplexes for crispr/cas9 based gene editing at ultra-low dose." *J Control Release* 370 (2024): 239-55. 10.1016/j.jconrel.2024.04.037.
145. Yazdi, M., J. Pohmerer, M. Hasanzadeh Kafshgari, J. Seidl, M. Grau, M. Hohn, V. Vetter, C. C. Hoch, B. Wollenberg, G. Multhoff, *et al.* "In vivo endothelial cell gene silencing by sirna-lnps tuned with lipoamino bundle chemical and ligand targeting." *Small* 20 (2024): e2400643. 10.1002/smll.202400643. https://www.ncbi.nlm.nih.gov/pubmed/38923700.
146. Haase, F., J. Pöhmerer, M. Yazdi, M. Grau, Y. Zeyn, U. Wilk, T. Burghardt, M. Höhn, C. Hieber, M. Bros, *et al.* "Lipoamino bundle lnps for efficient mrna transfection of dendritic cells and macrophages show high spleen selectivity." *Eur J Pharm Biopharm* 194 (2024): 95-109. 10.1016/j.ejpb.2023.11.025.
147. Hashizume, H., P. Baluk, S. Morikawa, J. W. McLean, G. Thurston, S. Roberge, R. K. Jain and D. M. McDonald. "Openings between defective endothelial cells explain tumor vessel leakiness." *Am J Pathol* 156 (2000): 1363-80. 10.1016/S0002-9440(10)65006-7. https://www.ncbi.nlm.nih.gov/pubmed/10751361.
148. Jain, R. K. "Transport of molecules across tumor vasculature." *Cancer Metastasis Rev* 6 (1987): 559-93. 10.1007/BF00047468. https://www.ncbi.nlm.nih.gov/pubmed/3327633.
149. Song, F., N. Sakurai, A. Okamoto, H. Koide, N. Oku, T. Dewa and T. Asai. "Design of a novel pegylated liposomal vector for systemic delivery of sirna to solid tumors." *Biol Pharm Bull* 42 (2019): 996-1003. 10.1248/bpb.b19-00032. https://www.ncbi.nlm.nih.gov/pubmed/31155597.
150. Adams, D., A. Gonzalez-Duarte, W. D. O'Riordan, C. C. Yang, M. Ueda, A. V. Kristen, I. Tournev, H. H. Schmidt, T. Coelho, J. L. Berk, *et al.* "Patisiran, an rnai therapeutic, for hereditary transthyretin amyloidosis." *N Engl J Med* 379 (2018): 11-21. 10.1056/NEJMoa1716153.
151. Akinc, A., W. Querbes, S. De, J. Qin, M. Frank-Kamenetsky, K. N. Jayaprakash, M. Jayaraman, K. G. Rajeev, W. L. Cantley, J. R. Dorkin, *et al.* "Targeted delivery of rnai therapeutics with endogenous and exogenous ligand-based mechanisms." *Mol Ther* 18 (2010): 1357-64. https://doi.org/10.1038/mt.2010.85.
152. Katakowski, J. A., G. Mukherjee, S. E. Wilner, K. E. Maier, M. T. Harrison, T. P. DiLorenzo, M. Levy and D. Palliser. "Delivery of sirnas to dendritic cells using dec205-targeted lipid nanoparticles to inhibit immune responses." *Mol Ther* 24 (2016): 146-55. 10.1038/mt.2015.175. https://www.ncbi.nlm.nih.gov/pubmed/26412590.
153. Parhiz, H., V. V. Shuvaev, N. Pardi, M. Khoshnejad, R. Y. Kiseleva, J. S. Brenner, T. Uhler, S. Tuyishime, B. L. Mui, Y. K. Tam, *et al.* "Pecam-1 directed re-targeting of exogenous mrna providing two orders of magnitude enhancement of vascular delivery and expression in lungs independent of apolipoprotein e-mediated uptake." *J Control Release* 291 (2018): 106-15. 10.1016/j.jconrel.2018.10.015. https://www.ncbi.nlm.nih.gov/pubmed/30336167.

154. Veiga, N., M. Goldsmith, Y. Diesendruck, S. Ramishetti, D. Rosenblum, E. Elinav, M. A. Behlke, I. Benhar and D. Peer. "Leukocyte-specific sirna delivery revealing irf8 as a potential anti-inflammatory target." *J Control Release* 313 (2019): 33-41. 10.1016/j.jconrel.2019.10.001. https://www.ncbi.nlm.nih.gov/pubmed/31634546.
155. Rosenblum, D., A. Gutkin, R. Kedmi, S. Ramishetti, N. Veiga, A. M. Jacobi, M. S. Schubert, D. Friedmann-Morvinski, Z. R. Cohen, M. A. Behlke, *et al.* "Crispr-cas9 genome editing using targeted lipid nanoparticles for cancer therapy." *Sci Adv* 6 (2020): 10.1126/sciadv.abc9450. https://www.ncbi.nlm.nih.gov/pubmed/33208369.
156. Tombácz, I., D. Laczkó, H. Shahnawaz, H. Muramatsu, A. Natesan, A. Yadegari, T. E. Papp, M. G. Alameh, V. Shuvaev, B. L. Mui, *et al.* "Highly efficient cd4+ t cell targeting and genetic recombination using engineered cd4+ cell-homing mrna-lnps." *Mol Ther* 29 (2021): 3293-304. 10.1016/j.ymthe.2021.06.004.
157. Escudé Martinez de Castilla, P., V. Verdi, W. de Voogt, M. Estapé Sentí, A. C. Koekman, J. Rietveld, S. van Kempen, Q. Yang, J. van Merris, G. Jenster, *et al.* "Nanobody-decorated lipid nanoparticles for enhanced mrna delivery to tumors in vivo." *Adv Healthc Mater* (2025): e2500605. 10.1002/adhm.202500605.
158. Papp, T. E., J. Zeng, H. Shahnawaz, A. Akyianu, L. Breda, A. Yadegari, J. Steward, R. Shi, Q. Li, B. L. Mui, *et al.* "Cd47 peptide-cloaked lipid nanoparticles promote cell-specific mrna delivery." *Mol Ther* 33 (2025): 3195-208. 10.1016/j.ymthe.2025.03.018.
159. Wang, Y. F., Y. Zhou, J. Sun, X. Wang, Y. Jia, K. Ge, Y. Yan, K. A. Dawson, S. Guo, J. Zhang, *et al.* "The yin and yang of the protein corona on the delivery journey of nanoparticles." *Nano Res* 16 (2023): 715-34. 10.1007/s12274-022-4849-6.
160. Vetter, V. C. and E. Wagner. "Targeting nucleic acid-based therapeutics to tumors: Challenges and strategies for polyplexes." *J Control Release* 346 (2022): 110-35. 10.1016/j.jconrel.2022.04.013.
161. Erbacher, P., J. S. Remy and J. P. Behr. "Gene transfer with synthetic virus-like particles via the integrin-mediated endocytosis pathway." *Gene Ther.* 6 (1999): 138-45.
162. Carlisle, R. C., M. L. Read, M. A. Wolfert and L. W. Seymour. "Self-assembling poly(l-lysine)/DNA complexes capable of integrin-mediated cellular uptake and gene expression." *Colloids and Surfaces B: Biointerfaces* 16 (1999): 261-72. https://doi.org/10.1016/S0927-7765(99)00077-6. https://www.sciencedirect.com/science/article/pii/S0927776599000776.
163. Kircheis, R., A. Kichler, G. Wallner, M. Kursa, M. Ogris, T. Felzmann, M. Buchberger and E. Wagner. "Coupling of cell-binding ligands to polyethylenimine for targeted gene delivery." *Gene Ther.* 4 (1997): 409-18. PM:9274717.
164. Wagner, E., C. Plank, K. Zatloukal, M. Cotten and M. L. Birnstiel. "Influenza virus hemagglutinin ha-2 n-terminal fusogenic peptides augment gene transfer by transferrin-polylysine-DNA complexes: Toward a synthetic virus-like gene-transfer vehicle." *Proc.Natl.Acad.Sci.U.S.A* 89 (1992): 7934-38. PM:1518816.
165. Schafer, A., A. Pahnke, D. Schaffert, W. M. van Weerden, C. M. de Ridder, W. Rodl, A. Vetter, C. Spitzweg, R. Kraaij, E. Wagner, *et al.* "Disconnecting the yin and yang relation of epidermal growth factor receptor (egfr)-mediated delivery: A fully synthetic, egfr-targeted gene transfer system avoiding receptor activation." *Hum Gene Ther* 22 (2011): 1463-73. 10.1089/hum.2010.231. http://www.ncbi.nlm.nih.gov/entrez/query.fcgi?cmd=Retrieve&db=PubMed&dopt=Citation&list_uids=21644815.
166. Erbacher, P., J. S. Remy and J. P. Behr. "Gene transfer with synthetic virus-like particles via the integrin-mediated endocytosis pathway." *Gene Therapy* 6 (1999): 138-45. 10.1038/sj.gt.3300783. https://doi.org/10.1038/sj.gt.3300783.
167. Mickler, F. M., L. Mockl, N. Ruthardt, M. Ogris, E. Wagner and C. Brauchle. "Tuning nanoparticle uptake: Live-cell imaging reveals two distinct endocytosis mechanisms

mediated by natural and artificial egfr targeting ligand." *Nano Lett* 12 (2012): 3417-23. 10.1021/nl300395q.
168. Rodl, W., D. Schaffert, E. Wagner and M. Ogris. "Synthesis of polyethylenimine-based nanocarriers for systemic tumor targeting of nucleic acids." *Methods Mol Biol* 948 (2013): 105-20. 10.1007/978-1-62703-140-0_8.
169. Steffens, R. C., S. Thalmayr, E. Weidinger, J. Seidl, P. Folda, M. Hohn and E. Wagner. "Modulating efficacy and cytotoxicity of lipoamino fatty acid nucleic acid carriers using disulfide or hydrophobic spacers." *Nanoscale* 16 (2024): 13988-4005. 10.1039/d4nr01357c. https://www.ncbi.nlm.nih.gov/pubmed/38984864.
170. Morys, S., A. Krhac Levacic, S. Urnauer, S. Kempter, S. Kern, J. O. Radler, C. Spitzweg, U. Lachelt and E. Wagner. "Influence of defined hydrophilic blocks within oligoaminoamide copolymers: Compaction versus shielding of pdna nanoparticles." *Polymers (Basel)* 9 (2017): 10.3390/polym9040142.
171. Smith, R. J., R. W. Beck and L. E. Prevette. "Impact of molecular weight and degree of conjugation on the thermodynamics of DNA complexation and stability of polyethylenimine-graft-poly(ethylene glycol) copolymers." *Biophys Chem* 203-204 (2015): 12-21. 10.1016/j.bpc.2015.04.005.
172. Koning, G. A., H. W. Morselt, J. A. Kamps and G. L. Scherphof. "Uptake and intracellular processing of peg-liposomes and peg-immunoliposomes by kupffer cells in vitro." *J Liposome Res* 11 (2001): 195-209. 10.1081/LPR-100108462. https://www.ncbi.nlm.nih.gov/pubmed/19530933.
173. Mishra, S., P. Webster and M. E. Davis. "Pegylation significantly affects cellular uptake and intracellular trafficking of non-viral gene delivery particles." *Eur.J Cell Biol.* 83 (2004): 97-111. PM:15202568.
174. Lai, T. C., K. Kataoka and G. S. Kwon. "Pluronic-based cationic block copolymer for forming pdna polyplexes with enhanced cellular uptake and improved transfection efficiency." *Biomaterials* 32 (2011): 4594-603. 10.1016/j.biomaterials.2011.02.065. https://www.ncbi.nlm.nih.gov/pubmed/21453964.
175. Chen, J., S. Gamou, A. Takayanagi and N. Shimizu. "A novel gene delivery system using egf receptor-mediated endocytosis." *FEBS Lett* 338 (1994): 167-69.
176. Kircheis, R., E. Ostermann, M. F. Wolschek, C. Lichtenberger, C. Magin-Lachmann, L. Wightman, M. Kursa and E. Wagner. "Tumor-targeted gene delivery of tumor necrosis factor-alpha induces tumor necrosis and tumor regression without systemic toxicity." *Cancer Gene Ther* 9 (2002): 673-80. 10.1038/sj.cgt.7700487.
177. Bellocq, N. C., S. H. Pun, G. S. Jensen and M. E. Davis. "Transferrin-containing, cyclodextrin polymer-based particles for tumor-targeted gene delivery." *Bioconjug.Chem.* 14 (2003): 1122-32. PM:14624625.
178. Merdan, T., J. Callahan, H. Petersen, K. Kunath, U. Bakowsky, P. Kopeckova, T. Kissel and J. Kopecek. "Pegylated polyethylenimine-fab' antibody fragment conjugates for targeted gene delivery to human ovarian carcinoma cells." *Bioconjug.Chem.* 14 (2003): 989-96. PM:13129403.
179. Oba, M., S. Fukushima, N. Kanayama, K. Aoyagi, N. Nishiyama, H. Koyama and K. Kataoka. "Cyclic rgd peptide-conjugated polyplex micelles as a targetable gene delivery system directed to cells possessing alphavbeta3 and alphavbeta5 integrins." *Bioconjug Chem* 18 (2007): 1415-23. PM:17595054.
180. Oba, M., K. Aoyagi, K. Miyata, Y. Matsumoto, K. Itaka, N. Nishiyama, Y. Yamasaki, H. Koyama and K. Kataoka. "Polyplex micelles with cyclic rgd peptide ligands and disulfide cross-links directing to the enhanced transfection via controlled intracellular trafficking." *Mol Pharm* 5 (2008): 1080-92.

181. Liu, L., M. Zheng, D. Librizzi, T. Renette, O. M. Merkel and T. Kissel. "Efficient and tumor targeted sirna delivery by polyethylenimine-graft-polycaprolactone-block-poly(ethylene glycol)-folate (pei-pcl-peg-fol)." *Mol Pharm* 13 (2016): 134-43. 10.1021/acs.molpharmaceut.5b00575.
182. Kim, M. W., H. Y. Jeong, S. J. Kang, M. J. Choi, Y. M. You, C. S. Im, T. S. Lee, I. H. Song, C. G. Lee, K. J. Rhee, *et al.* "Cancer-targeted nucleic acid delivery and quantum dot imaging using egf receptor aptamer-conjugated lipid nanoparticles." *Sci Rep* 7 (2017): 9474. 10.1038/s41598-017-09555-w. https://www.ncbi.nlm.nih.gov/pubmed/28842588.
183. Ren, H., L. Zhou, M. Liu, W. Lu and C. Gao. "Peptide ge11–polyethylene glycol–polyethylenimine for targeted gene delivery in laryngeal cancer." *Medical Oncology* 32 (2015): 185. 10.1007/s12032-015-0624-9. https://doi.org/10.1007/s12032-015-0624-9.
184. Lee, D., Y. M. Lee, J. Kim, M. K. Lee and W. J. Kim. "Enhanced tumor-targeted gene delivery by bioreducible polyethylenimine tethering egfr divalent ligands." *Biomaterials Science* 3 (2015): 1096-104. 10.1039/C5BM00004A. http://dx.doi.org/10.1039/C5BM00004A.
185. Schmohl, K. A., A. Gupta, G. K. Grunwald, M. Trajkovic-Arsic, K. Klutz, R. Braren, M. Schwaiger, P. J. Nelson, M. Ogris, E. Wagner, *et al.* "Imaging and targeted therapy of pancreatic ductal adenocarcinoma using the theranostic sodium iodide symporter (nis) gene." *Oncotarget* 8 (2017): 33393-404. 10.18632/oncotarget.16499.
186. Wang, Y., J. Luo, I. Truebenbach, S. Reinhard, P. M. Klein, M. Höhn, S. Kern, S. Morys, D. M. Loy, E. Wagner, *et al.* "Double click-functionalized sirna polyplexes for gene silencing in epidermal growth factor receptor-positive tumor cells." *ACS Biomater Sci Eng* 6 (2020): 1074-89. 10.1021/acsbiomaterials.9b01904.
187. Yu, L., Q. Wang, R. C. H. Wong, S. Zhao, D. K. P. Ng and P.-C. Lo. "Synthesis and biological evaluation of phthalocyanine-peptide conjugate for egfr-targeted photodynamic therapy and bioimaging." *Dyes and Pigments* 163 (2019): 197-203. https://doi.org/10.1016/j.dyepig.2018.11.055.
188. Kursa, M., G. F. Walker, V. Roessler, M. Ogris, W. Roedl, R. Kircheis and E. Wagner. "Novel shielded transferrin-polyethylene glycol-polyethylenimine/DNA complexes for systemic tumor-targeted gene transfer." *Bioconjug Chem* 14 (2003): 222-31. 10.1021/bc0256087.
189. Maurstad, G., B. T. Stokke, K. M. Varum and S. P. Strand. "Pegylated chitosan complexes DNA while improving polyplex colloidal stability and gene transfection efficiency." *Carbohydr Polym* 94 (2013): 436-43. 10.1016/j.carbpol.2013.01.015. https://www.ncbi.nlm.nih.gov/pubmed/23544560.
190. Tang, M. X. and F. C. Szoka. "The influence of polymer structure on the interactions of cationic polymers with DNA and morphology of the resulting complexes." *Gene Ther* 4 (1997): 823-32. PM:9338011.
191. Needham, D., T. J. McIntosh and D. D. Lasic. "Repulsive interactions and mechanical stability of polymer-grafted lipid membranes." *Biochim Biophys Acta* 1108 (1992): 40-48.
192. Oupicky, D., M. Ogris, K. A. Howard, P. R. Dash, K. Ulbrich and L. W. Seymour. "Importance of lateral and steric stabilization of polyelectrolyte gene delivery vectors for extended systemic circulation." *Mol Ther* 5 (2002): 463-72. PM:11945074.
193. Pun, S. H. and M. E. Davis. "Development of a nonviral gene delivery vehicle for systemic application." *Bioconjugate Chemistry* 13 (2002): 630-9. http://www.ncbi.nlm.nih.gov/pubmed/12009955.
194. Vader, P., L. J. van der Aa, J. F. Engbersen, G. Storm and R. M. Schiffelers. "Physicochemical and biological evaluation of sirna polyplexes based on pegylated poly(amido amine)s." *Pharm Res* 29 (2012): 352-61. 10.1007/s11095-011-0545-z.

195. Adolph, E. J., C. E. Nelson, T. A. Werfel, R. Guo, J. M. Davidson, S. A. Guelcher and C. L. Duvall. "Enhanced performance of plasmid DNA polyplexes stabilized by a combination of core hydrophobicity and surface pegylation." *J Mater Chem B* 2 (2014): 8154-64. 10.1039/C4TB00352G. https://www.ncbi.nlm.nih.gov/pubmed/25530856.
196. Wu, T., L. Wang, S. Ding and Y. You. "Fluorinated peg-polypeptide polyplex micelles have good serum-resistance and low cytotoxicity for gene delivery." *Macromol Biosci* 17 (2017): 10.1002/mabi.201700114. https://www.ncbi.nlm.nih.gov/pubmed/28524376.
197. Paunovska, K., C. D. Sago, C. M. Monaco, W. H. Hudson, M. G. Castro, T. G. Rudoltz, S. Kalathoor, D. A. Vanover, P. J. Santangelo, R. Ahmed, *et al.* "A direct comparison of in vitro and in vivo nucleic acid delivery mediated by hundreds of nanoparticles reveals a weak correlation." *Nano Lett* 18 (2018): 2148-57. 10.1021/acs.nanolett.8b00432.
198. Paunovska, K., D. Loughrey, C. D. Sago, R. Langer and J. E. Dahlman. "Using large datasets to understand nanotechnology." *Adv Mater* 31 (2019): e1902798. 10.1002/adma.201902798.
199. Huayamares, S. G., M. P. Lokugamage, R. Rab, A. J. Da Silva Sanchez, H. Kim, A. Radmand, D. Loughrey, L. Lian, Y. Hou, B. R. Achyut, *et al.* "High-throughput screens identify a lipid nanoparticle that preferentially delivers mrna to human tumors in vivo." *J Control Release* 357 (2023): 394-403. 10.1016/j.jconrel.2023.04.005.
200. Berger, S., M. Berger, C. Bantz, M. Maskos and E. Wagner. "Performance of nanoparticles for biomedical applications: The in vitro/in vivo discrepancy." *Biophys Rev (Melville)* 3 (2022): 011303. 10.1063/5.0073494. https://www.ncbi.nlm.nih.gov/pubmed/38505225.
201. Dilliard, S. A., Y. Sun, M. O. Brown, Y. C. Sung, S. Chatterjee, L. Farbiak, A. Vaidya, X. Lian, X. Wang, A. Lemoff, *et al.* "The interplay of quaternary ammonium lipid structure and protein corona on lung-specific mrna delivery by selective organ targeting (sort) nanoparticles." *J Control Release* 361 (2023): 361-72. 10.1016/j.jconrel.2023.07.058.
202. Alberg, I., S. Kramer, M. Schinnerer, Q. Hu, C. Seidl, C. Leps, N. Drude, D. Möckel, C. Rijcken, T. Lammers, *et al.* "Polymeric nanoparticles with neglectable protein corona." *Small* 16 (2020): e1907574. 10.1002/smll.201907574.
203. Zhang, X., S. Si, I. Lieberwirth, K. Landfester and V. Mailänder. "Engineered protein corona sustains stealth functionality of nanocarriers in plasma." *J Nanobiotechnology* 23 (2025): 512. 10.1186/s12951-025-03565-x.
204. Voke, E., M. Arral, H. J. Squire, T. J. Lin, R. Coreas, A. Lui, A. T. Iavarone, R. L. Pinals, K. A. Whitehead and M. Landry. "Protein corona formed on lipid nanoparticles compromises delivery efficiency of mrna cargo." *bioRxiv* (2025): 10.1101/2025.01.20.633942.
205. Rademacker, S., S. Pinto Carneiro, M. Molbay, F. Catapano, I. Forné, A. Imhof, R. Wibel, C. Heidecke, P. Hölig and O. M. Merkel. "The impact of lipid compositions on sirna and mrna lipid nanoparticle performance for pulmonary delivery." *Eur J Pharm Sci* 212 (2025): 107182. 10.1016/j.ejps.2025.107182.
206. He, X., R. Wang, Y. Cao, Y. Ding, Y. Chang, H. Dong, R. Xie, G. Zhong, H. Yang and J. Li. "Lung-specific mrna delivery by ionizable lipids with defined structure-function relationship and unique protein corona feature." *Adv Sci (Weinh)* 12 (2025): e2416525. 10.1002/advs.202416525.
207. van Straten, D., H. Sork, L. van de Schepop, R. Frunt, K. Ezzat and R. M. Schiffelers. "Biofluid specific protein coronas affect lipid nanoparticle behavior in vitro." *J Control Release* 373 (2024): 481-92. 10.1016/j.jconrel.2024.07.044.
208. Lundqvist, M., J. Stigler, G. Elia, I. Lynch, T. Cedervall and K. A. Dawson. "Nanoparticle size and surface properties determine the protein corona with possible implications for biological impacts." *Proc Natl Acad Sci U S A* 105 (2008): 14265-70. 10.1073/pnas.0805135105. https://www.ncbi.nlm.nih.gov/pubmed/18809927.

209. Lundqvist, M., J. Stigler, T. Cedervall, T. Berggard, M. B. Flanagan, I. Lynch, G. Elia and K. Dawson. "The evolution of the protein corona around nanoparticles: A test study." *ACS Nano* 5 (2011): 7503-9. 10.1021/nn202458g. https://www.ncbi.nlm.nih.gov/pubmed/21861491.
210. Cedervall, T., I. Lynch, S. Lindman, T. Berggard, E. Thulin, H. Nilsson, K. A. Dawson and S. Linse. "Understanding the nanoparticle-protein corona using methods to quantify exchange rates and affinities of proteins for nanoparticles." *Proc Natl Acad Sci U S A* 104 (2007): 2050-5. 10.1073/pnas.0608582104. https://www.ncbi.nlm.nih.gov/pubmed/17267609.
211. Vilanova, O., J. J. Mittag, P. M. Kelly, S. Milani, K. A. Dawson, J. O. Radler and G. Franzese. "Understanding the kinetics of protein-nanoparticle corona formation." *ACS Nano* 10 (2016): 10842-50. 10.1021/acsnano.6b04858. https://www.ncbi.nlm.nih.gov/pubmed/28024351.
212. Milani, S., F. B. Bombelli, A. S. Pitek, K. A. Dawson and J. Radler. "Reversible versus irreversible binding of transferrin to polystyrene nanoparticles: Soft and hard corona." *ACS Nano* 6 (2012): 2532-41. 10.1021/nn204951s. https://www.ncbi.nlm.nih.gov/pubmed/22356488.
213. Zelphati, O., L. S. Uyechi, L. G. Barron and F. C. Szoka, Jr. "Effect of serum components on the physico-chemical properties of cationic lipid/oligonucleotide complexes and on their interactions with cells." *Biochim.Biophys.Acta* 1390 (1998): 119-33. PM:9507083.
214. Senior, J. H., K. R. Trimble and R. Maskiewicz. "Interaction of positively-charged liposomes with blood: Implications for their application in vivo." *Biochim.Biophys.Acta* 1070 (1991): 173-79. PM:1751523.
215. Casper, J., S. H. Schenk, E. Parhizkar, P. Detampel, A. Dehshahri and J. Huwyler. "Polyethylenimine (pei) in gene therapy: Current status and clinical applications." *J Control Release* 362 (2023): 667-91. 10.1016/j.jconrel.2023.09.001. https://www.ncbi.nlm.nih.gov/pubmed/37666302.

8 PUBLICATIONS

8.1 RESEARCH

Folda, P.; Weidinger, E.; Seidl, J.; Yazdi, M.; Pöhmerer, J.; Grau, M.; Minde, D.P.; Ali, M.; Kimna, C.; Wagner, E. PEGylation Enhances Colloidal Stability and Promotes Ligand-Mediated Targeting of LAF–Xenopeptide mRNA Complexes. *Polymers* 2025, 17, 2979.

Steffens RC, Thalmayr S, Weidinger E, Seidl J, **Folda P**, Höhn M, Wagner E. (2024) Modulating efficacy and cytotoxicity of lipoamino fatty acid nucleic acid carriers using disulfide or hydrophobic spacers, *Nanoscale* 2024 Jul 25;16(29):13988-14005

Steffens RC, **Folda P**, Fendler NL, Höhn M, Bücher-Schossau K, Kempter S, Snyder NL, Hartmann L, Wagner E, Berger S. (2024) GalNAc- or Mannose-PEG-Functionalized Polyplexes Enable Effective Lectin-Mediated DNA Delivery, *Bioconjug Chem.* 2024 Mar 20;35(3):351-370

Thalmayr S, Grau M, Peng L, Pöhmerer J, Wilk U, **Folda P**, Yazdi M, Weidinger E, Burghardt T, Höhn M, Wagner E, Berger S. (2023) Molecular Chameleon Carriers for Nucleic Acid Delivery: The Sweet Spot between Lipoplexes and Polyplexes, *Adv. Mater.* 2023 Jun;35(25):e2211105

8.2 POSTER PRESENTATION

Benli-Hoppe, T.; Yazdi, M.; **Folda, P.**; Wagner, E.; Berger, S., Optimizing four-armed carriers for pDNA and siRNA delivery: Impact of type and position of hydrophobic amino acids (Poster #P11). DG-GT Symposium 2022 “Making Gene Therapy a Clinical Reality”, Hannover, Germany; March 23-25, 2022.

8.3 PATENT APPLICATION

Ernst Wagner, Lun Peng, Simone Berger, Sophie Thalmayr, **Paul Folda**, Franziska Haase, Melina Grau, Janin Germer, Mina Yazdi, Eric Weidinger, Tobias Burghardt, Johanna Seidl, Ricarda Steffens, Novel carriers for nucleic acid and/or protein delivery, WO/2024/110492, EP4622673 US 19/132,459

9 ACKNOWLEDGEMENTS

I would like to sincerely thank Prof. Dr. Ernst Wagner for enabling me to pursue my PhD within his research group. I am extremely thankful for your support and valuable guidance throughout my PhD. Particularly, learning from you how to design and conduct experiments, interpret data, and prepare scientific manuscripts was invaluable. I benefited greatly from your experience, creativity, and scientific vision. Moreover, I am also very thankful for the constant supply of chocolate pralines and the excellent original "Sacher Torte" for the whole lab.

I would like to express my gratitude to all members of the examination committee, and especially to Prof. Dr. Wolfgang Frieß, my second examiner, for their careful and thorough evaluation of my thesis.

I would like to thank my collaboration partners, Dr. Ceren Kimna, Dr. David-Paul Minde, and Dr. Mayar Ali, for their valuable contributions to the protein corona investigation of LAF-Xenopeptides.

I would also like to thank all technicians of the AK Wagner group. Wolfgang your technical expertise saved more than one piece of equipment from an early retirement. For your-well deserved retirement, I wish you all the best. Also thank you Melinda and Miriam for your relentless support in cell culture. Lorina, thank you for your continuous help in the lab, and more importantly, for inviting me to your parties, even though you never manage to attend mine. Olga, thank you for the great organization. Markus, thank you for having always been so positive and for providing "sweets" for the team.

Special thanks go to Theo and Simone. You both supported me at the beginning of my PhD, particular for introducing me to cell culture and synthesis.

Many thanks to Johanna, Sophie, Eric, Melina, Victoria, Jana, Uli, Franzi, Ricarda, Anni, Janin, Mina, Alex, Fengrong, Faqian, Lun and Xianjin. Beyond your outstanding scientific advice and support, I am so happy to be your friend.

Countless moments, whether shared as Christmas parties, ski retreats or Octoberfest visits made my PhD a time, that I do not want to miss.

Sophie, I have known you for twelve years, and I really enjoy getting old and wise with you. I am lucky to have you as a friend. Melina, thank you for constantly providing carriers. It was always a pleasure gossiping with you, and thank you for inviting me and Johanna to the annual Barthelmarkt in Oberstimm. I am fortunate to be your friend. Eric thank you for your friendship, your help with my manuscript, and for introducing me to the world of cars. Victoria, thank you for being my friend and for showing me how to eat cake in an appropriate way. Mina, I am so thankful for the many discussions and your excellent scientific advice. Franzi, thank you for being the perfect office partner and for the many discussions. Mina (again) and Jana, thank you for planning and performing the animal experiments. And Tobi, thank you for baking the best cakes and measuring MALDI. Fengrong, Faqian, Lun and Xianjin I am happy and lucky to have met you. Especially, the Chinese hot pot dinner evenings are memories I will never forget.

A special thank you goes to you, Johanna. I am so lucky to have met you here, and this alone made my PhD journey a success. Without you, this time would have been only half as enjoyable and successful.

Finally, I would like to thank my family. First of all, thank you to my grandparents, Opa Franz, Oma Gertrud, Großvater Siegfried and Omi Hildegard. And thank you also to Papa, Mama, Franz (Jr.), Ida, Dejan, Herbert, Stefan, Anne und Ulla and the “whole rest”. From supporting me during school, university, and in my PhD, without you I would not have achieved this. Not all of you can celebrate with me in person, but I am sure we will one day. I am so happy and fortunate to call you my family.